

Fig. 6.16 Microhardness of phases measured by a 0.098N indentation across the austenite layer at prior austenite grain boundaries.

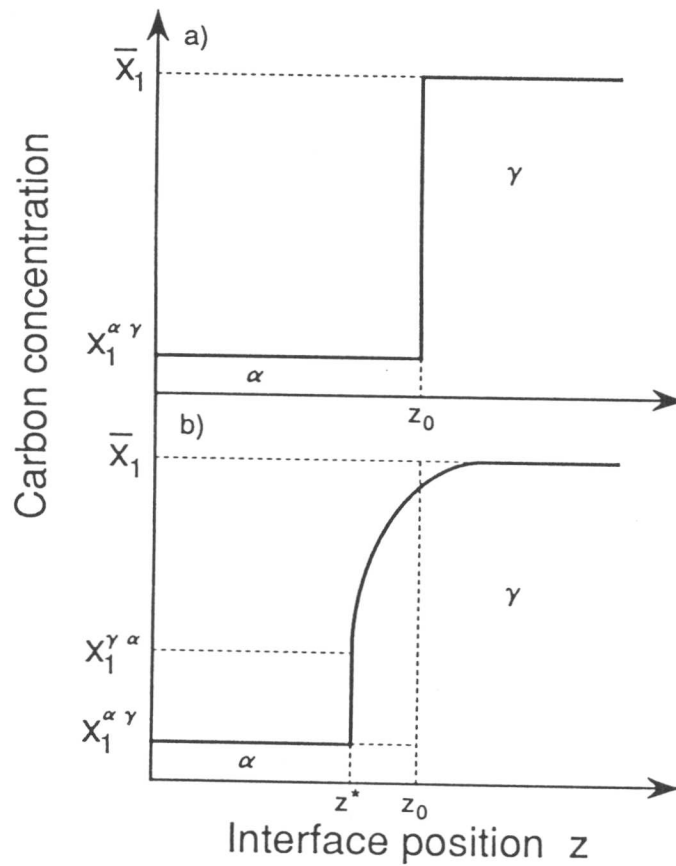


Fig. 6.17 Illustrative carbon profile in austenite near interface during the growth event of the austenite which exists in the initial microstructure of a mixture of bainite and austenite.

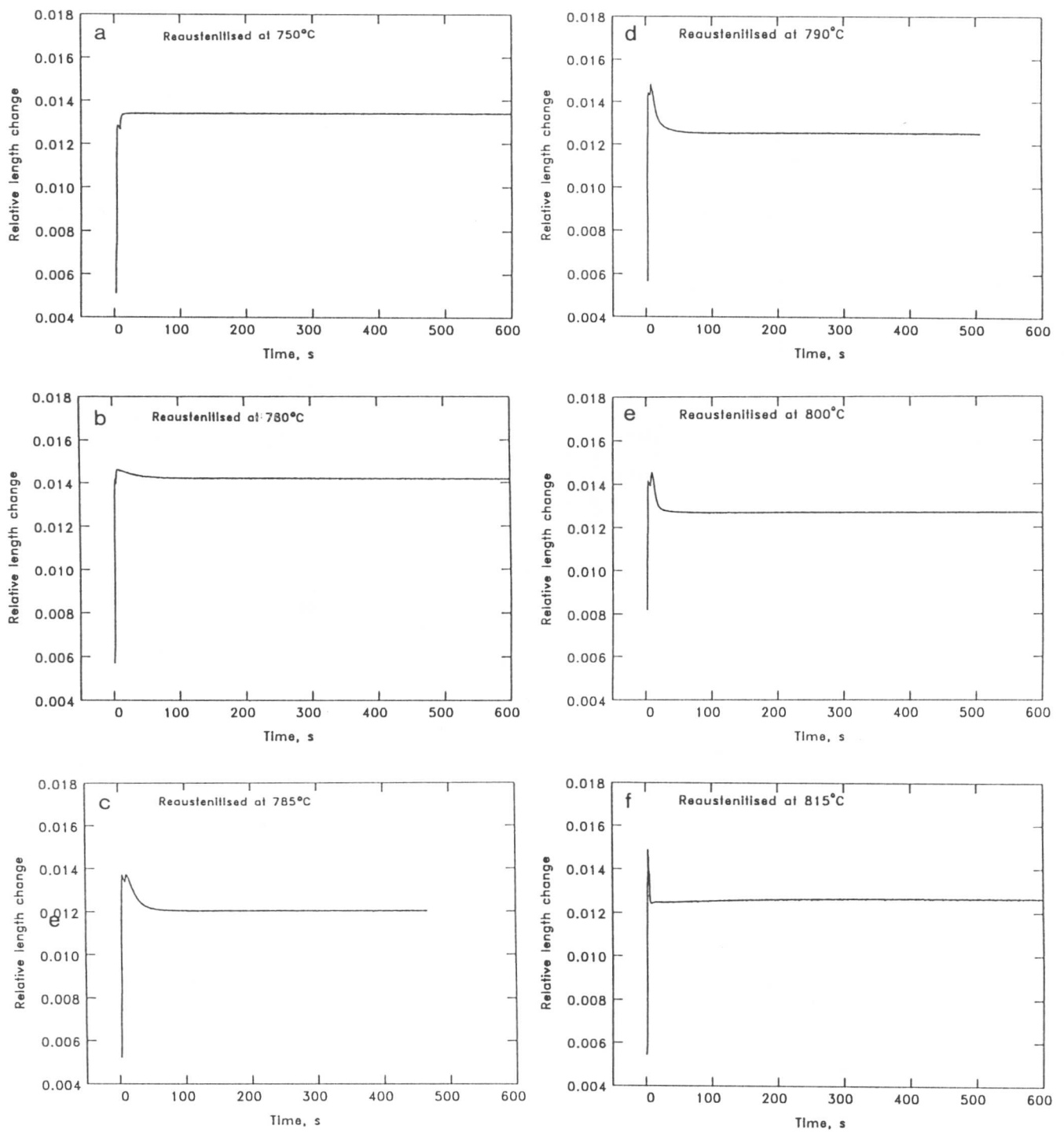


Fig. 6.18 Relative length changes obtained during isothermal re-austenitisation from martensite, which was obtained by quenching from 1100 °C, at a) 750 °C, b) 780 °C, c) 785 °C, d) 790 °C, e) 800 °C and f) 815 °C in the Fe-0.3C-4.08Cr wt.% alloy.

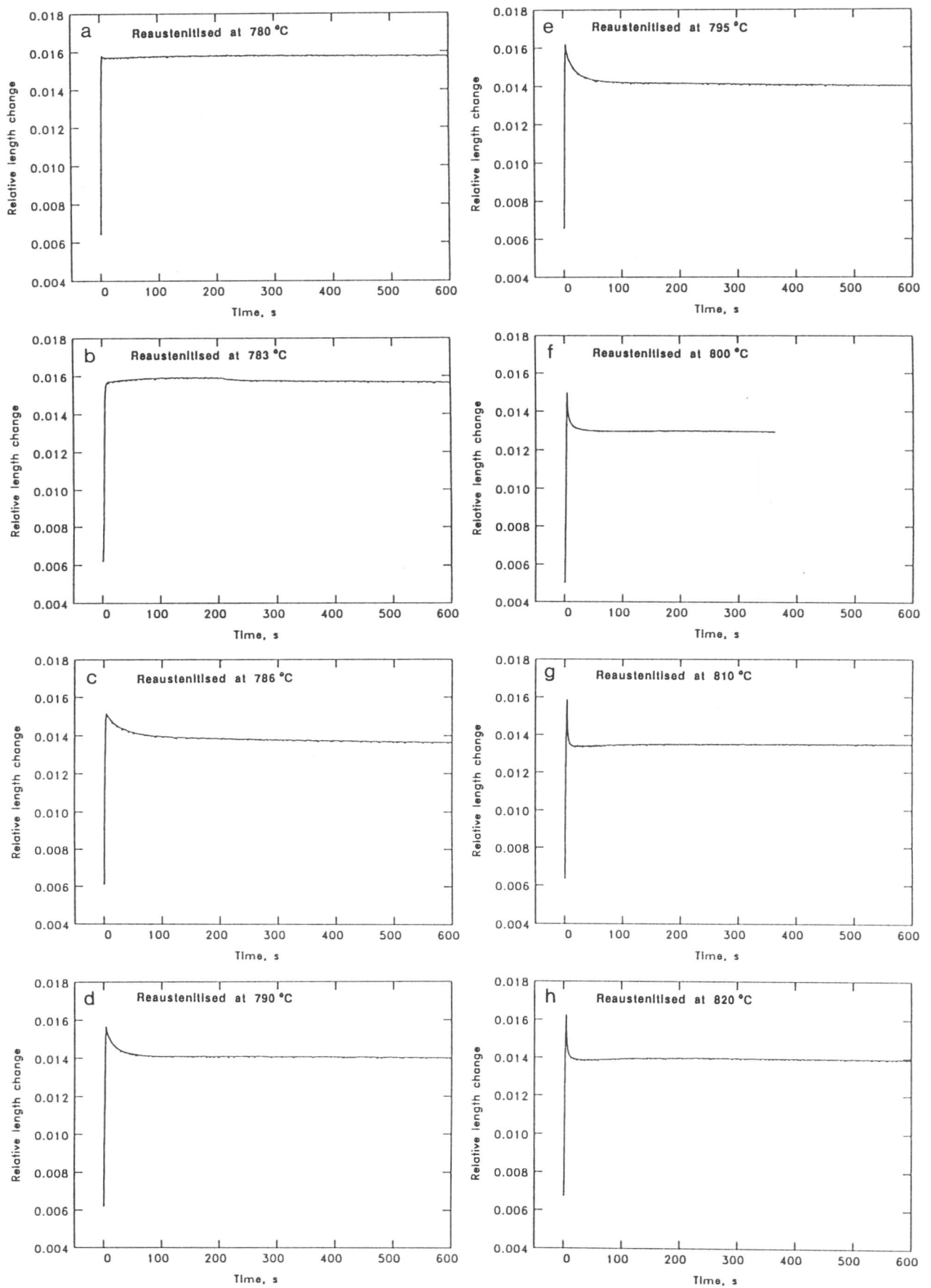


Fig. 6.19 Relative length changes obtained during isothermal re-austenitisation from martensite, which was obtained by quenching from 1250 °C, at a) 780 °C, b) 783 °C, c) 786 °C, d) 790 °C, e) 795 °C, f) 800 °C, g) 810 °C and h) 820 °C in the Fe-0.3C-4.08Cr wt.% alloy.

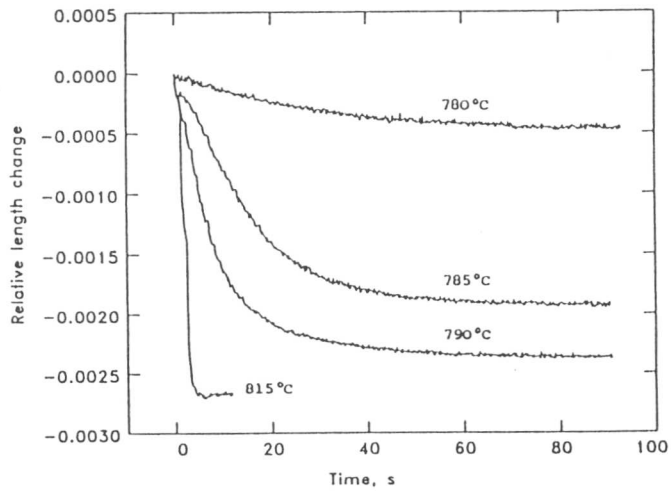


Fig. 6.20 Effect of the reaction temperature on the temperature corrected relative length change during the isothermal re-austenitisation from martensite.

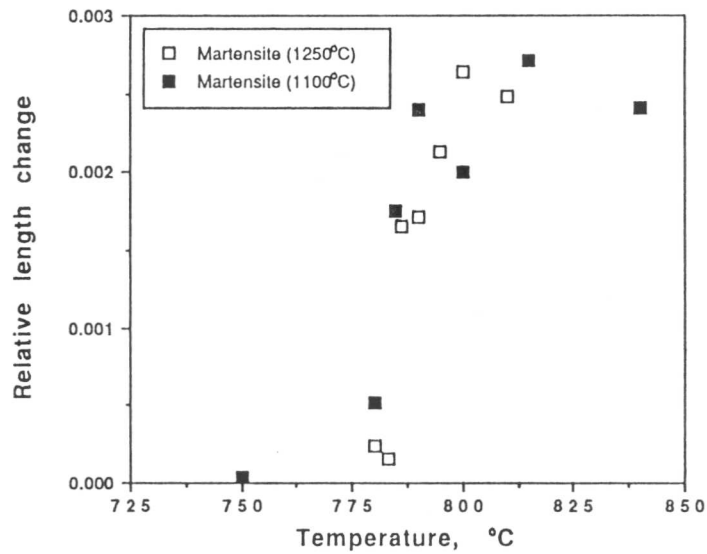


Fig. 6.21 Maximum relative length changes during 30 min of isothermal re-austenitisation from martensite which was obtained by quenching from either 1100°C or 1250°C in the Fe-0.3C-4.08Cr wt.% alloy.

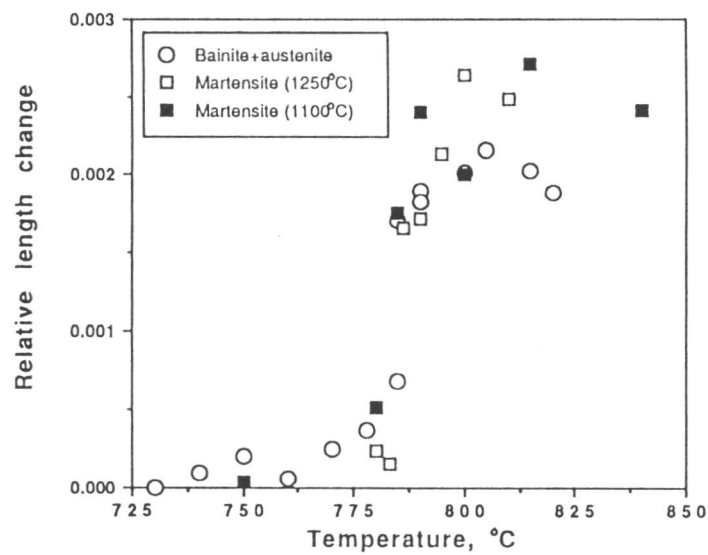


Fig. 6.22 Maximum relative length changes during 30 min of isothermal re-austenitisation from martensite and from the mixture of bainite and austenite in the Fe-0.3C-4.08Cr wt.% alloy.

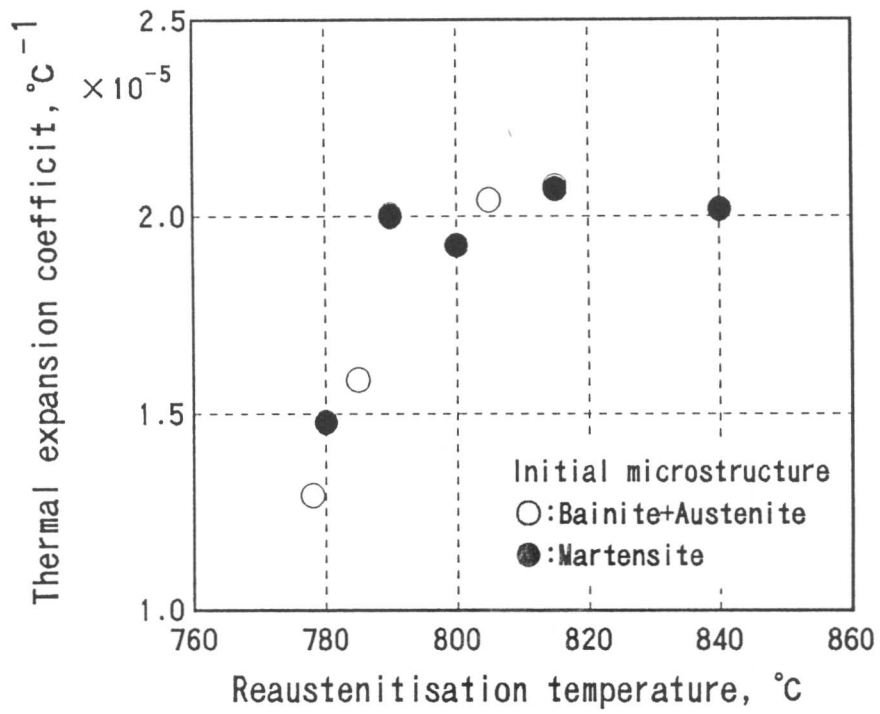


Fig. 6.23 Thermal expansion coefficient during cooling after 30 min of isothermal reaustenitisation from martensite as a function of reaction temperature.

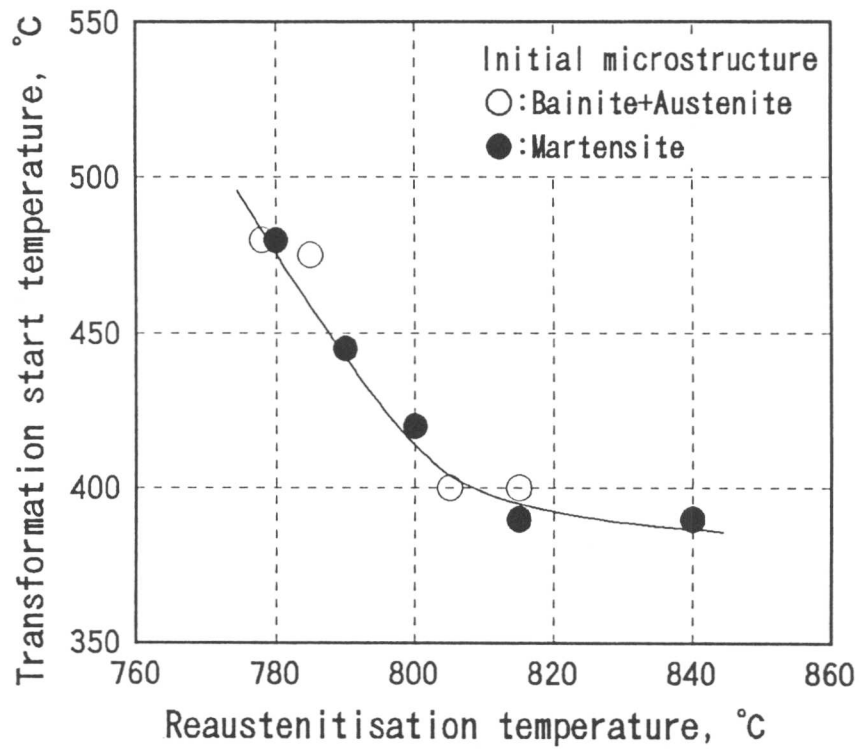


Fig. 6.25 Decomposition-start temperature during cooling after 30 min of isothermal reaustenitisation from martensite as a function of reaction temperature.

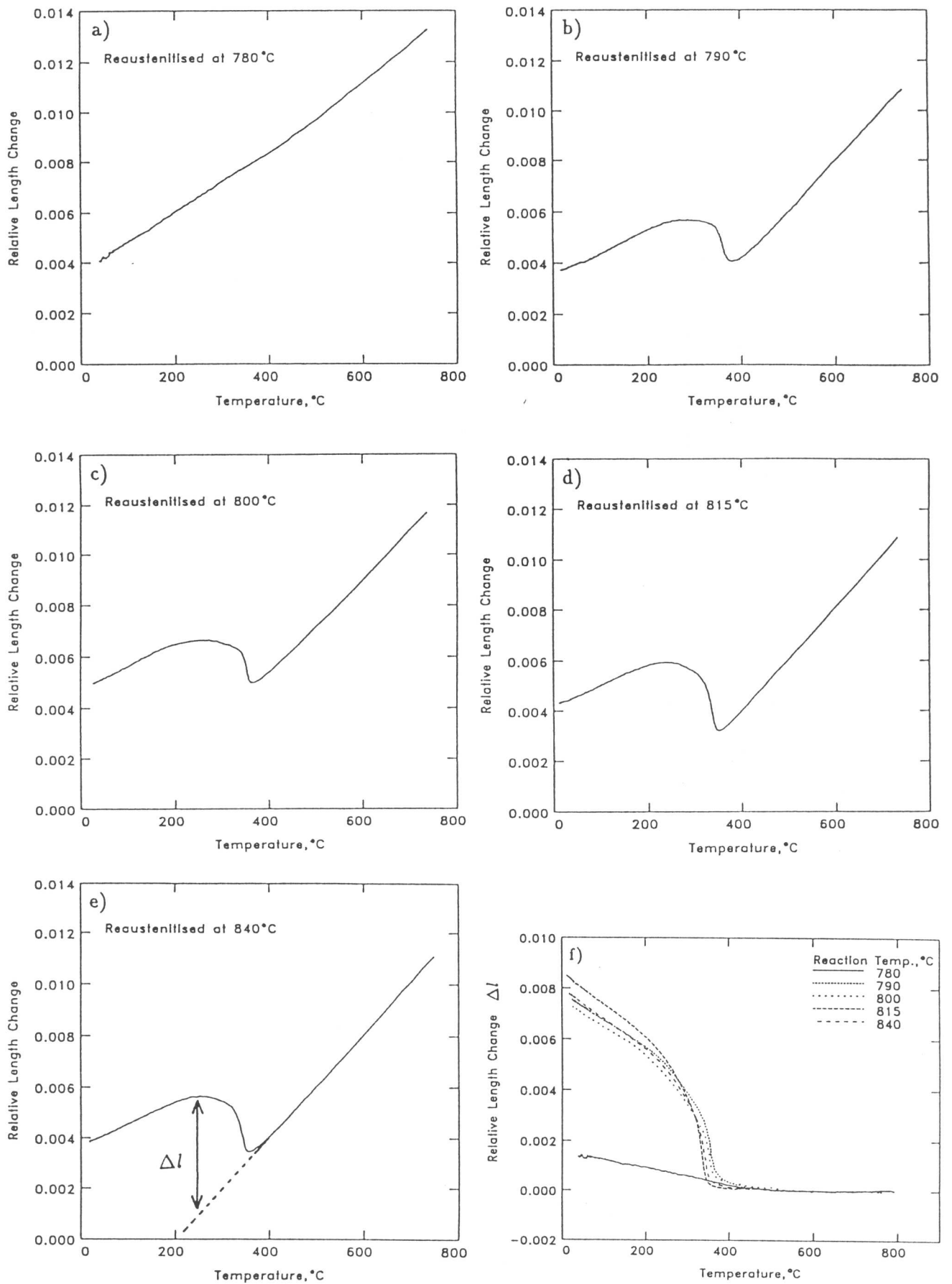


Fig. 6.24 Relative length change during helium quenching after 30 min of isothermal re-austenitisation at each temperatures.

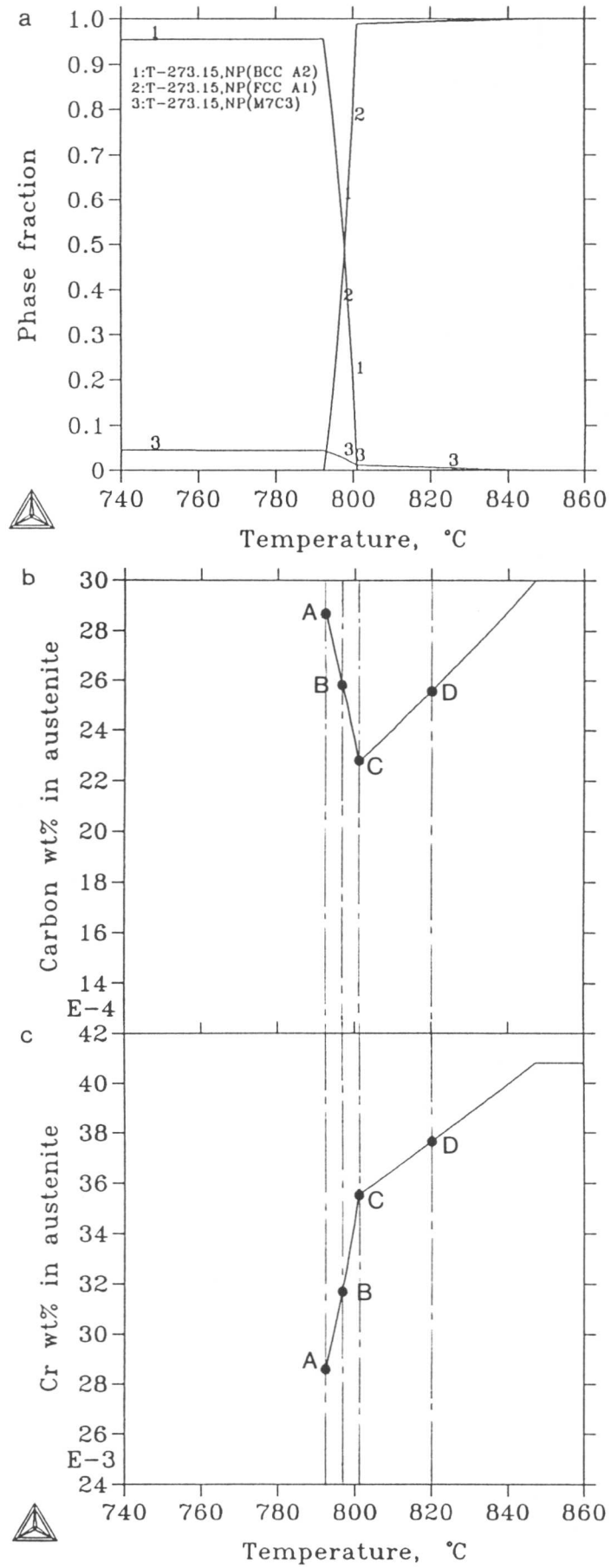


Fig. 6.26 Calculated phase boundaries and chemical compositions in austenite formed at intercritical temperatures. Calculation was carried out using "Thermo-Calc".

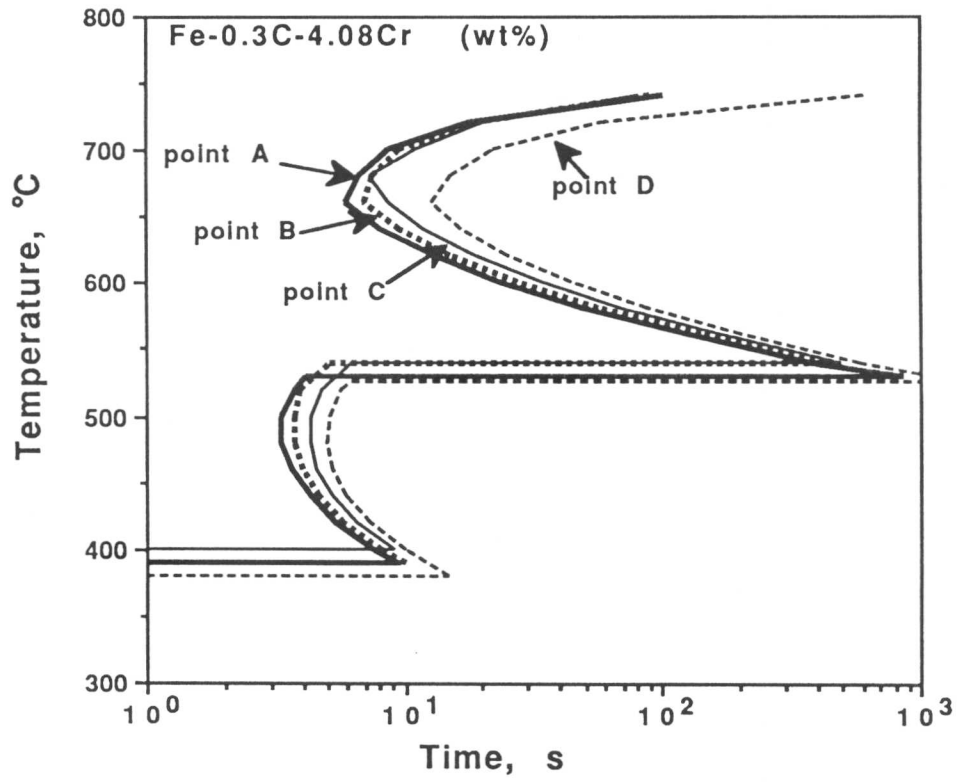


Fig. 6.27 Calculated TTT curves for austenite formed at points *A*, *B*, *C* and *D* in Fig. 6.28.

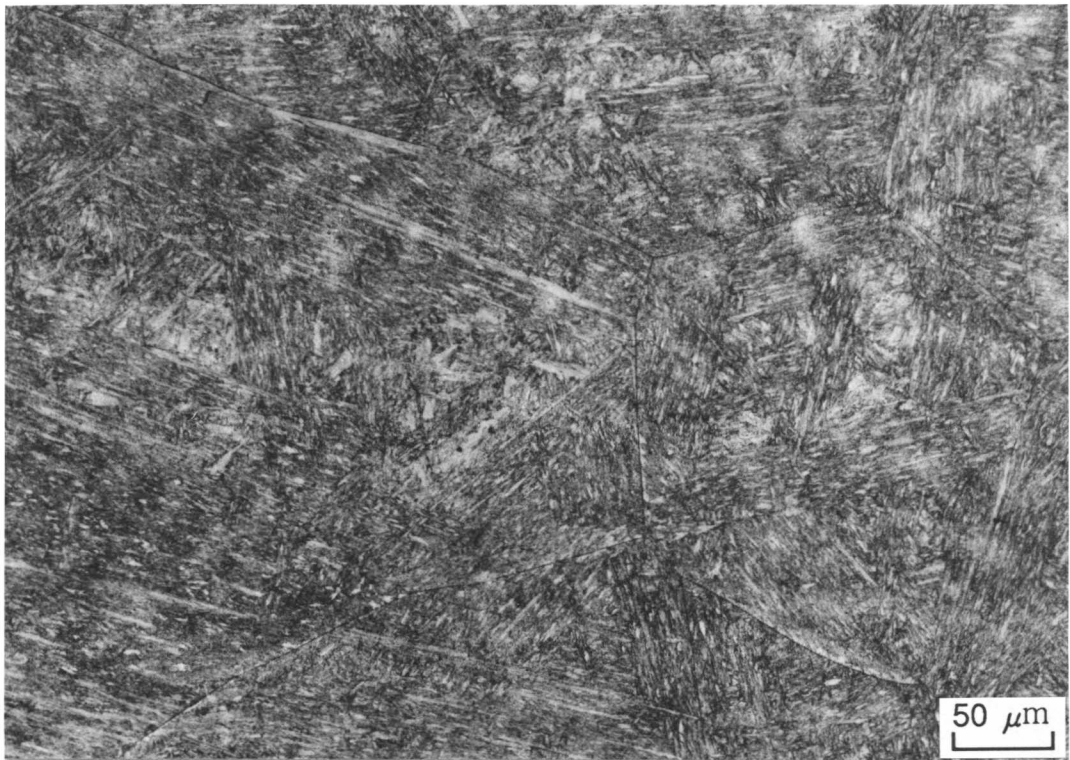


Fig. 6.28 Optical micrograph of a specimen water quenched after tempering of martensite at 500°C for 17 hours in the Fe-0.3C-4.08Cr wt.% alloy.

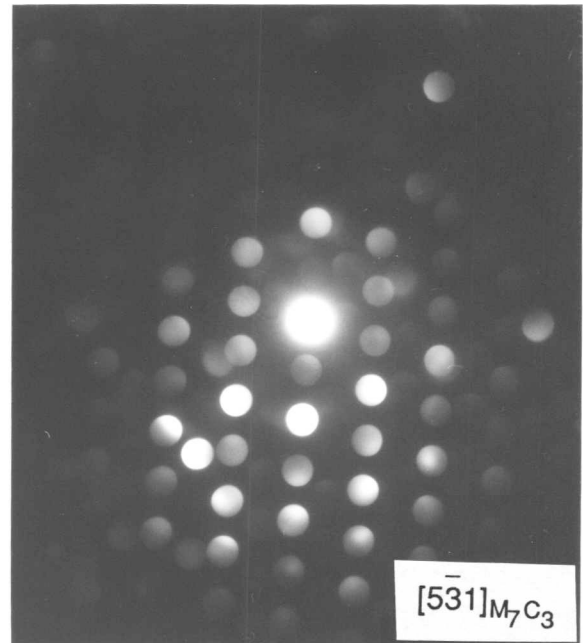
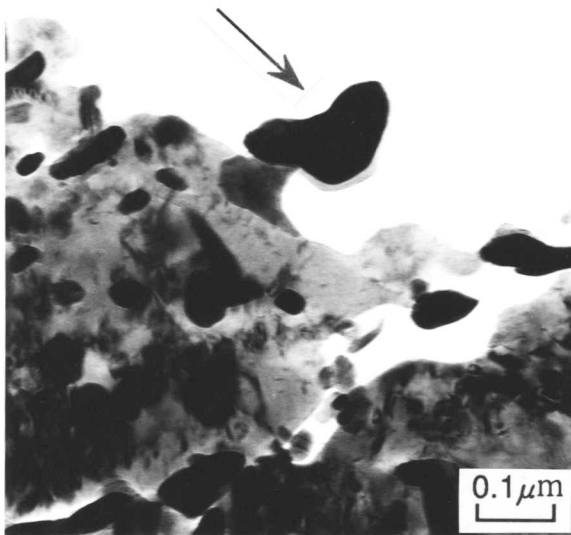
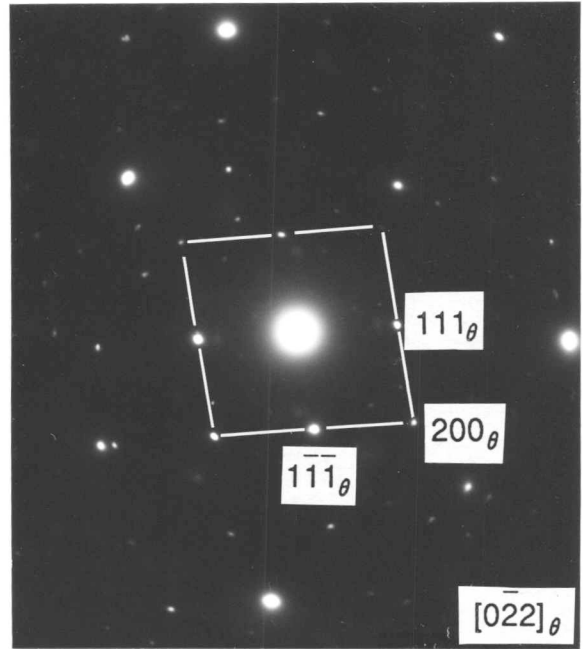
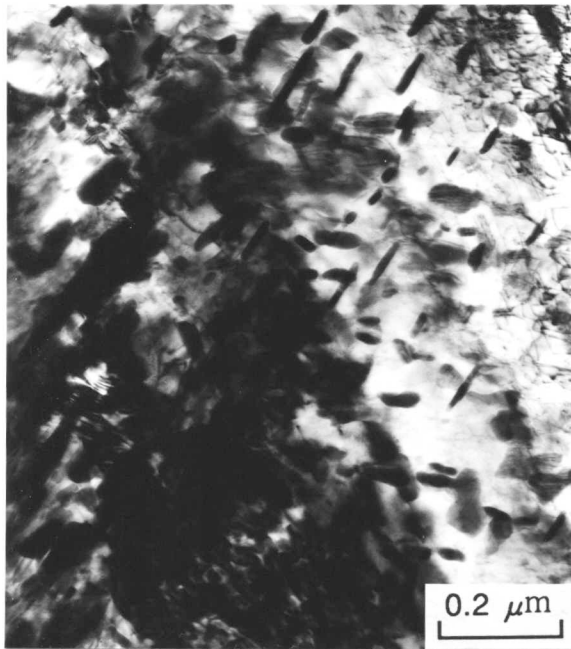


Fig. 6.29 TEM bright field images of a specimen water quenched after tempering of martensite at 500 °C for 17 hours in the Fe-0.3C-4.08Cr wt.% alloy.

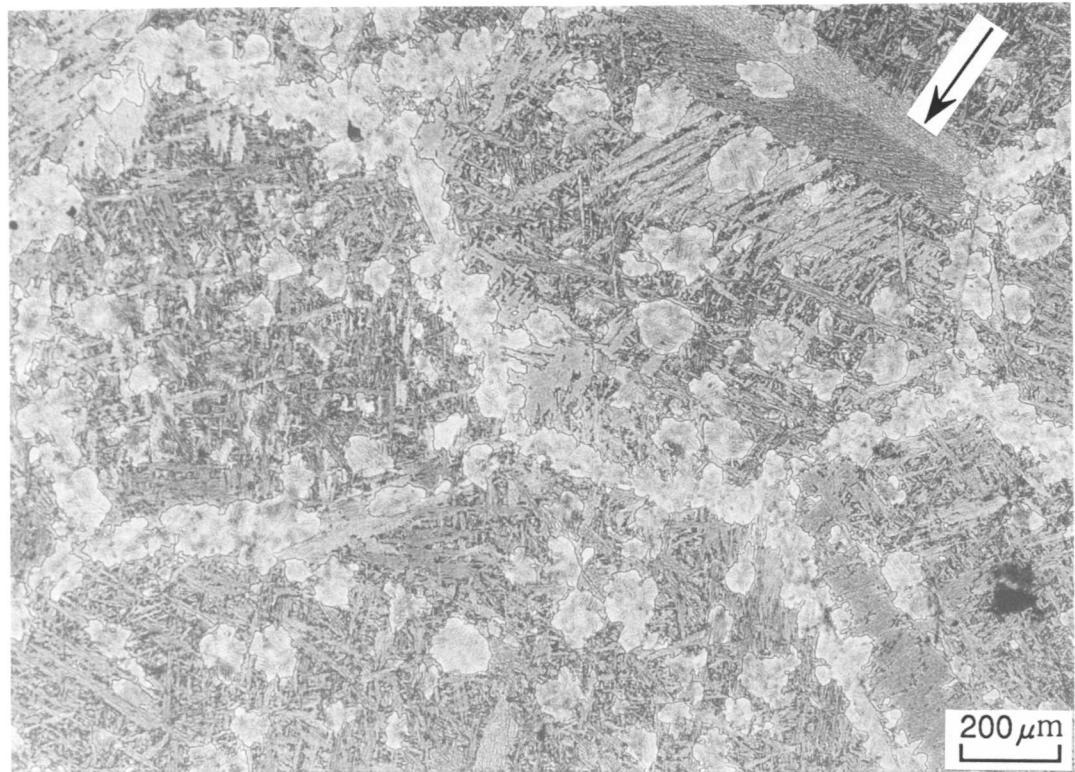


Fig. 6.30 Optical micrograph of a specimen helium quenched after 30 min of isothermal re-austenitization from tempered martensite at 784 °C in the Fe-0.3C-4.08Cr wt.% alloy.



Fig. 6.31 Optical micrograph of a specimen water quenched after tempering of martensite at 700 °C for 51 hours.

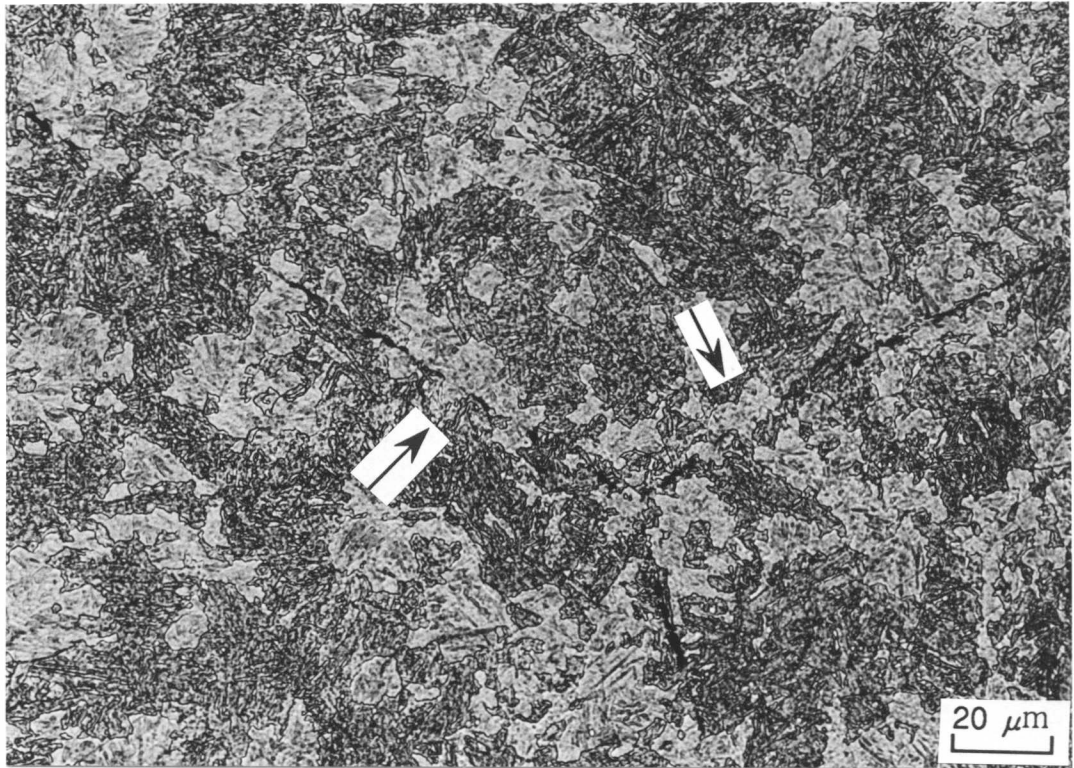


Fig. 6.32 Optical micrograph of a specimen helium quenches after 30 min of isothermal reaustenitisation from tempered martensite, which was obtained at 700 °C, at 785 °C.



Fig. 6.33 TEM bright field image of a specimen helium quenches after 30 min of isothermal reaustenitisation from tempered martensite, which was obtained at 700 °C, at 785 °C.

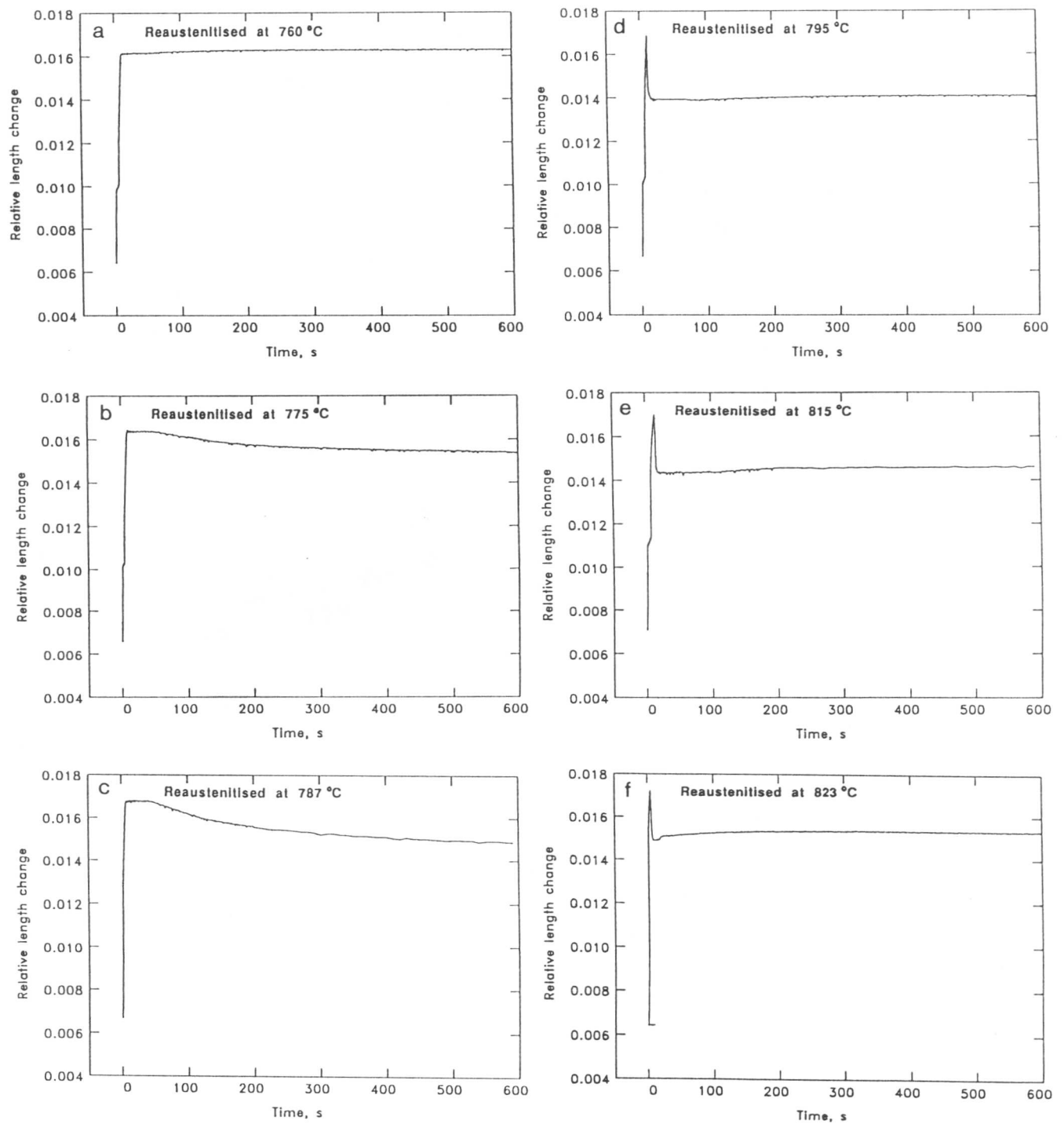


Fig. 6.34 Relative length change during 30 min of isothermal re-austenitisation from tempered martensite which was obtained at 500 °C.

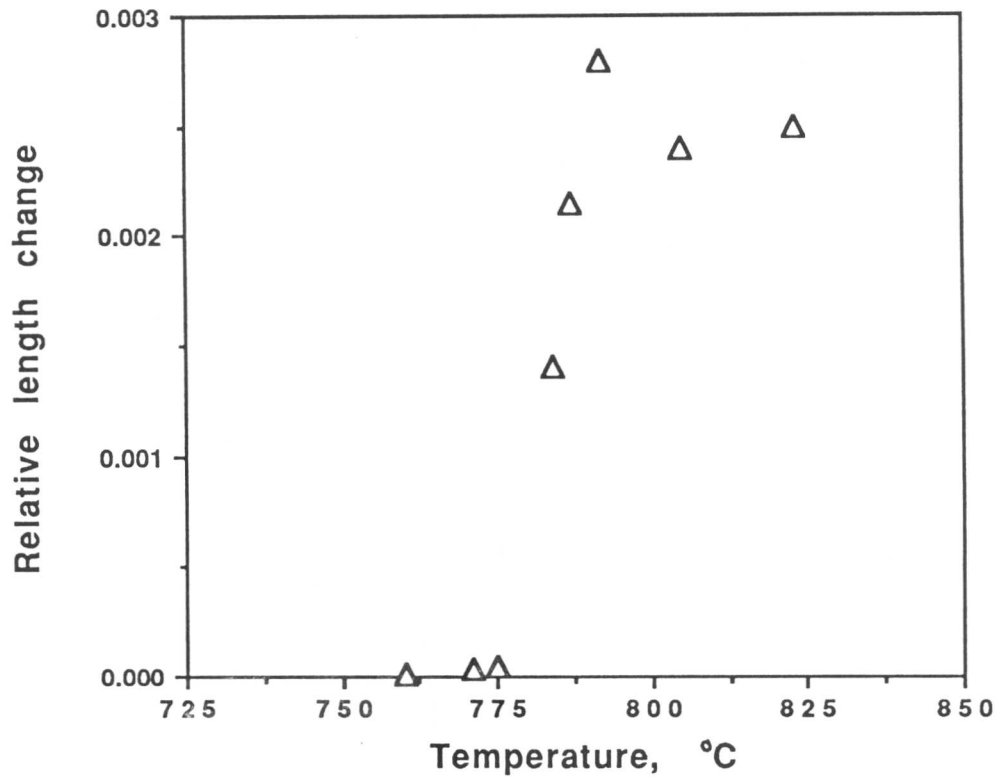


Fig. 6.35 Maximum relative length changes during 30 min of isothermal re-austenitisation from tempered martensite which was obtained at 500°C.

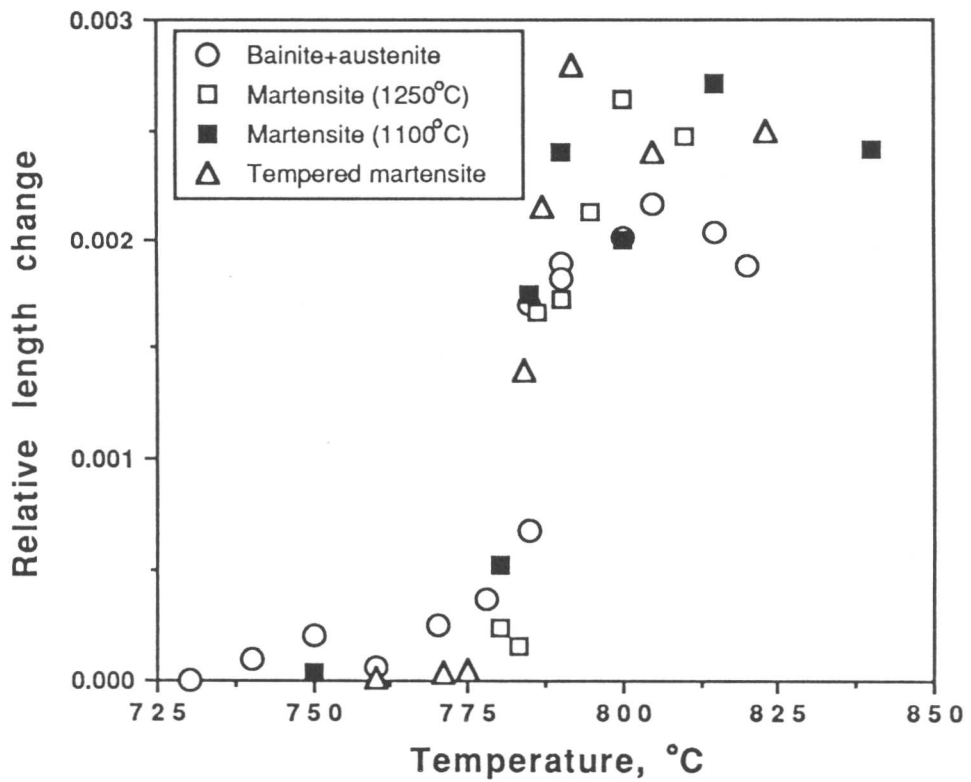


Fig. 6.36 Maximum relative length changes during 30 min of isothermal re-austenitisation from martensite, from the mixture of bainite and austenite, and from tempered martensite at 500°C in the Fe-0.3C-4.08Cr wt.% alloy.

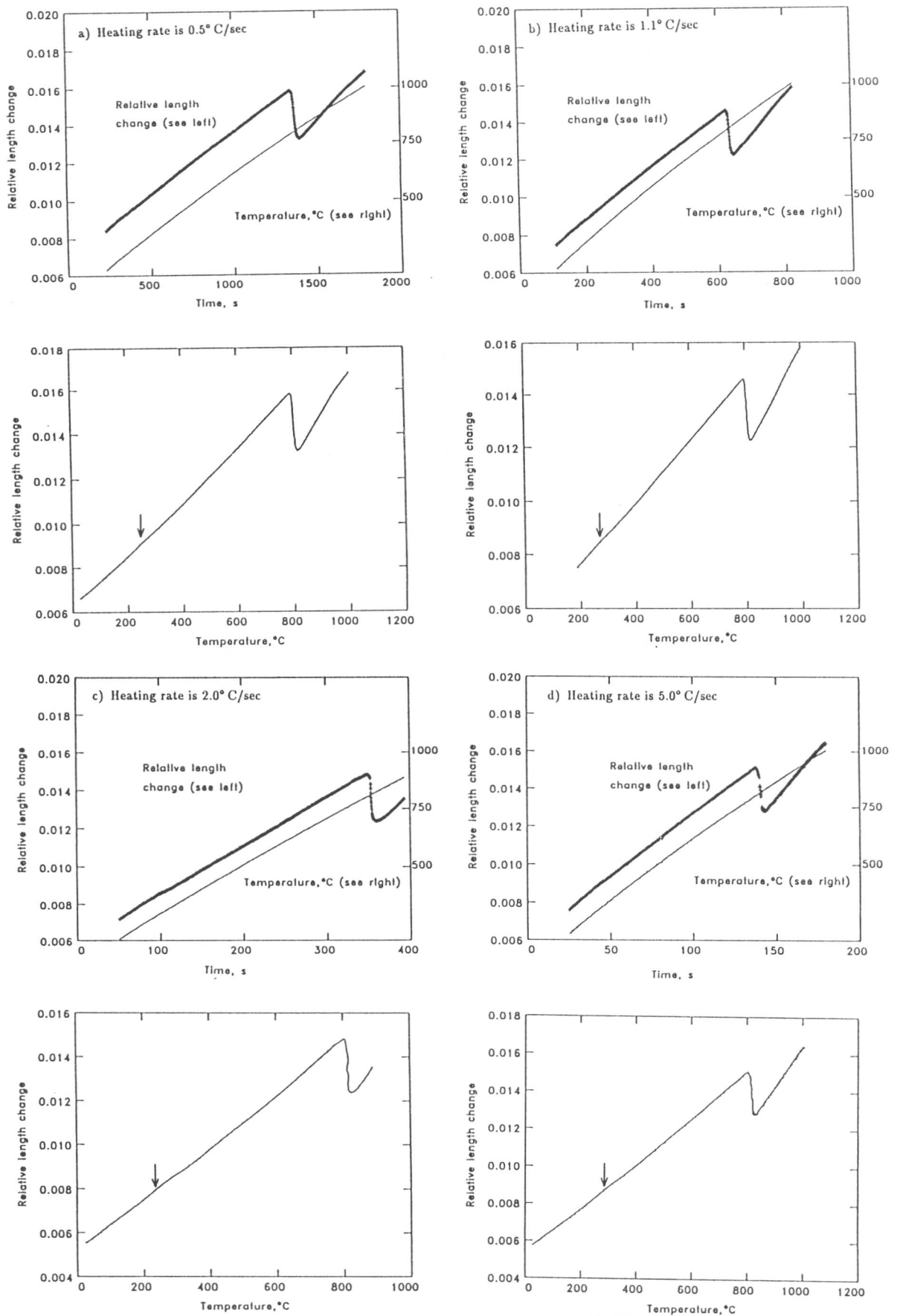


Fig. 6.37 Relative length changes during continuous heating at constant heating rates from the martensitic initial microstructure.

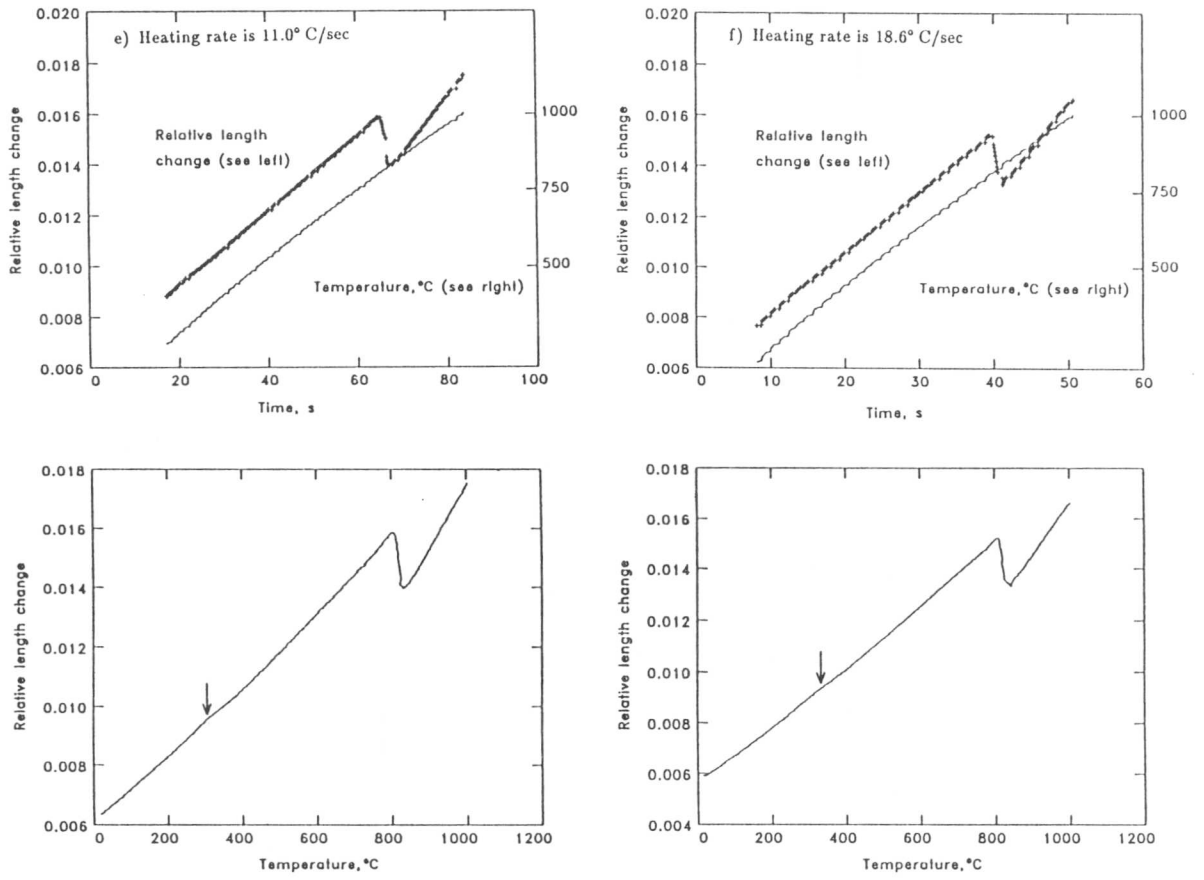


Fig. 6.37 (continued)

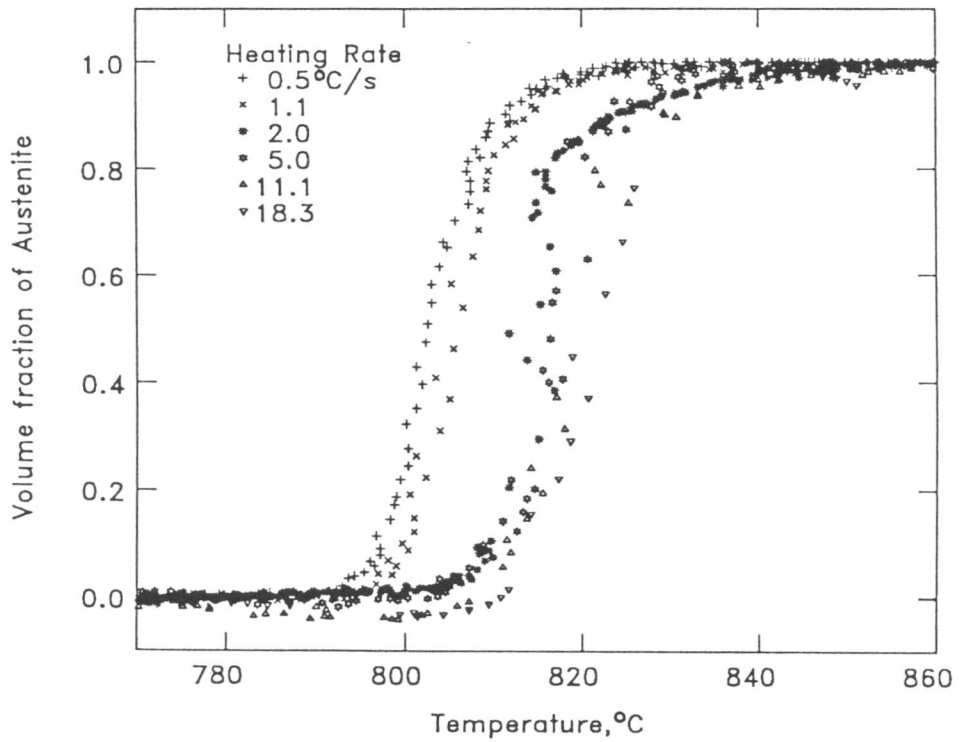


Fig. 6.38 Overall reaustenitisation behaviour during heating at constant heating rate from the martensitic initial microstructure.

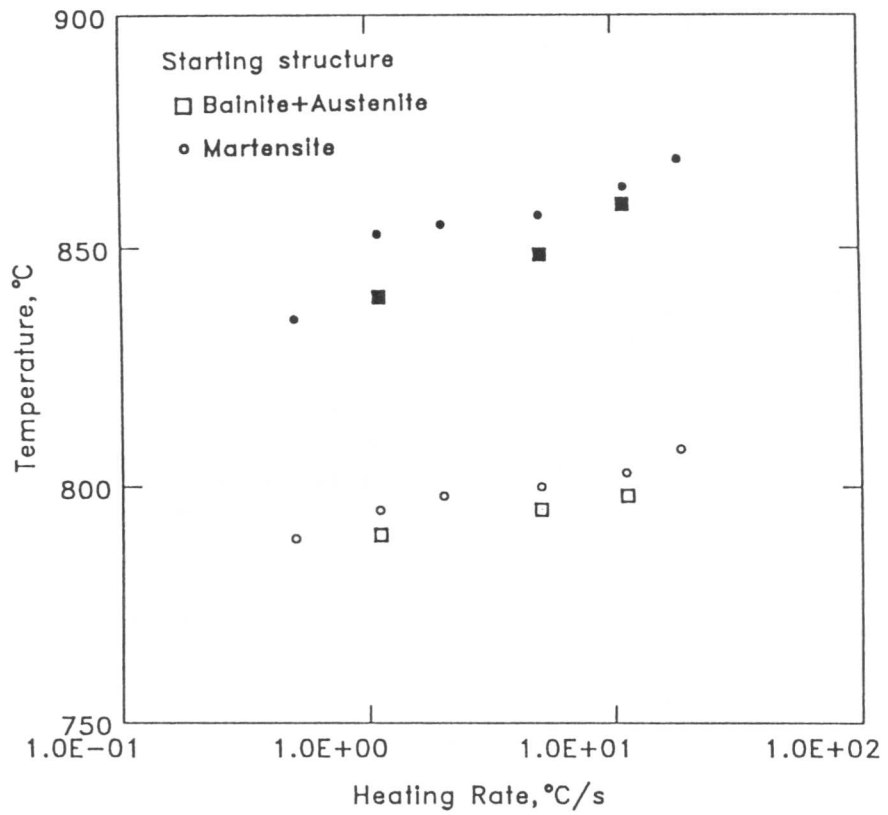


Fig. 6.39 Effect of heating rate on transformation-start and -finish temperatures during continuous heating at constant heating rates from the martensitic initial microstructure.

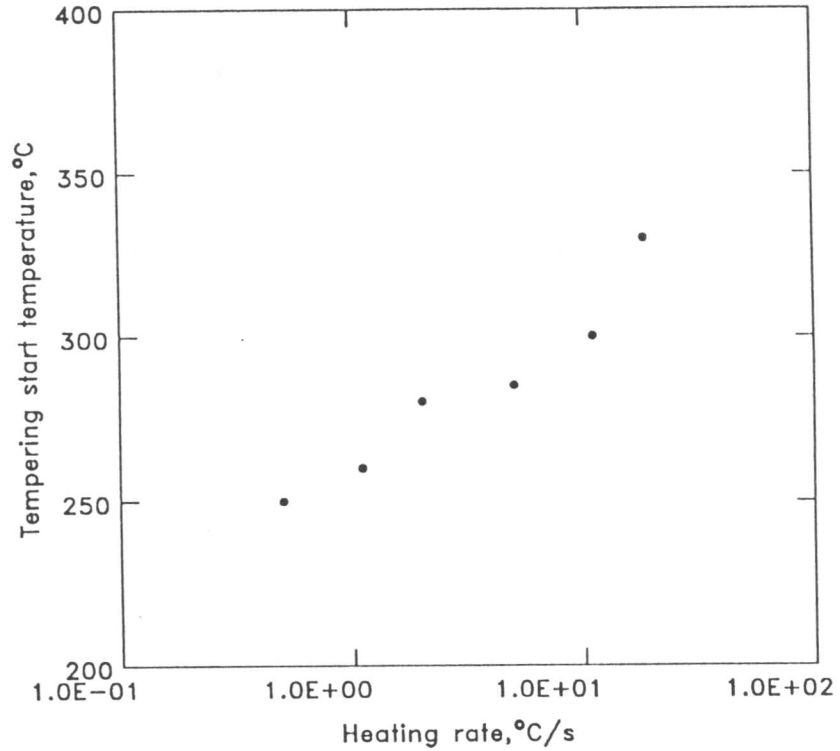


Fig. 6.40 Effect of heating rate on temperature at which tempering of martensite starts during continuous heating re-austenitisation from martensite.

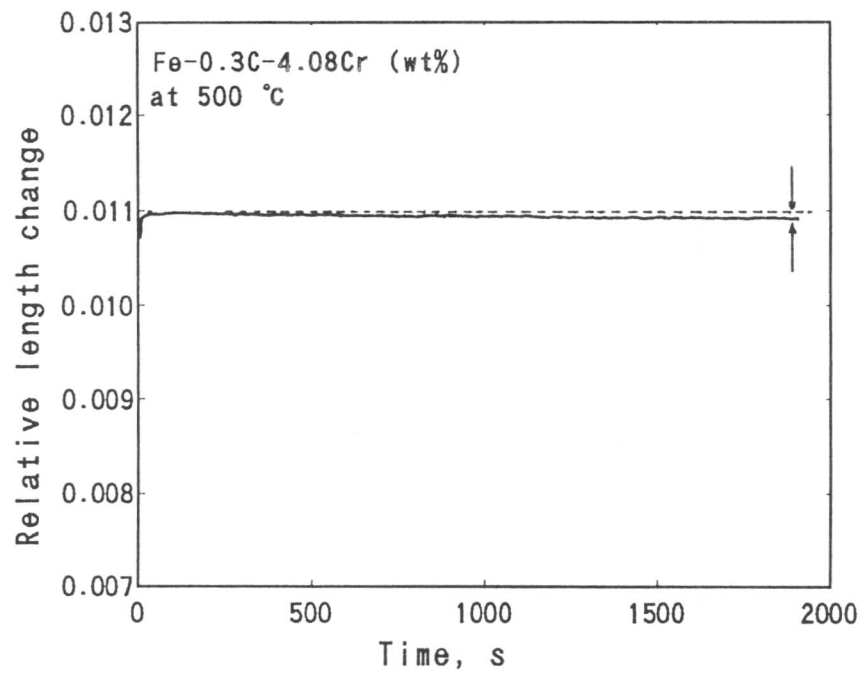


Fig. 6.41 Relative length change during 30 min of isothermal tempering of martensite at 500 °C.

CHAPTER 7

THERMODYNAMICS OF REAUSTENITISATION IN TERNARY ALLOYS

7.1 INTRODUCTION

The conditions which exist at the transformation interface during the growth of ferrite from austenite in steels have been discussed in much more detail than is the case for the reverse transformation from ferrite to austenite. The thermodynamic theory which has been developed for the decomposition of austenite should in principle be adaptable for the reverse transformation, but as will be seen later, there are some important differences which need to be taken into account.

The thermodynamics of the reconstructive formation of ferrite from austenite will be summarised first in order to summarise the techniques available for handling transformation in ternary steels, and an attempt will then be made to deduce a similar framework for the reverse transformation processes.

7.2 RECONSTRUCTIVE FORMATION OF FERRITE FROM AUSTENITE

Ferrite formation is expected to occur when austenite is cooled down below the equilibrium $\gamma/(\alpha + \gamma)$ transformation temperature Ae_3 . It is well established that it is possible to obtain various kinds of transformation products, whose mechanism of transformation may be different, depending on a level of supercooling below the equilibrium transformation temperature. The key characteristics of these transformation products in steels have been summarised by Bhadeshia [1].

7.2.1 Reconstructive growth of ferrite in multi-component systems

Since the main interest here is the reconstructive formation of austenite, we begin with a summary of the thermodynamics dealing with the reconstructive transformation of austenite to ferrite in multi-component systems, with a view to using some of the principles for the reverse case.

In multi-component steels, a variety of different modes of equilibrium can be maintained locally at the moving transformation interface because of the existence of a remarkable difference in the diffusivities of interstitial atoms and substitutional alloying elements in iron [2-13]. These modes can be classified into three categories; 1) partitioning local equilibrium (PLE) 2) negligible local equilibrium (NPLE) and 3) paraequilibrium (PE).

In a system such as Fe-C-X, the diffusion rate of carbon in the austenite may be as much as $10^7 - 10^9$ times greater than that of a substitutional atom in the temperature range of interest. These very different rates of atomic migration mean that true equilibrium segregation with regard to all components may not be produced at a migrating interface. It is, however, possible to envisage growth under diffusion control with local equilibrium at the interface in the sense that the compositions of two phases at the interface are related by a tie line of the equilibrium diagram, even though this tie line may not pass through the point representing the initial (or average) composition of the alloy. When these kinetic restrictions apply, the two phases may differ either significantly or negligibly in substitutional solute content. A qualitative analysis for ternary steels was first developed by Hillert [5], and a simplified quantitative theory in which diffusion cross terms are neglected was developed by Kirkaldy [6], Purdy *et al.* [7] and Coates

[10]; the effect of the cross terms was later examined by Coates [11,12]. The simple theory shows that for the diffusion-controlled growth of ferrite from austenite in an Fe-C-X alloy with initial composition near the $\gamma/(\alpha + \gamma)$ phase boundary (*i.e.* with a small supersaturation), the tie line selected will have the carbon composition of austenite at the interface almost equal to that of the bulk alloy so that the activity of carbon is nearly constant in the austenite, thus reducing the driving force for carbon diffusion almost to zero. There will be a concentration gradient of the substitutional solute ahead of the interface, resulting in appreciable partition, and the relatively slow growth rate will be determined by the diffusion rate of this solute (Fig. 7.1a). For large supersaturations, the tie line will have the Fe+X composition of the ferrite virtually identical with that of the bulk austenite, and partitioning of the substitutional solute will be extremely small, with a relatively fast growth rate (Fig. 7.1b). These are referred to as the partitioning local equilibrium (PLE) and negligible partitioning local equilibrium (NPLE) growth modes [7,11,12], and for a high ratio of the diffusivities, the theory predicts an abrupt transition from one to the other as the supersaturation increases.

In the NPLE mode, the concentration of the substitutional alloying element is uniform except for a small “spike” in the parent phase adjacent to the interface. As the ratio of interstitial and substitutional diffusion rates increases, the width of this spike decreases, and when it becomes of the order of atomic dimension, the concept of local equilibrium at the interface is invalid and has to be replaced (assuming the growth is nevertheless diffusion-controlled) by that of paraequilibrium [5,2,3,8,9]. In conditions of paraequilibrium, there is no redistribution of Fe + X atoms between the phases, the Fe/X ratio remaining uniform right up to the interface. One interpretation of the paraequilibrium limit is that reconstructive transformation occurs with all displacements of the Fe+X atoms taking place in the incoherent interface; another interpretation might be that only displacive transformation can occur. In either case, to quote from Coates [10], “the slow diffuser and the solvent participate only in the change of crystal structure”. Paraequilibrium implies that the growth rate is controlled by the interstitial diffusivity, the interface compositions now being given by the tie lines of the pseudoequilibrium between the two phases under the constraint of a constant Fe/X ratio.

7.2.2 Calculation of tie lines for reconstructive formation of ferrite in ternary systems

For simplification, a ternary system Fe-C-X, where C and X denote respectively carbon and a substitutional alloying element, will be discussed in this section to demonstrate briefly the way to calculate tie lines and the growth rate of the product phase in different equilibrium modes. The bulk composition of austenite is designated $(\bar{x}_1^\gamma, \bar{x}_2^\gamma)$, and the interface compositions, which will be determined in the manner discussed below, are $x_1^{\gamma\alpha}$, $x_1^{\alpha\gamma}$, $x_2^{\gamma\alpha}$, and $x_2^{\alpha\gamma}$, where the subscripts denote carbon and the substitutional alloying element concentrations respectively, and the superscripts $\gamma\alpha$ and $\alpha\gamma$ represent respectively the interface compositions in austenite (γ) and in ferrite (α) which are in equilibrium.

Because the reaction is now controlled by the diffusion of both carbon and the substitutional alloying element, Fick’s Law for both species has to be solved simultaneously. The one-dimensional diffusion equations in austenite are expressed as follows. (Note that the concept can easily be extended to two and three dimensional problems: see for example [11,12]):

$$\frac{\partial x_1^\gamma}{\partial t} = \frac{\partial}{\partial z} \left(D_{11}^\gamma \frac{\partial x_1^\gamma}{\partial z} \right) + \frac{\partial}{\partial z} \left(D_{12}^\gamma \frac{\partial x_2^\gamma}{\partial z} \right) \quad (7.1)$$

$$\frac{\partial x_2^\gamma}{\partial t} = \frac{\partial}{\partial z} \left(D_{22}^\gamma \frac{\partial x_2^\gamma}{\partial z} \right) + \frac{\partial}{\partial z} \left(D_{21}^\gamma \frac{\partial x_1^\gamma}{\partial z} \right) \quad (7.2)$$

where z is the space co-ordinate normal to the transformation interface, D_{11}^γ and D_{22}^γ are the interdiffusion coefficients of carbon and X in austenite respectively, and D_{12}^γ and D_{21}^γ are the cross interdiffusion coefficients in the ternary system taking account of the dependence of the flux of one alloy element on the concentration gradient of another. Since the product phase is here assumed to grow with a constant composition, it is necessary only to consider the diffusion equations within the parent austenite phase.

The requirement of mass conservation at the interface is expressed by the following two equations

$$(x_1^{\gamma\alpha} - x_1^{\alpha\gamma})v = J_1|_{z=z^*} \quad (7.3)$$

$$(x_2^{\gamma\alpha} - x_2^{\alpha\gamma})v = J_2|_{z=z^*} \quad (7.4)$$

where v is the growth rate of the product phase, z^* is the position of the moving interface along the space co-ordinate z , and the fluxes of carbon and X at the moving interface, $J_1|_{z=z^*}$ and $J_2|_{z=z^*}$, are expressed by

$$J_1|_{z=z^*} = -D_{11}^\gamma \frac{\partial x_1^\gamma}{\partial z} \Big|_{z=z^*} - D_{12}^\gamma \frac{\partial x_2^\gamma}{\partial z} \Big|_{z=z^*} \quad (7.5)$$

$$J_2|_{z=z^*} = -D_{22}^\gamma \frac{\partial x_2^\gamma}{\partial z} \Big|_{z=z^*} - D_{21}^\gamma \frac{\partial x_1^\gamma}{\partial z} \Big|_{z=z^*} \quad (7.6)$$

where the differentiations should be taken at the interface.

The four interface compositions in the mass conservation equations are the components of two ends of the tie line in an isothermal section of the ternary equilibrium phase diagram at the reaction temperature of the system concerned. As has been discussed (for example see [11,12]), only one of them is independent given equilibrium since the chemical potentials of the species have to be identical in the phases concerned, giving the additional equations:

$$\mu_i^\alpha = \mu_i^\gamma; i = 0, 1, 2 \quad (7.7)$$

where i 's ($i=0,1$ and 2) correspond to iron, carbon and X respectively. Therefore the two mass conservation equations contain only two independent variables, one of which represents compositions at the interface, and the other the growth rate of the product phase. A unique solution can therefore be obtained from these equations.

When the supersaturation is low (*i.e.* at higher temperatures in the $\alpha + \gamma$ two phase field where the bulk concentration is close to the γ phase field), the PLE condition will be maintained at the interface (see Fig. 7.1a). In order to get a reduced driving force for carbon diffusion in austenite, the interface compositions in austenite are determined by the intersection between the carbon isoactivity line passing through the bulk composition (point **A** in Fig. 7.1a) and the $\gamma/(\gamma + \alpha)$ phase boundary. The other end of the tie line is then obtained via equations 7.7.

On the other hand at relatively higher supersaturations (NPLE) where the bulk alloy composition is close to the α phase field, the tie line is fixed by the intersection between a horizontal line ($x = \bar{x}_2^\gamma$) which passes through the bulk composition (point **B** in Fig. 7.1b) and

the $\alpha/(\alpha + \gamma)$ phase boundary, making the extent of partitioning of X effectively negligible and hence increasing its gradient in the austenite and allowing its flux to keep up with that of carbon. The other end of the tie line is again obtained from equations 7.7.

The intersection of two lines, one of which is the horizontal line passing through the ferrite end of the tie line, and the other is the carbon isoactivity line in austenite passing through the austenite end of the tie line, form the transition line between the PLE to the NPLE modes of growth. When the bulk composition is on the left hand side of the transition line, the NPLE condition will be maintained, whereas the PLE condition will otherwise be achieved (Fig. 7.1a,b).

Although the method discussed above is convenient for discussion, the required rigorous solution (*i.e.* the interface compositions and the growth rate) can be obtained only when the five equations, two of which are the mass conservation conditions at the moving interface and the others the equilibrium equations, are solved simultaneously.

7.3 THERMODYNAMICS OF REAUSTENITISATION

Austenite can be expected to form when steels which contain ferrite, carbide, austenite and their combinations, are heated to a temperature in the $\alpha + \gamma$ two phase region or into the austenite single phase field. When the reaction temperature is raised; *i.e.* the supersaturation is increased, the mobility of atoms also increases. This contrasts with transformation to ferrite from austenite, in which atomic mobility decreases as supercooling increases. Consequently, during austenite formation, the mechanism of transformation is likely to be reconstructive, especially for low alloy steels, whereas the tendency to form ferrite by displacive transformation increases as the undercooling is increased.

7.3.1 Local equilibrium conditions during reaustenitisation

In the case of reaustenitisation in steels, local equilibrium has been usually assumed to exist at the interface between austenite precipitate and ferrite matrix (see for example [14-16]), although Ågren suggested the possibility of partitionless transformation of ferrite to austenite at very high temperatures (higher than 847° C) in Fe-1.5 wt.% Mn system [16].

Assuming local equilibrium, when the reaction temperature is low (low supersaturation), the growth of austenite may be expected to occur by a PLE mechanism, and by the NPLE mechanism at relatively higher supersaturations. The procedure has been discussed qualitatively by Hillert [17]; to calculate the operative tie lines requires a model for the ferrite and austenite solid solution and the dilute solution, the Wagner interaction parameter method is adopted below. The transition line from the PLE to the NPLE condition in an isothermal section of the ternary equilibrium phase diagram is expressed by the line **RQ** instead of **PS** (Fig. 7.2), which is the transition line for the *decomposition* process of austenite [17].

When a steel, which is initially fully ferritic (*i.e.* a low carbon steel), is superheated to an intercritical temperature, it might be a good assumption that local equilibrium will be maintained at the interfaces between austenite and ferrite matrix, because of the high mobility of alloying elements at that temperature. In order to simplify the discussion, attention is focused initially on the reconstructive formation of austenite under conditions of local equilibrium, in a ternary alloy Fe-C-X. When the bulk composition of the steel (see point **I**{ \bar{x}_1, \bar{x}_2 } in Fig. 7.3) at the temperature T is in the NPLE condition (region **RQS** in Fig. 7.3), the operative tie line can be obtained as follows. In the NPLE mode, the gradient of X in the parent phase must be large: this can be achieved by allowing $x_2^{\gamma\alpha} \rightarrow \bar{x}_2$. One end of the tie line is, therefore,

obtained as the intersection of the $\gamma/(\alpha + \gamma)$ phase boundary and a horizontal $x_2 = \bar{x}_2$ line, which gives the point $\{x_1^{\gamma\alpha}, x_2^{\gamma\alpha}\}$ designated “**A**” in Fig. 7.3. The other end of the tie line follows automatically as the point **B** $\{x_1^{\alpha\gamma}, x_2^{\alpha\gamma}\}$ (Fig. 7.3), from the fact that for a tie line,

$$\mu_i^{\alpha\gamma} = \mu_i^{\gamma\alpha}; i = 0, 1, 2. \quad (7.8)$$

Kirkaldy and his co-workers [18-20] have used dilute solution methods to calculate the tie lines in multi-component systems. The requirement of identical chemical potentials both in austenite and in ferrite at the interface, leads to the approximation [18].

$$\frac{\Delta G_i^{0\alpha\rightarrow\gamma}}{RT} = \ln \frac{x_i^\alpha}{x_i^\gamma} + \ln \frac{\Gamma_i^\alpha}{\Gamma_i^\gamma}; i = 0, 1, 2 \quad (7.9)$$

where $\Delta G_i^{0\alpha\rightarrow\gamma}$ is the standard free energy change between α and γ for each element, and Γ_i are the activity coefficients for each of the elements, given by,

$$\ln \Gamma_1 = \epsilon_{11}x_1 + \epsilon_{12}x_2 \quad (7.10)$$

$$\ln \Gamma_2 = \epsilon_{12}x_1 + \epsilon_{22}x_2 \quad (7.11)$$

$$\ln \Gamma_0 = -\frac{\epsilon_{11}}{2}x_1^2 - \epsilon_{12}x_1x_2 - \frac{\epsilon_{22}}{2}x_2^2. \quad (7.12)$$

where ϵ_{ij} are empirical coefficients known as the Wagner interaction parameters. Therefore, from the fact that the alloying element concentration in austenite at the interface is identical to that of the bulk, it is possible to calculate the interfacial compositions (points **A** and **B** in Fig. 7.3) which satisfy the thermodynamic equations listed above, simultaneously. Then one can obtain the point **M** $\{x_1^T, x_2^T\}$ on the transition line **RQ** (Fig. 7.3), which is the intersection of the isoactivity line of carbon in ferrite passing through the point **B**, and the constant substitutional alloying element line **IA**. † The activity of carbon at the points **B** and **M** (a_B and a_M respectively) in a dilute ternary system are given as follows, ignoring the higher-order terms of the expansion [21]:

$$\ln a_B^c = \ln x_1^{\alpha\gamma} + \epsilon_{11}x_1^{\alpha\gamma} + \epsilon_{12}x_2^{\alpha\gamma}$$

$$\ln a_M^c = \ln x_1^T + \epsilon_{11}x_1^T + \epsilon_{12}x_2^T.$$

Using these two equations, and by ignoring the small difference between the products $\epsilon_{11}x_1^{\alpha\gamma}$ and $\epsilon_{11}x_1^T$, we obtain

$$\ln x_1^T = \ln x_1^{\alpha\gamma} + \epsilon_{12}x_2^{\alpha\gamma} - \epsilon_{12}x_2^T. \quad (7.13)$$

On replacing x_2^T by \bar{x}_2 , x_1^T can be calculated given the interface compositions $x_1^{\gamma\alpha}$ and $x_2^{\alpha\gamma}$. Because the bulk composition is now in the NPLE region, it should be noted that $x_1^T < \bar{x}_1$.

In the case of the PLE condition, in contrast, it is expected that $x_1^T > \bar{x}_1$. The following method is used in order to determine the tie line in this situation. When the bulk composition of ferrite is in the PLE region (see point **K** $\{\bar{x}_1, \bar{x}_2\}$ in Fig. 7.4), it is necessary to ensure that the gradient of carbon in the parent phase is reduced to a level consistent with the sluggishness of X element diffusion. This can be done by ensuring that the carbon isoactivity line in ferrite passes

† Note that **IA** is not strictly parallel to the carbon axis since it is really the ratio of Fe/X atoms is constant along **IA**.

through the bulk composition \mathbf{K} ; the intersection of that isoactivity line with the $\alpha/(\alpha + \gamma)$ phase boundary (see point $\mathbf{B}\{x_1^{\alpha\gamma}, x_2^{\alpha\gamma}\}$ in Fig. 7.4), then defines the operative tie line.

However, when the phase boundary is to be determined simultaneously with the tie line, it is possible to use a more convenient method to calculate these values. It is noted that the operative tie line AB for the bulk composition \mathbf{K} is the NPLE tie line for an alloy whose bulk composition is same as the point \mathbf{M} in Fig. 7.4, which is an intersection between the transition line and the isoactivity line of carbon in ferrite passing through the bulk composition \mathbf{K} . Therefore the operative tie line AB can be obtained by finding the point \mathbf{M} and then calculating the NPLE tie line for the point.

First, one can calculate the point $\mathbf{G}\{x_1^T, x_2^{\alpha\gamma}\}$ corresponding to the point \mathbf{K} using equation 7.13 and the NPLE interface compositions determined for the bulk composition \mathbf{K} ; *i.e.* under the condition of $x_2^{\gamma\alpha} = \bar{x}_2$. Since the bulk composition is now in the PLE region, it is expected that $x_1^T > \bar{x}_1$. We now rename these points for simplicity: the bulk composition and the corresponding point \mathbf{G} are now called $\mathbf{K}_0\{\bar{x}_{1,0}, \bar{x}_{2,0}\}$ and $\mathbf{G}_0\{x_{1,0}^T, x_{2,0}^T\}$ respectively (Fig. 7.4b). In order to find the point \mathbf{M} effectively, a point $\mathbf{K}_1\{\bar{x}_{1,1}, \bar{x}_{2,1}\}$ on the isoactivity line of carbon in ferrite (*i.e.*, line \mathbf{BK}), which has a slightly higher alloying element composition than that of the bulk; *i.e.* $\bar{x}_{2,1} > \bar{x}_{2,0}$, is selected. And the corresponding point $\mathbf{G}_1(x_{1,1}^T, x_{2,1}^T)$ on the transition line is determined as mentioned above. Now one can estimate the point $\mathbf{G}_2(x_{1,2}^T, x_{2,2}^T)$ which may be close to the point \mathbf{M} using points $\mathbf{K}_0, \mathbf{K}_1, \mathbf{G}_0$ and \mathbf{G}_1 by the following equations:

$$\bar{x}_{2,i+1} = \frac{\bar{x}_{2,i-1}(x_{1,i}^T - \bar{x}_{1,i}) - \bar{x}_{2,i}(x_{1,i-1}^T - \bar{x}_{1,i-1})}{(x_{1,i}^T - \bar{x}_{1,i}) - (x_{1,i-1}^T - \bar{x}_{1,i-1})} \quad (7.14)$$

and

$$\bar{x}_{1,i+1} = \exp\{\ln \bar{x}_{1,1} + \epsilon_{12}\bar{x}_{2,1} - \epsilon_{12}\bar{x}_{2,i+1}\}. \quad (7.15)$$

The point \mathbf{M} is obtained by repeating this calculation until the difference between $\bar{x}_{1,i+1}$ and $x_{1,i+1}^T$ becomes smaller than the accuracy required. Then one can use exactly the same method to determine the tie line corresponding the point \mathbf{M} as was used for the determination of the tie line for the NPLE condition. This tie line is, in fact, the operative tie line for the bulk composition \mathbf{K} in Fig. 7.4.

7.3.2 Reconstructive growth of austenite under the local equilibrium

- starting from a mixture of ferrite and austenite of compositions \bar{x}_i^α and \bar{x}_i^γ

When the initial microstructure is a mixture of bainitic ferrite and austenite whose carbon concentration was determined by the T_0' curve at the bainite transformation temperature, tie lines for the local equilibrium mode can, in this case, also be determined using the method discussed above. The chemical distributions in both phases are, however, different from those in the case of reaustenitisation from a fully ferritic sample. Since the initial carbon and X concentrations in austenite are different from those at the interface, fluxes of carbon and X in austenite are also expected to exist. Illustrative chemical distributions are shown with an isothermal section of the equilibrium phase diagram in Fig. 7.5 and Fig. 7.6.

As mentioned in the previous section, rigorous solutions of the interface compositions and the growth rate of the product phase (*i.e.* austenite), can be obtained only when the mass conservation equations are solved giving the growth rate of the product phase which satisfies the equilibrium conditions at the interface.

Because there are now diffusional fields both in the matrix (*i.e.* ferrite) and in the product (*i.e.* austenite) phases, it is necessary to handle the diffusion equations in both phases, in a way which satisfies the mass conservation conditions at the interface. The one-dimensional diffusion equations in the ferrite matrix and austenite precipitate phase are expressed as follows.

$$\frac{\partial x_1^\gamma}{\partial t} = \frac{\partial}{\partial z} \left(D_{11}^\gamma \frac{\partial x_1^\gamma}{\partial z} \right) + \frac{\partial}{\partial z} \left(D_{12}^\gamma \frac{\partial x_2^\gamma}{\partial z} \right) \quad (7.16)$$

$$\frac{\partial x_2^\gamma}{\partial t} = \frac{\partial}{\partial z} \left(D_{22}^\gamma \frac{\partial x_2^\gamma}{\partial z} \right) + \frac{\partial}{\partial z} \left(D_{21}^\gamma \frac{\partial x_1^\gamma}{\partial z} \right) \quad (7.17)$$

$$\frac{\partial x_1^\alpha}{\partial t} = \frac{\partial}{\partial z} \left(D_{11}^\alpha \frac{\partial x_1^\alpha}{\partial z} \right) + \frac{\partial}{\partial z} \left(D_{12}^\alpha \frac{\partial x_2^\alpha}{\partial z} \right) \quad (7.18)$$

$$\frac{\partial x_2^\alpha}{\partial t} = \frac{\partial}{\partial z} \left(D_{22}^\alpha \frac{\partial x_2^\alpha}{\partial z} \right) + \frac{\partial}{\partial z} \left(D_{21}^\alpha \frac{\partial x_1^\alpha}{\partial z} \right) \quad (7.19)$$

The requirement for conservation of mass at the interface gives the following two equations:

$$(x_1^{\gamma\alpha} - x_1^{\alpha\gamma})v = -J_1^\alpha|_{z=z^*} + J_1^\gamma|_{z=z^*} \quad (7.20)$$

$$(x_2^{\gamma\alpha} - x_2^{\alpha\gamma})v = -J_2^\alpha|_{z=z^*} + J_2^\gamma|_{z=z^*} \quad (7.21)$$

where v is the growth rate of the product phase. We emphasise again that the fluxes in both the matrix and product phases contribute to mass conservation at the interface, and thus, to the growth rate of the product phase. The fluxes of carbon and the substitutional alloying element at the moving interface are given by,

$$J_1^\gamma|_{z=z^*} = -D_{11}^\gamma \frac{\partial x_1^\gamma}{\partial z} \Big|_{z=z^*} - D_{12}^\gamma \frac{\partial x_2^\gamma}{\partial z} \Big|_{z=z^*} \quad (7.22)$$

$$J_2^\gamma|_{z=z^*} = -D_{22}^\gamma \frac{\partial x_2^\gamma}{\partial z} \Big|_{z=z^*} - D_{21}^\gamma \frac{\partial x_1^\gamma}{\partial z} \Big|_{z=z^*} \quad (7.23)$$

$$J_1^\alpha|_{z=z^*} = -D_{11}^\alpha \frac{\partial x_1^\alpha}{\partial z} \Big|_{z=z^*} - D_{12}^\alpha \frac{\partial x_2^\alpha}{\partial z} \Big|_{z=z^*} \quad (7.24)$$

$$J_2^\alpha|_{z=z^*} = -D_{22}^\alpha \frac{\partial x_2^\alpha}{\partial z} \Big|_{z=z^*} - D_{21}^\alpha \frac{\partial x_1^\alpha}{\partial z} \Big|_{z=z^*} \quad (7.25)$$

where the differentials are taken in the respective phases at the interface.

Because analytical equations of the concentration distributions in both matrix and product phases (for the cases where diffusion fields in both phases should be considered simultaneously) are not available, linear chemical concentration gradients are assumed in both phases for the calculation of the growth rate of the product phase; this is the so-called Zener approximation.

As it is illustrated in Fig. 7.7, the diffusion distances of carbon and the substitutional alloying element in ferrite and in austenite are respectively, L_γ , L_α , l_γ and l_α . The fluxes of carbon and the substitutional alloying element at the moving boundary are then given by,

$$J_1^\gamma|_{z=z^*} = -D_{11}^\gamma \frac{\bar{x}_1^\gamma - x_1^{\gamma\alpha}}{L_\gamma} - D_{12}^\gamma \frac{\bar{x}_2^\gamma - x_2^{\gamma\alpha}}{l_\gamma} \quad (7.26)$$

$$J_2^\gamma|_{z=z^*} = -D_{22}^\gamma \frac{\bar{x}_2^\gamma - x_2^{\gamma\alpha}}{l_\gamma} - D_{21}^\gamma \frac{\bar{x}_1^\gamma - x_1^{\gamma\alpha}}{L_\gamma} \quad (7.27)$$

$$J_1^\alpha|_{z=z^*} = -D_{11}^\alpha \frac{\bar{x}_1^\alpha - x_1^{\alpha\gamma}}{L_\alpha} - D_{12}^\alpha \frac{\bar{x}_2^\alpha - x_2^{\alpha\gamma}}{l_\alpha} \quad (7.28)$$

$$J_2^\alpha|_{z=z^*} = -D_{22}^\alpha \frac{\bar{x}_2^\alpha - x_2^{\alpha\gamma}}{l_\alpha} - D_{21}^\alpha \frac{\bar{x}_1^\alpha - x_1^{\alpha\gamma}}{L_\alpha} \quad (7.29)$$

where $\bar{x}_1^{\alpha,\gamma}$ and $\bar{x}_2^{\alpha,\gamma}$ are average concentrations of carbon and the substitutional alloying element in each phase, and z^* is the position of the moving interface. The conservation conditions for carbon and the substitutional alloying element in the system as a whole provide the following equations:

$$(L_\gamma - z^*)(\bar{x}_1^\gamma - \bar{x}_1^\alpha) = \frac{L_\gamma}{2}[(x_1^{\gamma\alpha} - \bar{x}_1^\alpha) + (\bar{x}_1^\gamma - \bar{x}_1^\alpha)] - \frac{L_\alpha}{2}(\bar{x}_1^\alpha - x_1^{\alpha\gamma}) \quad (7.30)$$

$$\frac{l_\alpha}{2}(\bar{x}_2^\alpha - x_2^{\alpha\gamma}) = \frac{l_\gamma}{2}(x_2^{\gamma\alpha} - \bar{x}_2^\gamma). \quad (7.31)$$

In addition to these equations, because the decrease in the amount of carbon (or X) in ferrite is equal to the integrated flux of carbon (or X) at the interface from $t = 0$ to $t = t$, one can introduce two further equations given below:

$$\int_0^t \left(\frac{D_{11}^\alpha(\bar{x}_1^\alpha - x_1^{\alpha\gamma})}{L_\alpha} + \frac{D_{12}^\alpha(\bar{x}_2^\alpha - x_2^{\alpha\gamma})}{l_\alpha} \right) dt = \frac{1}{2}(L_\alpha + 2z^*)(\bar{x}_1^\alpha - x_1^{\alpha\gamma}) \quad (7.32)$$

$$\int_0^t \frac{D_{22}^\alpha(\bar{x}_2^\alpha - x_2^{\alpha\gamma})}{l_\alpha} dt = \frac{1}{2}(l_\alpha + 2z^*)(\bar{x}_2^\alpha - x_2^{\alpha\gamma}). \quad (7.33)$$

As discussed in Appendix, the interface position z^* and the diffusion distances L_γ , L_α , l_γ , and l_α are proportional to $t^{1/2}$:

$$\begin{aligned} z^* &= \alpha_1 t^{1/2} \\ L_\gamma &= k_{C\gamma} t^{1/2} \\ L_\alpha &= k_{C\alpha} t^{1/2}, \\ l_\gamma &= k_{X\gamma} t^{1/2} \\ l_\alpha &= k_{X\alpha} t^{1/2} \end{aligned}$$

and, therefore, the growth rate of the product phase is given by:

$$v = \frac{dz^*}{dt} = \frac{1}{2}\alpha_1 t^{-1/2}, \quad (7.34)$$

where α_1 is one-dimensional parabolic thickening rate constant. Equations (7.32) and (7.33) give the following relations for the proportionality constants for the diffusion distances in ferrite:

$$\begin{aligned} k_{X\alpha} &= -\alpha_1 + \sqrt{\alpha_1^2 + 4D_{22}^\alpha} \\ k_{C\alpha} &= -k_\alpha + \sqrt{k_\alpha^2 + 4D_{11}^\alpha} \end{aligned}$$

with

$$k_\alpha = \alpha_1 - \frac{2D_{12}^\alpha(\bar{x}_2^\alpha - x_2^{\alpha\gamma})}{\bar{x}_1^\alpha - x_1^{\alpha\gamma}} \frac{1}{k_{X\alpha}}.$$

From equations 7.30 and 7.31, $k_{C\gamma}$ and $k_{X\gamma}$ are expressed by α_1 , $k_{C\alpha}$, and $k_{X\alpha}$, giving,

$$k_{X\gamma} = k_{X\alpha} \frac{\bar{x}_2^\alpha - x_2^{\alpha\gamma}}{x_2^{\gamma\alpha} - \bar{x}_2^\gamma}$$

$$k_{C\gamma} = 2\alpha_1 \frac{\bar{x}_1^\gamma - \bar{x}_1^\alpha}{\bar{x}_1^\gamma - x_1^{\gamma\alpha}} - k_{C\alpha} \frac{\bar{x}_1^\alpha - x_1^{\alpha\gamma}}{\bar{x}_1^\alpha - x_1^{\gamma\alpha}}$$

Now, these four diffusion distances and the interface position can be substituted into the mass conservation equations 7.30 and 7.31 to obtain the interface compositions and the growth rate of the product phase, assuming that the cross interdiffusion coefficient D_{21} is negligible [21]:

$$\alpha_1^2 - C_1\alpha_1 - C_2 = 0 \quad (7.35)$$

$$\alpha_1^2 - C_3 = 0 \quad (7.36)$$

with

$$C_1 = \frac{k_{C\alpha} \bar{x}_1^\alpha - x_1^{\alpha\gamma}}{2 \bar{x}_1^\gamma - \bar{x}_1^\alpha} + \frac{2D_{11}^\alpha \bar{x}_1^\alpha - x_1^{\alpha\gamma}}{k_{C\alpha} x_1^{\gamma\alpha} - x_1^{\alpha\gamma}}$$

$$+ \frac{2D_{12}^\alpha \bar{x}_2^\alpha - x_2^{\alpha\gamma}}{k_{X\alpha} x_1^{\gamma\alpha} - x_1^{\alpha\gamma}} - \frac{2D_{12}^\gamma (x_2^{\gamma\alpha} - \bar{x}_2^\gamma)^2}{k_{X\alpha} (x_1^{\gamma\alpha} - x_1^{\alpha\gamma})(\bar{x}_2^\alpha - x_2^{\alpha\gamma})}$$

$$C_2 = D_{11}^\gamma \frac{(\bar{x}_1^\gamma - x_1^{\gamma\alpha})^2}{(x_1^{\gamma\alpha} - x_1^{\alpha\gamma})(\bar{x}_1^\gamma - \bar{x}_1^\alpha)} + \frac{k_{C\alpha} D_{12}^\gamma \bar{x}_1^\alpha - x_1^{\alpha\gamma}}{k_{X\alpha} (x_1^{\gamma\alpha} - x_1^{\alpha\gamma})(\bar{x}_1^\gamma - \bar{x}_1^\alpha)} \frac{(x_2^{\gamma\alpha} - \bar{x}_2^\gamma)^2}{\bar{x}_2^\alpha - x_2^{\alpha\gamma}}$$

$$- D_{11}^\alpha \frac{(\bar{x}_1^\alpha - x_1^{\alpha\gamma})^2}{(x_1^{\gamma\alpha} - x_1^{\alpha\gamma})(\bar{x}_1^\gamma - \bar{x}_1^\alpha)} - \frac{k_{C\alpha} D_{12}^\alpha (\bar{x}_1^\alpha - x_1^{\alpha\gamma})(\bar{x}_2^\alpha - x_2^{\alpha\gamma})}{k_{X\alpha} (x_1^{\gamma\alpha} - x_1^{\alpha\gamma})(\bar{x}_1^\gamma - \bar{x}_1^\alpha)}$$

$$C_3 = \frac{2D_{22}^\alpha \bar{x}_2^\alpha - x_2^{\alpha\gamma}}{k_{X\alpha} x_2^{\gamma\alpha} - x_2^{\alpha\gamma}} - \frac{2D_{22}^\gamma (x_2^{\gamma\alpha} - \bar{x}_2^\gamma)^2}{k_{X\alpha} (x_2^{\gamma\alpha} - x_2^{\alpha\gamma})(\bar{x}_2^\alpha - x_2^{\alpha\gamma})}$$

One can then calculate the interface compositions and the growth rate of austenite by solving equations 7.35 and 7.36 and three thermodynamic equations 7.8 simultaneously.

It is worth noting that the flux in austenite may be negligible in the case of the formation of austenite from a fully ferritic initial microstructure by analogy with the reconstructive ferrite formation from austenite in which the ferrite is usually assumed to grow with a constant composition. Therefore the growth of austenite, in this case, is controlled only by diffusion of atoms in ferrite instead of in austenite. This is the same situation as the formation of ferrite from austenite despite the fact that the growth of ferrite is in later case controlled by diffusion in austenite. For the formation of austenite either from a mixture of ferrite and carbide particles, or from a mixture of bainitic ferrite and austenite, on the other hand, concentration gradients of carbon and X in austenite are expected to exist, and therefore, the growth of austenite will depend on diffusion in austenite as well as that in ferrite.

7.3.3 Reconstructive growth of austenite under paraequilibrium

When the supersaturation of ferrite is very high; *i.e.* at very high temperatures, paraequilibrium might be the condition which governs the growth of austenite.

According to the definition of the paraequilibrium, an identical X/Fe atoms ratio is now expected both in the matrix and product phases:

$$\frac{x_2^\gamma}{x_0^\gamma} = \frac{x_2^\alpha}{x_0^\alpha} = \frac{\bar{x}_2^\alpha}{\bar{x}_0^\alpha} = k_2. \quad (7.37)$$

Although the chemical potential of the substitutional alloying element or iron are no longer identical in the two phases at the interface, subject to that constraint, the carbon at the interface achieves equality of chemical potentials in both phases [18], giving

$$\frac{\Delta G_1^{0\alpha\rightarrow\gamma}}{RT} = \ln \frac{x_1^\alpha}{x_1^\gamma} + \ln \frac{\Gamma_1^\alpha}{\Gamma_1^\gamma}. \quad (7.38)$$

The following equation is used in order to define the paraequilibrium tie line [18].

$$\frac{\Delta G_2^{0\alpha\rightarrow\gamma}}{RT} - \ln \frac{x_2^\alpha}{x_2^\gamma} - \ln \frac{\Gamma_2^\alpha}{\Gamma_2^\gamma} = -\frac{1}{k_2} \frac{\Delta G_0^{0\alpha\rightarrow\gamma}}{RT} - \ln \frac{x_0^\alpha}{x_0^\gamma} - \ln \frac{\Gamma_0^\alpha}{\Gamma_0^\gamma} \quad (7.39)$$

These three equations allow the interface compositions to be calculated independently from the mass conservation equation at the moving interface. Therefore one can calculate the interface compositions first, and then put them into the mass conservation equation to obtain the growth rate of the product phase at the moving interface. Because of the definition of paraequilibrium, no flux of X atoms needs to be considered in this case. As a result, it is necessary only to set the mass conservation for carbon at the interface. The growth of the product phase is, therefore, controlled by carbon diffusion in both ferrite and austenite phases. The mass conservation equation for carbon, in this case, can be simplified as follows:

$$\begin{aligned} \alpha_1^2 - \alpha_1 & \left[\frac{k_{C\alpha}}{2} \frac{\bar{x}_1^\alpha - x_1^{\alpha\gamma}}{\bar{x}_1^\gamma - \bar{x}_1^\alpha} + \frac{2D_{11}^\alpha}{k_{C\alpha}} \frac{\bar{x}_1^\alpha - x_1^{\alpha\gamma}}{x_1^{\gamma\alpha} - x_1^{\alpha\gamma}} \right] \\ & = D_{11}^\gamma \frac{(\bar{x}_1^\gamma - x_1^{\gamma\alpha})^2}{(x_1^{\gamma\alpha} - x_1^{\alpha\gamma})(\bar{x}_1^\gamma - \bar{x}_1^\alpha)} - D_{11}^\alpha \frac{(\bar{x}_1^\alpha - x_1^{\alpha\gamma})^2}{(x_1^{\gamma\alpha} - x_1^{\alpha\gamma})(\bar{x}_1^\gamma - \bar{x}_1^\alpha)} \end{aligned} \quad (7.40)$$

Fig. 7.8 and Fig. 7.9 represent illustrative phase diagrams for reaustenitisation from a ferritic initial microstructure, and from an initial microstructure which is a mixture of bainitic ferrite and austenite respectively.

7.3.4 Special cases

As mentioned earlier, with some exceptions, it is necessary to consider diffusion in both the ferrite matrix and austenite precipitate during reaustenitisation. However, there might exist circumstances where diffusion in just one of the two phases largely controls the growth of the product phase. The mass conservation equations derived in the previous section can then be simplified and also, more rigorous solutions for the chemical distributions in the phase are then available [6,11,12].

When a fully ferritic initial microstructure is heated into the $\alpha + \gamma$ two phase region, it may be a good approximation that there is no flux in the precipitate phase (*i.e.* austenite). For ferrite growth from austenite, the approximation is often very good because of the low solubility of carbon and in ferrite. On the other hand, in the case of the austenite growth from ferrite, the product phase usually has a high solubility for carbon and the substitutional alloying element. Therefore the assumption of no flux in austenite should be examined experimentally. In addition to this, fluxes in austenite may exist when soft impingement occurs: overlapping of diffusion fields can lead to a change in the boundary conditions.

Reaustenitisation from a mixture of bainitic ferrite and austenite or from a mixture of ferrite and carbides shows rather different features. The carbon concentration of the initial austenite at the reaustenitisation temperature is usually expected to be higher than the equilibrium

concentration at the interface at the reaction temperature [22-25], leading to the fact that the supersaturation level in carbon could be larger in austenite than that in ferrite. As a consequence, the contribution of fluxes in ferrite may be negligible [25] to the overall problem.

In the case of reaustenitisation from an initial microstructure of ferrite and cementite, the austenite is found to nucleate preferentially at the junctions between ferrite/ferrite grain boundaries and carbide particles [14,26-29]. The dissolution of carbide particles happens essentially happens after becoming engulfed by austenite. The early stages of the growth of austenite is then controlled by carbon diffusion through the austenite envelope [14,15]. Because the equilibrium carbon concentration in austenite at the interface between austenite and cementite is much larger than that at the interface between austenite and ferrite, the carbon concentration gradient in austenite is expected to be correspondingly larger than that in ferrite. Hence any flux in the ferrite may be considered negligible [14,15].

Under the circumstances where one of the two phases is not important in terms of the diffusion field which controls the growth of the product phase, the mass conservation equations relate to the first one of the two phases, giving:

$$(x_1^{\gamma\alpha} - x_1^{\alpha\gamma})v = J_1|_{z=z^*} \quad (7.41)$$

$$(x_2^{\gamma\alpha} - x_2^{\alpha\gamma})v = J_2|_{z=z^*} \quad (7.42)$$

where $J_1|_{z=z^*}$ and $J_2|_{z=z^*}$ are fluxes either in ferrite or in austenite depending on the phase which dominates as far as diffusion is concerned.

Growth of austenite from a ferritic sample

When the initial microstructure is ferritic, the growth of austenite might be controlled by fluxes of carbon and X in ferrite instead of in austenite as mentioned earlier. Assuming the approximation of the linear gradients of chemical compositions, the following equations for the conservation of mass at the interface (see Fig. 7.10) are obtained:

$$v(x_1^{\gamma\alpha} - x_1^{\alpha\gamma}) = \frac{D_{11}^\alpha}{L_\alpha}(\bar{x}_1^\alpha - x_1^{\alpha\gamma}) + \frac{D_{12}^\alpha}{l_\alpha}(\bar{x}_2^\alpha - x_2^{\alpha\gamma}) \quad (7.43)$$

$$v(x_2^{\gamma\alpha} - x_2^{\alpha\gamma}) = \frac{D_{22}^\alpha}{l_\alpha}(\bar{x}_2^\alpha - x_2^{\alpha\gamma}). \quad (7.44)$$

The mass conservation conditions for carbon and X for the whole system give the following two equations (Fig. 7.10):

$$z^*(x_1^{\gamma\alpha} - \bar{x}_1^\alpha) = \frac{L_\alpha}{2}(\bar{x}_1^\alpha - x_1^{\alpha\gamma}) \quad (7.45)$$

$$z^*(x_2^{\gamma\alpha} - \bar{x}_2^\alpha) = \frac{l_\alpha}{2}(\bar{x}_2^\alpha - x_2^{\alpha\gamma}). \quad (7.46)$$

The one-dimensional parabolic thickening rate constant for the growth of austenite is therefore given by the simultaneous solution of:

$$\alpha_1^2 = D_{11}^\alpha \frac{(\bar{x}_1^\alpha - x_1^{\alpha\gamma})^2}{(x_1^{\gamma\alpha} - x_1^{\alpha\gamma})(x_1^{\gamma\alpha} - \bar{x}_1^\alpha)} + D_{12}^\alpha \frac{(\bar{x}_2^\alpha - x_2^{\alpha\gamma})^2}{(x_2^{\gamma\alpha} - x_2^{\alpha\gamma})(x_2^{\gamma\alpha} - \bar{x}_2^\alpha)} \quad (7.47)$$

$$\alpha_1^2 = D_{22}^\alpha \frac{(\bar{x}_2^\alpha - x_2^{\alpha\gamma})^2}{(x_2^{\gamma\alpha} - x_2^{\alpha\gamma})(x_2^{\gamma\alpha} - \bar{x}_2^\alpha)}. \quad (7.48)$$

For paraequilibrium austenite growth, the interface compositions are calculated independently from the thermodynamic equations as discussed earlier. The parabolic rate constant of austenite in that case is given by:

$$\alpha_1^2 = D_{11}^\alpha \frac{(\bar{x}_1^\alpha - x_1^{\alpha\gamma})^2}{(x_1^{\gamma\alpha} - x_1^{\alpha\gamma})(x_1^{\gamma\alpha} - \bar{x}_1^\alpha)}. \quad (7.49)$$

Growth of austenite from a mixture of ferrite and austenite

When the initial microstructure contains ferrite and austenite of equilibrium chemical composition, the growth of the pre-existing austenite into ferrite is mainly controlled by the diffusion fields in austenite if the superheating is high (Fig. 7.11). For that case, the mass conservation of carbon and the substitutional alloying element at the interface, and in the whole system give the following equations (see Fig. 7.11):

$$v(x_1^{\gamma\alpha} - x_1^{\alpha\gamma}) = \frac{D_{11}^\gamma}{L_\gamma}(\bar{x}_1^\gamma - x_1^{\gamma\alpha}) + \frac{D_{12}^\gamma}{l_\gamma}(\bar{x}_2^\gamma - x_2^{\gamma\alpha}) \quad (7.50)$$

$$v(x_2^{\gamma\alpha} - x_2^{\alpha\gamma}) = \frac{D_{22}^\gamma}{l_\gamma}(\bar{x}_2^\gamma - x_2^{\gamma\alpha}) \quad (7.51)$$

$$(L_\gamma - z^*)(\bar{x}_1^\gamma - x_1^{\alpha\gamma}) = \frac{L_\gamma}{2}[(\bar{x}_1^\gamma - x_1^{\alpha\gamma}) + (x_1^{\gamma\alpha} - x_1^{\alpha\gamma})] \quad (7.52)$$

$$(l_\gamma - z^*)(\bar{x}_2^\gamma - x_2^{\alpha\gamma}) = \frac{l_\gamma}{2}[(\bar{x}_2^\gamma - x_2^{\alpha\gamma}) + (x_2^{\gamma\alpha} - x_2^{\alpha\gamma})]. \quad (7.53)$$

The one-dimensional parabolic thickening rate constant of austenite is therefore given by the simultaneous solution of:

$$\alpha_1^2 = D_{11}^\gamma \frac{(\bar{x}_1^\gamma - x_1^{\gamma\alpha})^2}{(x_1^{\gamma\alpha} - x_1^{\alpha\gamma})(\bar{x}_1^\gamma - x_1^{\alpha\gamma})} + D_{12}^\gamma \frac{(\bar{x}_2^\gamma - x_2^{\gamma\alpha})^2}{(x_2^{\gamma\alpha} - x_2^{\alpha\gamma})(\bar{x}_2^\gamma - x_2^{\alpha\gamma})} \quad (7.54)$$

$$\alpha_1^2 = D_{22}^\gamma \frac{(\bar{x}_2^\gamma - x_2^{\gamma\alpha})^2}{(x_2^{\gamma\alpha} - x_2^{\alpha\gamma})(\bar{x}_2^\gamma - x_2^{\alpha\gamma})}. \quad (7.55)$$

For the case of paraequilibrium, the rate constant is given by:

$$\alpha_1^2 = D_{11}^\gamma \frac{(\bar{x}_1^\gamma - x_1^{\gamma\alpha})^2}{(x_1^{\gamma\alpha} - x_1^{\alpha\gamma})(\bar{x}_1^\gamma - x_1^{\alpha\gamma})}. \quad (7.56)$$

Growth of austenite controlled by dissolution of cementite

In the case of reaustenitisation from a mixture of ferrite and cementite particles, the nucleation of austenite occurs preferentially at the junctions between ferrite/ferrite grain boundaries and cementite particles which locate on the grain boundaries. The austenite particles, then, engulf the cementite particles. The growth of austenite particles after this stage is mainly controlled by the dissolution of cementite particles within the austenite, if the supersaturation is reasonably low, and the effect of the dissolution of cementite particles within the ferrite matrix is small (see for example [15]). Assuming linear gradients of chemical composition in austenite (Fig. 7.12), we can obtain the following equations to satisfy the mass conservation at the interface and for the whole system:

$$v(x_1^{\gamma\alpha} - x_1^{\alpha\gamma}) = \frac{D_{11}^{\gamma}}{l_{\theta} + z^*}(x_1^{\gamma\theta} - x_1^{\gamma\alpha}) + \frac{D_{12}^{\gamma}}{l_{\theta} + z^*}(x_2^{\gamma\theta} - x_2^{\gamma\alpha}) \quad (7.57)$$

$$v(x_2^{\gamma\alpha} - x_2^{\alpha\gamma}) = \frac{D_{22}^{\gamma}}{l_{\theta} + z^*}(x_2^{\gamma\theta} - x_2^{\gamma\alpha}) \quad (7.58)$$

$$l_{\theta}(x_1^{\theta\gamma} - x_1^{\alpha\gamma}) = \frac{l_{\theta} + z^*}{2} [(x_1^{\gamma\theta} - x_1^{\alpha\gamma}) + (x_1^{\gamma\alpha} - x_1^{\alpha\gamma})] \quad (7.59)$$

$$l_{\theta}(x_2^{\theta\gamma} - x_2^{\alpha\gamma}) = \frac{l_{\theta} - z^*}{2} [(x_2^{\gamma\theta} - x_2^{\alpha\gamma}) + (x_2^{\gamma\alpha} - x_2^{\alpha\gamma})]. \quad (7.60)$$

where l_{θ} is the dissolution thickness of cementite (see Fig. 7.12), $x^{\theta\gamma}$, $x^{\gamma\theta}$ are respectively carbon (or X) concentrations at the interface in cementite and in austenite. From these equations, we can obtain the following two expressions which on simultaneous solution can yield the one-dimensional parabolic thickening rate constant:

$$\alpha_1^2 = D_{11}^{\gamma} \frac{(x_1^{\gamma\theta} - x_1^{\gamma\alpha})(2x_1^{\theta\gamma} - x_1^{\gamma\theta} - x_1^{\gamma\alpha})}{(x_1^{\gamma\alpha} - x_1^{\alpha\gamma})(x_1^{\theta\gamma} - x_1^{\alpha\gamma})} + D_{12}^{\gamma} \frac{(x_2^{\gamma\theta} - x_2^{\gamma\alpha})(2x_1^{\theta\gamma} - x_1^{\gamma\theta} - x_1^{\gamma\alpha})}{(x_2^{\gamma\alpha} - x_2^{\alpha\gamma})(x_2^{\theta\gamma} - x_2^{\alpha\gamma})} \quad (7.61)$$

$$\alpha_1^2 = D_{22}^{\gamma} \frac{(x_2^{\gamma\theta} - x_2^{\gamma\alpha})(2x_2^{\theta\gamma} - x_2^{\gamma\theta} - x_2^{\gamma\alpha})}{(x_2^{\gamma\alpha} - x_2^{\alpha\gamma})(x_2^{\theta\gamma} - x_2^{\alpha\gamma})}. \quad (7.62)$$

For the paraequilibrium growth of austenite, it follows that:

$$\alpha_1^2 = D_{11}^{\gamma} \frac{(x_1^{\gamma\theta} - x_1^{\gamma\alpha})(2x_1^{\theta\gamma} - x_1^{\gamma\theta} - x_1^{\gamma\alpha})}{(x_1^{\gamma\alpha} - x_1^{\alpha\gamma})(x_1^{\theta\gamma} - x_1^{\alpha\gamma})}. \quad (7.63)$$

The chemical compositions at the interface between austenite and cementite also need to be determined. A method of this has been discussed by Hashiguchi and Kirkaldy [20].

Analytical solutions

When only one of the two phases is important in terms of the control of the growth of the product phase, analytical expressions for chemical distributions are available. The equations for the concentration distributions in each phase (*i.e.* ferrite and austenite) can be obtained from the diffusion equations [6] independently when no interaction between the fluxes in two phases exists. If the cross interdiffusion coefficient D_{21} is negligible [21], it is possible to simplify the general equation [6] as follows [10]:

$$\begin{aligned} x_1^{\alpha} &= \bar{x}_1^{\alpha} + \frac{D_{12}^{\alpha}(x_2^{\alpha\gamma} - \bar{x}_2^{\alpha})}{D_{11}^{\alpha} - D_{22}^{\alpha}} \frac{\operatorname{erfc}\left\{\frac{z}{2\sqrt{D_{22}^{\alpha}t}}\right\}}{\operatorname{erfc}\left\{\frac{z^*}{2\sqrt{D_{22}^{\alpha}t}}\right\}} \\ &+ \left[(x_1^{\alpha\gamma} - \bar{x}_1^{\alpha}) - \frac{D_{12}^{\alpha}(x_2^{\alpha\gamma} - \bar{x}_2^{\alpha})}{D_{11}^{\alpha} - D_{22}^{\alpha}} \right] \frac{\operatorname{erfc}\left\{\frac{z}{2\sqrt{D_{11}^{\alpha}t}}\right\}}{\operatorname{erfc}\left\{\frac{z^*}{2\sqrt{D_{11}^{\alpha}t}}\right\}} \\ x_1^{\gamma} &= \bar{x}_1^{\gamma} + \frac{D_{12}^{\gamma}(x_2^{\gamma\alpha} - \bar{x}_2^{\gamma})}{D_{11}^{\gamma} - D_{22}^{\gamma}} \frac{\operatorname{erfc}\left\{\frac{z}{2\sqrt{D_{22}^{\gamma}t}}\right\}}{\operatorname{erfc}\left\{\frac{z^*}{2\sqrt{D_{22}^{\gamma}t}}\right\}} \end{aligned} \quad (7.64)$$

$$+ \left[(x_1^{\gamma\alpha} - \bar{x}_1^\gamma) - \frac{D_{12}^\gamma (x_2^{\gamma\alpha} - \bar{x}_2^\gamma)}{D_{11}^\gamma - D_{22}^\gamma} \right] \frac{\operatorname{erfc}\left\{\frac{z}{2\sqrt{D_{11}^\gamma t}}\right\}}{\operatorname{erfc}\left\{\frac{z^*}{2\sqrt{D_{11}^\gamma t}}\right\}} \quad (7.65)$$

$$x_2^\alpha = \bar{x}_2^\alpha + (x_2^{\alpha\gamma} - \bar{x}_2^\alpha) \frac{\operatorname{erfc}\left\{\frac{z}{2\sqrt{D_{22}^\alpha t}}\right\}}{\operatorname{erfc}\left\{\frac{z^*}{2\sqrt{D_{22}^\alpha t}}\right\}} \quad (7.66)$$

$$x_2^\gamma = \bar{x}_2^\gamma + (x_2^{\gamma\alpha} - \bar{x}_2^\gamma) \frac{\operatorname{erfc}\left\{\frac{z}{2\sqrt{D_{22}^\gamma t}}\right\}}{\operatorname{erfc}\left\{\frac{z^*}{2\sqrt{D_{22}^\gamma t}}\right\}}. \quad (7.67)$$

It should be noted that these equations are not applicable if the diffusion fields in the two phases interact with each other; this is expected to happen in most real circumstances. The interface position is expressed by the diffusion coefficients and growth rate constants η_i (see for example [10]):

$$z^* = \eta_1^\gamma \sqrt{D_{11}^\gamma t} = \eta_2^\gamma \sqrt{D_{22}^\gamma t} = \eta_1^\alpha \sqrt{D_{11}^\alpha t} = \eta_2^\alpha \sqrt{D_{22}^\alpha t} \quad (7.68)$$

or,

$$z^* = \alpha_1 t^{1/2} \quad (7.69)$$

where α_1 is an one-dimensional parabolic thickening rate constant. The growth rate v is then given by:

$$v = \frac{dz^*}{dt} = \frac{\eta_i D_{ii}}{2\sqrt{D_{ii} t}} = \frac{1}{2} \alpha_1 t^{-1/2}. \quad (7.70)$$

Substituting the derivatives of the distributions of chemical composition and the growth rate of the product phase into the mass conservation equations at the interface, one can obtain the relations between the interface compositions and the growth rate of the product phase.

When the growth of austenite is controlled by the diffusion field in austenite, the relations are given as follows [10]:

$$\frac{x_1^{\gamma\alpha} - \bar{x}_1^\gamma}{x_1^{\gamma\alpha} - x_1^{\alpha\gamma}} = H\{D_{11}^\gamma\} - \frac{B_1 D_{12}^\gamma}{D_{11}^\gamma - D_{22}^\gamma} [H\{D_{22}^\gamma\} - H\{D_{11}^\gamma\}] \quad (7.71)$$

$$\frac{x_2^{\gamma\alpha} - \bar{x}_2^\gamma}{x_2^{\gamma\alpha} - x_2^{\alpha\gamma}} = H\{D_{22}^\gamma\} \quad (7.72)$$

where

$$H\{D_{ii}\} = \sqrt{\frac{\pi}{4D_{ii}}} \alpha_1 [\operatorname{erfc}\left\{\frac{\alpha_1}{\sqrt{4D_{ii}}}\right\}] \exp\left\{\frac{\alpha_1^2}{4D_{ii}}\right\}$$

$$B_1 = \frac{x_2^{\gamma\alpha} - x_2^{\alpha\gamma}}{x_1^{\gamma\alpha} - x_1^{\alpha\gamma}}.$$

On the other hand, when the growth of austenite is controlled by diffusion in ferrite only, the following equation applies:

$$\frac{x_1^{\alpha\gamma} - \bar{x}_1^\alpha}{x_1^{\alpha\gamma} - x_1^{\gamma\alpha}} = H\{D_{11}^\alpha\} - \frac{B_1 D_{12}^\alpha}{D_{11}^\alpha - D_{22}^\alpha} [H\{D_{22}^\alpha\} - H\{D_{11}^\alpha\}] \quad (7.73)$$

$$\frac{x_2^{\alpha\gamma} - \bar{x}_2^\alpha}{x_2^{\alpha\gamma} - x_2^{\gamma\alpha}} = H\{D_{22}^\alpha\}. \quad (7.74)$$

7.4 CALCULATED EXAMPLES

In order to demonstrate the calculation of tie lines under different equilibrium conditions as discussed in the previous section, re-austenitisation in a Fe-C-Cr ternary system will be discussed.

7.4.1 Thermodynamic parameters

The thermodynamic parameters for the system which are used for the calculation have represented by Kirkaldy and his co-workers [19,20]. Those parameters for the Fe-C-Cr system are listed below, with some correction of typographical errors.

$$\begin{aligned}\Delta G_0^{0\alpha \rightarrow \gamma} &= 8933 - 14.406T + 12.083 \times 10^{-3}T^2 - 11.51 \times 10^{-6}T^3 \\ &\quad + 5.23 \times 10^{-9}T^4, \text{ J mol}^{-1} \text{ (T < 1000K)} \\ &= 71659 - 216.84T + 24.773 \times 10^{-2}T^2 - 12.661 \times 10^{-5}T^3 \\ &\quad + 24.397 \times 10^{-9}T^4, \text{ J mol}^{-1} \text{ (T > 1000K)} \\ \Delta G_1^{0\alpha \rightarrow \gamma} &= -65562 + 32.949T, \text{ J mol}^{-1} \\ \Delta G_2^{0\alpha \rightarrow \gamma} &= -1534 - 19.472T + 2.749T \ln T, \text{ J mol}^{-1} \\ \epsilon_{11}^{\alpha} &= 1.3 \\ \epsilon_{11}^{\gamma} &= 4.786 + 5066/T \\ \epsilon_{22}^{\alpha} &= 2.819 - 6039/T \\ \epsilon_{22}^{\gamma} &= 7.655 - 3154/T - 0.661 \ln T \\ \epsilon_{12}^{\gamma} &= 14.19 - 30210/T \\ \epsilon_{12}^{\alpha} &= \epsilon_{12}^{\gamma}\end{aligned}$$

In order to calculate the growth rate of product phase and interface compositions satisfying the mass conservations at the moving interface and the diffusion equations in both phases, it is essential to know the diffusion coefficients of carbon and alloying elements both in ferrite and in austenite.

The diffusivity of carbon in austenite is known to vary significantly with carbon concentration. Therefore the diffusion equations should be solved with a diffusion coefficient which is a function of carbon concentration; thus it varies from place to place in austenite. However, it has also been shown that a weighted average diffusion coefficient of carbon in austenite, in which the average is taken between the minimum and maximum carbon concentrations in austenite, can be used in the calculation giving reasonable accuracy. Hence, in the present work, a weighted average diffusion coefficient of carbon in austenite will be used for further calculations. The average diffusion coefficient is expressed as follows [30]:

$$\bar{D} = \int_{\bar{x}_1^{\gamma}}^{x^{\gamma\alpha}} \frac{D dx}{(x^{\gamma\alpha} - \bar{x}_1^{\gamma})}. \quad (7.75)$$

This procedure is valid strictly for the situation where the concentration profile does not change with time, but is recognised to be a good approximation for non-steady state conditions, as exist during the growth of austenite into ferrite. For simplicity and consistency, we use a symbol D_{11}^{γ} as \bar{D} . As discussed by Brown and Kirkaldy [21], the cross coefficients are expressed by,

$$D_{12}^{\alpha,\gamma} = D_{11}^{\alpha,\gamma} \frac{\epsilon_{12}^{\alpha,\gamma} x_1^{\alpha,\gamma}}{1 + \epsilon_{11}^{\alpha,\gamma} x_1^{\alpha,\gamma}}. \quad (7.76)$$

The diffusion coefficient of carbon in ferrite is expressed as a function of temperature [16], giving,

$$D_{11}^{\alpha} = 0.02 \exp \left\{ -\frac{10115}{T} \right\} \exp \left\{ 0.5898 \left[1 + \frac{2}{\pi} \arctan \left(1.4985 - \frac{15309}{T} \right) \right] \right\}, \text{ cm}^2 \text{ s}^{-1}. \quad (7.77)$$

The diffusivities of alloying element in ferrite and austenite were discussed by Fridberg *et al.* [17]. On reproducing the data for Cr of figure 14 in their paper [17], the diffusion coefficients of Cr in ferrite and austenite are expressed as follows:

$$D_{22}^{\gamma} = 3.325 \exp \left\{ -\frac{286000}{RT} \right\}, \text{ cm}^2 \text{ s}^{-1} \quad (7.78)$$

$$\begin{aligned} D_{22}^{\alpha} &= 4.288 \exp \left\{ -\frac{240000}{RT} \right\}, \text{ cm}^2 \text{ s}^{-1} \text{ (paramagnetic ferrite)} \\ &= 1.340 \exp \left\{ -\frac{240000}{RT} \right\}, \text{ cm}^2 \text{ s}^{-1} \text{ (ferromagnetic ferrite)} \end{aligned} \quad (7.79)$$

Calculated isothermal sections of the phase diagram of a Fe-0.3C-4.08 wt.% alloy are presented in Fig. 7.13.

7.4.2 Growth of austenite from a mixture of bainite and austenite

When the initial microstructure contains a certain amount of austenite, nucleation of austenite might be unnecessary during reaustenitisation. Especially when the initial microstructure is a mixture of bainitic ferrite and residual austenite, the plate shape of the two phases may allow us to treat reaustenitisation process as an one-dimensional parabolic growth of the residual austenite plates.

Specimens are assumed to be heated up to the austenite phase field, and then quenched to and held at a bainite transformation temperature for a sufficient length of time to allow the specimens to complete the bainite transformation. Because of the nature of bainite transformation, the reaction stops when the carbon concentration in residual austenite reaches the point where the diffusionless formation of ferrite from austenite becomes thermodynamically impossible: this is referred to as the incomplete reaction phenomenon. Therefore, if the other reactions such as carbide precipitations and reconstructive formations of ferrite are sluggish, one can obtain a mixture of bainitic ferrite plates and residual austenite trapped in between those bainitic ferrite plates. The carbon concentration in the residual austenite has been reported to be in a good agreement with T_0' curve in the phase diagram of the system, where ferrite, whose free energy has been raised by a stored energy term (*i.e.* 400 J mol^{-1} , after Bhadeshia and Edmonds [31]) associated with the transformation strain, and austenite of identical composition have the same free energy. Since the decarburisation of bainitic ferrite occurs soon after the reaction, the carbon concentration in ferrite may be close to its equilibrium level. There is no partitioning of substitutional alloying elements during bainite transformation [32-35], the alloying element compositions in the two phases are identical as long as there is no reconstructive formation of ferrite. Thus, if one chooses a bainite reaction temperature, one can obtain the average chemical compositions in ferrite and residual austenite.

The specimens are then heated directly to a re-austenitisation temperature without being cooled below the bainite transformation temperature T_b . So the initial microstructure is a mixture of bainitic ferrite with the equilibrium carbon concentration at the bainite reaction temperature; $\bar{x}_1^\alpha = x_1^{\alpha\gamma}\{T_b\}$, and residual austenite with carbon concentration at T'_0 at the bainite transformation temperature; $\bar{x}_1^\gamma = x_{T'_0}\{T_b\}$.

One-dimensional parabolic thickening rate constants in the Fe-0.3C-4.08Cr wt.% alloy calculated for the paraequilibrium and the local equilibrium conditions are shown in Fig. 7.14. In order to show the effect of the initial carbon concentration on the rate constant, three different bainite transformation temperatures; 360, 420 and 480 °C, were selected. The calculated initial carbon concentrations in residual austenite and in ferrite are listed below [37,38].

$T_b, \text{ }^\circ\text{C}$	$x_{1,eq}^\alpha\{T_b\}$, mole fraction	$x_{T'_0}\{T_b\}$, mole fraction
360	0.000553	0.0265
420	0.000623	0.0228
480	0.000692	0.0163

Table 7.1: Carbon concentrations in bainitic ferrite and residual austenite at the end of bainite transformation at each temperature in Fe-0.3C-4.08Cr wt.% alloy.

It can be seen that the growth rate of austenite increases monotonically with temperature. It should be noted that the rate constant under local equilibrium is always larger than that under paraequilibrium. When the one dimensional parabolic rate constant for the growth of ferrite from austenite is calculated, it has been found that the rate constant under paraequilibrium is larger than that under local equilibrium at lower temperatures whereas the order swaps at higher temperatures. This could be understood as follows. Although the driving force for the formation of ferrite is always higher in local equilibrium than that under paraequilibrium, the diffusivity of the substitutional alloying element is remarkably low at low temperatures; this causes the retardation of the growth of austenite. Therefore the rate constant for the growth of ferrite under local equilibrium at lower temperatures is smaller than that under paraequilibrium (for example see [40]). At higher temperatures, on the other hand, the diffusivity of the substitutional alloying element becomes high and the driving force for the transformation under paraequilibrium decreases rapidly: in fact the driving force for the growth of ferrite under paraequilibrium becomes zero at the Ae'_3 temperature. As a consequence, the rate constant under local equilibrium becomes greater than that under paraequilibrium [40]. However it should be noted that a spike of the substitutional alloying element in austenite adjacent to the transformation interface, which is under local equilibrium, becomes sharper with decreasing temperature, and little difference will be expected for the rate constants calculated from local equilibrium and paraequilibrium conditions as can be seen in Enomoto's calculations [40].

In the case of re-austenitisation, however, the diffusivity of the substitutional alloying element is very high because of the elevated temperatures for re-austenitisation, leading to the fact that the rate constant for the growth of austenite under local equilibrium always remains higher than that under paraequilibrium.

The rate constants for the growth of austenite under paraequilibrium for the three different mixtures of bainitic ferrite and residual austenite are compared in Fig. 7.15. The rate constants decrease gently with temperature at higher temperatures, but fall down steeply to zero at lower

temperature showing the lowest possible temperature where austenite can actually grow. It can also be seen that the rate constant at a temperature is larger when the bainite transformation temperature is lower. This can be understood qualitatively from the fact that $x_{T_0}\{T_b\}$ is larger in lower bainite transformation temperature, which provides larger supersaturation of carbon in austenite at a reaction temperature and hence a larger growth rate of austenite. The reaustenitisation-start temperature under paraequilibrium; *i.e.* the lowest temperature where the growth of austenite can occur, also varies with the bainite transformation temperature. The reaustenitisation-start temperature from a mixture of bainitic ferrite and austenite can be understood in terms of the carbon concentration in residual austenite and the negative slope of the Ae_3 (or Ae'_3) curve [22-25].

However it should be noted that Yang and Bhadeshia ignored the effect of diffusion of carbon in ferrite [22-25], which might have a substantial effect on the reaustenitisation-start temperature. This was examined by comparing the rate constant for the growth of austenite under paraequilibrium calculated by equation 7.40; in which the diffusion of carbon in both phases are taken into account, or equation 7.56; where the diffusion field exists only in austenite. Calculated rate constants for the growth of austenite from two different mixtures of bainitic ferrite and austenite are shown in Fig. 7.16. The calculated rate constant assuming the diffusion field only in austenite is larger than that calculated for the case where the diffusion fields exist in both phases at lower temperatures, whereas the order changes at higher temperatures. This crossover in the rate constants can be interpreted as follows. At a temperature where carbon concentration in residual austenite reaches the Ae'_3 (note that this is not Ae_3) (see Fig. 7.17a), the growth of austenite can start if the diffusion of carbon in ferrite can be ignored. However, the growth of austenite is not yet possible in the case where the diffusion of carbon in both phases should be taken into account, since the negative gradient of carbon exists at the transformation interface in ferrite. This circumstance remains until the temperature is raised to a point at which the fluxes of carbon in ferrite and in austenite cancel each other out (Fig. 7.17b). Above this temperature, the growth of austenite can proceed even in the case where the diffusion of carbon in both phases is considered. In this circumstance, the growth rate of austenite calculated with carbon fluxes in both phases is smaller than that with the carbon diffusion only in austenite because of the negative slope of carbon in ferrite at the transformation interface. When the temperature reaches a point where the carbon concentration in the ferrite matrix is equal to that on the $\alpha/(\alpha + \gamma)$ phase boundary (see Fig. 7.17c), the rate constant calculated by the two different methods becomes identical since there is no flux of carbon in ferrite at the temperature. Above this temperature, the rate constant calculated with diffusion of the carbon in both phases becomes higher than that with the diffusion of carbon only in austenite since the positive flux of carbon in ferrite accelerates the movement of the transformation interface (Fig. 7.17d).

It is also suggested that the smaller the initial carbon concentration in ferrite the larger the difference in reaustenitisation temperatures calculated by the two different methods since more superheating is required to reach the temperature shown in Fig. 7.17b. In fact the difference in reaustenitisation-start temperatures calculated by the two different methods for the case of the bainite transformation at 360 °C was larger than the case of the 420 °C bainite transformation temperature, since in the former case the carbon concentration in the initial ferrite is lower than that of the later (see Table 7.1).

The calculated interface carbon concentrations during reaustenitisation under local equi-

The theory was applied to re-austenitisation from a mixture of bainitic ferrite and austenite, where nucleation of austenite may not be necessary since the initial microstructure contains austenite.

REFERENCES

1. H. K. D. H. Bhadeshia: "Phase Transformations '87", *Institute of Metals, London*, ed. G. W. Lorimer, 1987, 309.
2. A. Hultgren: *Jernkontorets Ann.*, 1951, **135**, 403.
3. E. Rudberg: *Jernkontorets Ann.*, 1952, **136**, 91.
4. M. Hillert: *Jernkontorets Ann.*, 1952, **136**, 25.
5. M. Hillert: *Internal Report, Swedish Institute of Metals Research*. 1953.
6. J. S. Kirkaldy: *Can. J. Phys.*, 1958, **36**, 907.
7. G. R. Purdy, D. H. Weichert and J. S. Kirkaldy: *TMS-AIME*, 1964, **230**, 1025.
8. H. I. Aaronson, H. A. Domian and G. M. Pound: *TMS-AIME*, 1966 **236**, 753.
9. H. I. Aaronson, H. A. Domian and G. M. Pound: *TMS-AIME*, 1966 **236**, 768.
10. D. E. Coates: *Metall. Trans.*, 1972, **3**, 1203.
11. D. E. Coates: *Metall. Trans.*, 1973, **4**, 1077.
12. D. E. Coates: *Metall. Trans.*, 1973, **4**, 2313.
13. H. K. D. H. Bhadeshia: *Progress in Materials Science*, 1985, **29**, 321.
14. R. R. Judd and H. W. Paxton: *TMS-AIME*, 1968, **242**, 206.
15. M. Hillert, K. Nilsson and L-E. Törndahl: *JISI*, 1971 **209**, 49.
16. J. Ågren: *Mat. Sci. and Eng.*, 1982, **55**, 135.
17. M. Hillert: "Mechanism of Phase Transformations in Crystalline Solid", *Monograph 13, Institute of Metals, London*, 1969, 231.
18. J. B. Gilmour, G. R. Purdy and J. S. Kirkaldy: *Metall. Trans.*, 1972, **3**, 1455.
19. J. S. Kirkaldy, B. A. Thomson and E. A. Baganis: "Hardenability Concepts with Applications to Steel", ed. D. V. Doane and J. S. Kirkaldy, *AIME*, 1978, 82.
20. K. Hashiguchi and J. S. Kirkaldy: *CALPHAD*, 1984, **8**, 173.
21. L. C. Brown and J. S. Kirkaldy: *Trans. AIME*, 1964, **230**, 223.
22. J-R. Yang and H. K. D. H. Bhadeshia: "Welding Metallurgy of Structural Steels", *TMS-AIME, Warrendale, Ohio*, ed. J. Y. Koo, 1987, 549.
23. J-R. Yang and H. K. D. H. Bhadeshia: "Phase Transformations '87", *The Institute of Metals, London*, ed. G. W. Lorimer, 1988, 203.
24. J-R. Yang and H. K. D. H. Bhadeshia: *Mat. Sci. and Eng.*, 1989, in press.
25. J-R. Yang: *Ph.D. Thesis, University of Cambridge*, 1988.
26. G. R. Speich and A. Szirmai: *TMS-AIME*, 1969, **245**, 1063.
27. C. I. Garcia and A. J. DeArdo: *Metall. Trans.*, 1981, **12A**, 521.
28. U. R. Lenel and R. W. K. Honeycombe: *Metal Science*, 1984, **18**, 201.
29. U. R. Lenel and R. W. K. Honeycombe: *Metal Science*, 1984, **18**, 503.
30. R. Trivedi and G. M. Pound: *J. Appl. Phys.*, 1967, **38**, 3569.
31. H. K. D. H. Bhadeshia: *Acta Metall.*, 1981, **29**, 1117.
32. H. K. D. H. Bhadeshia and A. R. Waugh: *Proc. of Int. Conf. on "Solid/Solid Phase Transformations"*, *Pittsburgh, ASM, Ohio, U.S.A.*, 1981, 1041.

33. H. K. D. H. Bhadeshia and A. R. Waugh: *Acta Metall.*, 1982, **30**, 775.
34. I. Stark, G. D. W. Smith and H. K. D. H. Bhadeshia: *Proc. of Int. Conf. on "Solid/Solid Phase Transformations"*, Institute of Metals, London, 1989, in press.
35. I. Stark, G. D. W. Smith and H. K. D. H. Bhadeshia: *Proc. of Int. Conf. on "The Bainite Transformation"*, Chicago, U.S.A, A.S.M., 1988, in press.
36. B. Josefsson and H. O. Andren: *Proc. of the 35th Int. Conf. on "Field Emission Symp."*, Oak Ridge, Tennessee, U.S.A. 18-22 July, 1988.
37. H. K. D. H. Bhadeshia and D. V. Edmonds: *Acta Metall.*, 1980, **28**, 1265.
38. H. K. D. H. Bhadeshia: *Metal Science*, 1982, **16**, 167.
39. J. W. Christian: *"The Theory of Transformation in Metals and Alloys"*, second ed. Part 1, Pergamon, Oxford, 1975.
40. M. Enomoto: 1988, Trans. ISIJ, **28**, 826.
41. K. R. Kinsman and H. I. Aaronson: *Metall. Trans.*, 1973, **4**, 959.

APPENDIX

The conservation of mass for the substitutional alloying element in a ternary system is expressed by the following three equations as discussed in the text:

$$v(x_2^{\gamma\alpha} - x_2^{\alpha\gamma}) = -\frac{D_{22}^{\gamma}}{l_{\gamma}}(x_2^{\gamma\alpha} - \bar{x}_2) + \frac{D_{22}^{\alpha}}{l_{\alpha}}(\bar{x}_2 - x_2^{\alpha\gamma}) \quad (7.81)$$

$$\frac{l_{\alpha}}{2}(\bar{x}_2^{\alpha} - x_2^{\alpha\gamma}) = \frac{l_{\gamma}}{2}(x_2^{\gamma\alpha} - \bar{x}_2^{\gamma}) \quad (7.82)$$

$$\int_0^t \frac{D_{22}^{\alpha}(\bar{x}_2^{\alpha} - x_2^{\alpha\gamma})}{l_{\alpha}} dt = \frac{1}{2}(l_{\alpha} + 2z^*)(\bar{x}_2^{\alpha} - x_2^{\alpha\gamma}). \quad (7.83)$$

On eliminating l_{γ} from equations 7.81 and 7.82, a relation between v and l_{α} can be obtained:

$$vl_{\alpha} = -\frac{D_{22}^{\gamma}(x_2^{\gamma\alpha} - \bar{x}_2)^2}{(x_2^{\gamma\alpha} - x_2^{\alpha\gamma})(\bar{x}_2 - x_2^{\alpha\gamma})} + \frac{D_{22}^{\alpha}(\bar{x}_2 - x_2^{\alpha\gamma})}{x_2^{\gamma\alpha} - x_2^{\alpha\gamma}} \quad (7.84)$$

The right hand side of equation 7.84 is independent on time as long as soft impingement does not occur. Equation 7.84 can therefore be rewritten as follows regarding the fact that $v = dz/dt$:

$$l_{\alpha} \frac{dz}{dt} = C_1 \quad (7.85)$$

where C_1 is a constant which is equal to the right hand side of equation 7.84. In equation 7.85 l_{α} and z are both functions of time. Since $l_{\alpha} = 0$ at $t = 0$, it might be reasonable to assume the expression for l_{α} as follows:

$$l_{\alpha} = C_2 t^a \quad (7.86)$$

where C_1 and a are constants. Thus equation 7.85 becomes:

$$\frac{dz}{dt} = \frac{C_1}{C_2} t^{-a} \quad (7.87)$$

leading the expression for z :

$$z = C_3 t^{-a+1} \quad (7.88)$$

where $C_3 = \frac{C_1}{C_2(-a+1)}$ is a constant. On substituting equations 7.86 and 7.88 into 7.83, one can obtain the following expression:

$$\left(\frac{2D_{22}^{\alpha}}{C_2^2(-a+1)} - \frac{2C_3}{C_2} \right) t^{-2a+1} = 1 \quad (7.89)$$

Since equation 7.89 should be satisfied for any value of time t , the time exponent have to be equal to zero:

$$-2a + 1 = 0 \quad (7.90)$$

As a result, $a = 1/2$ is obtained.

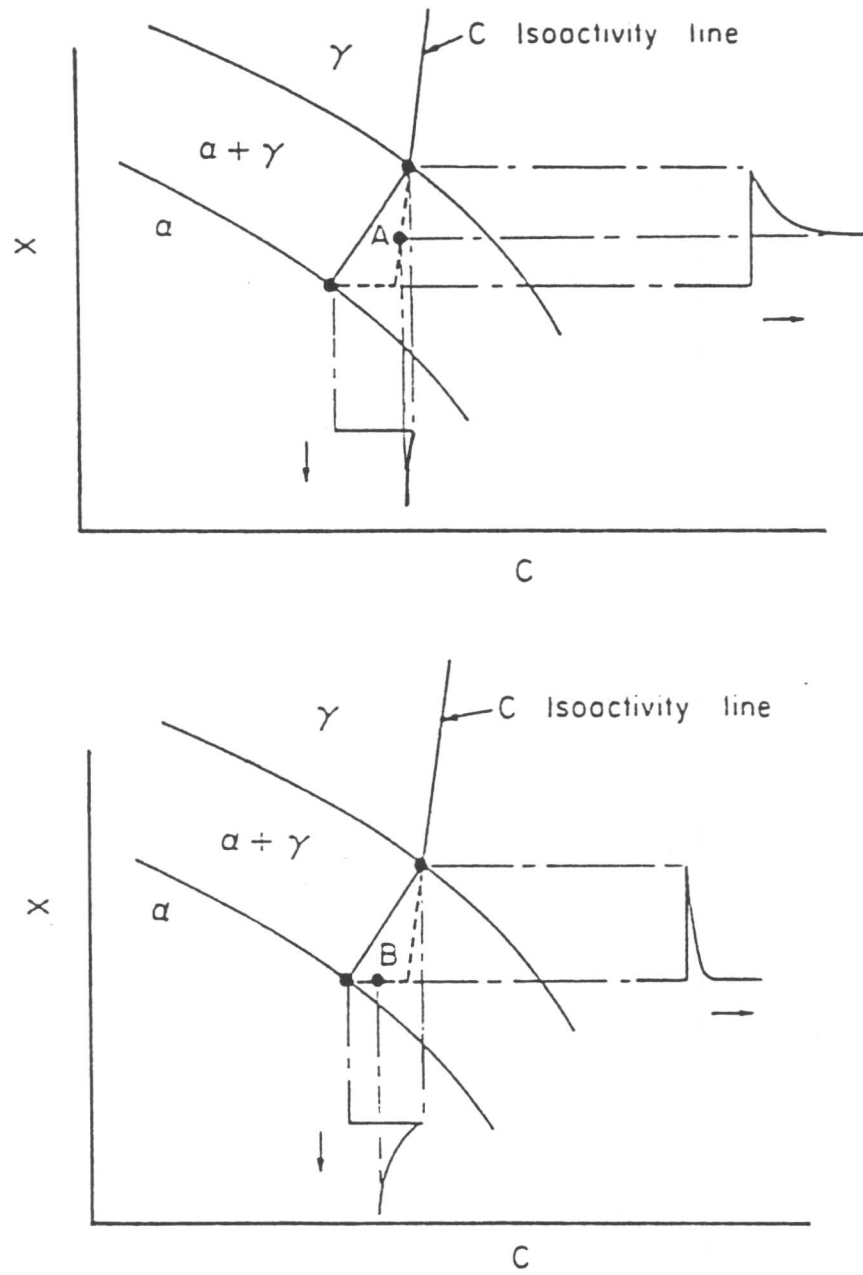


Fig. 7.1 Schematic isothermal section of a Fe-C-X ternary system, illustrating ferrite growth occurring with local equilibrium at the α/γ interface. (a) Growth at low supersaturations (PLE) with bulk composition of X, and (b) growth at high supersaturations (NPLE) with negligible partitioning of X during transformation. The bulk alloy compositions are designated "A" and "B" respectively.

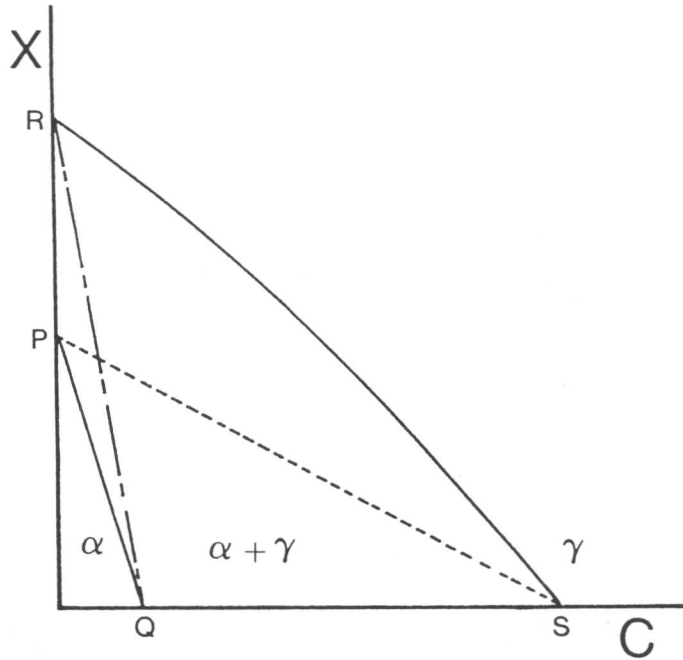


Fig. 7.2 Isothermal section of a ternary Fe-C-X phase diagram, with the $(\alpha + \gamma)$ phase field lying within the region **PQSR**. The decomposition of austenite by the NPLE mechanism can occur if the bulk composition lies in the region **QPS**, whereas the growth of austenite by the NPLE mechanism can only occur if the ferrite is superheated into the region **QRS**.

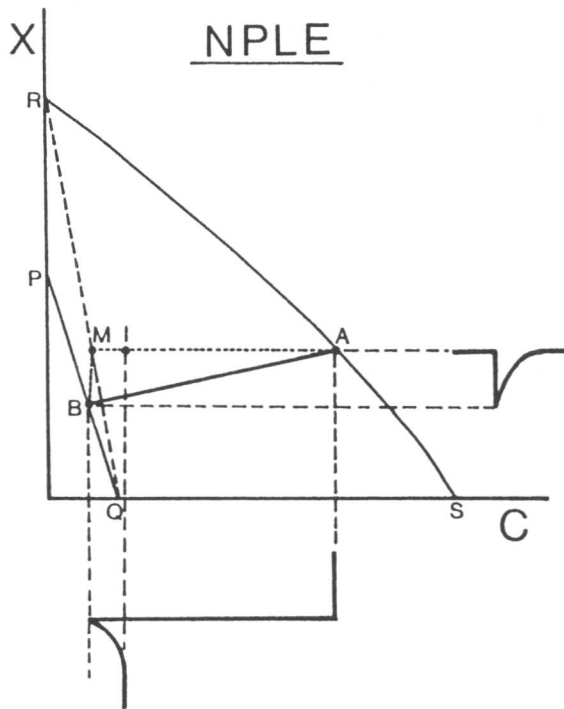


Fig. 7.3 The NPLE growth of austenite as a consequence of the superheating of a fully ferritic sample of bulk composition "I" to a temperature T .

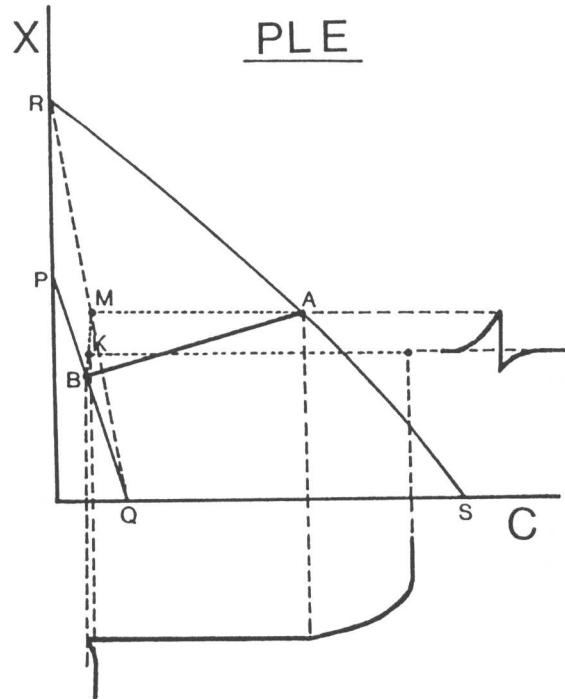


Fig. 7.6 The PLE growth of austenite as a consequence of the superheating of a sample with a mixture of bainitic ferrite and residual austenite initial microstructure of bulk composition "K" to a temperature T .

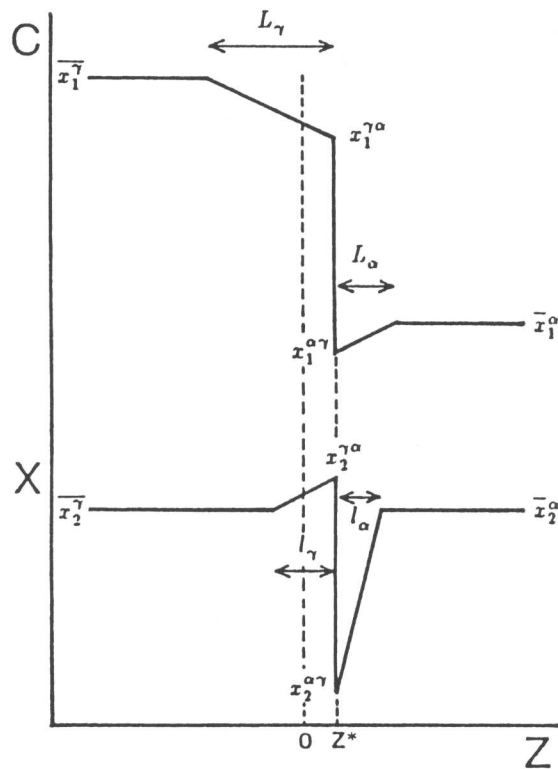


Fig. 7.7 Schematic diagram of carbon and X profiles during reconstructive growth of austenite from a mixture of bainitic ferrite and austenite assuming linear gradients. z^* designate the position of the transformation interface along a space coordinate normal to the interface.

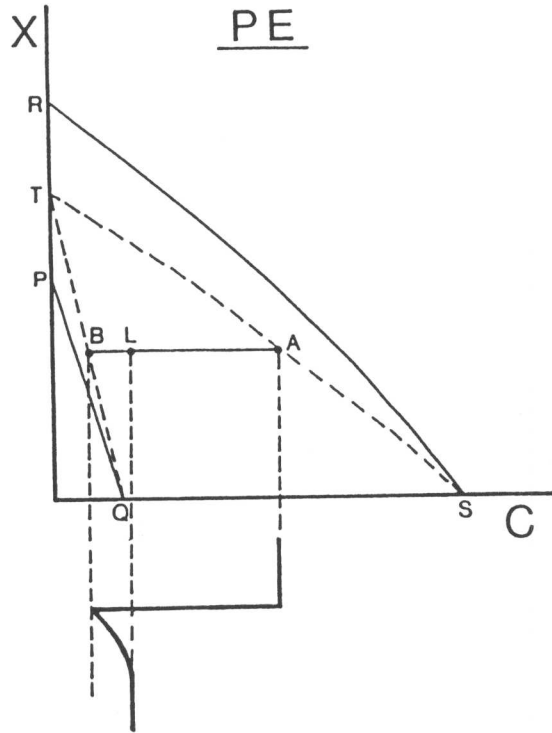


Fig. 7.8 The paraequilibrium growth of austenite as a consequence of the superheating of a fully ferritic sample of bulk composition "L" to a temperature T .

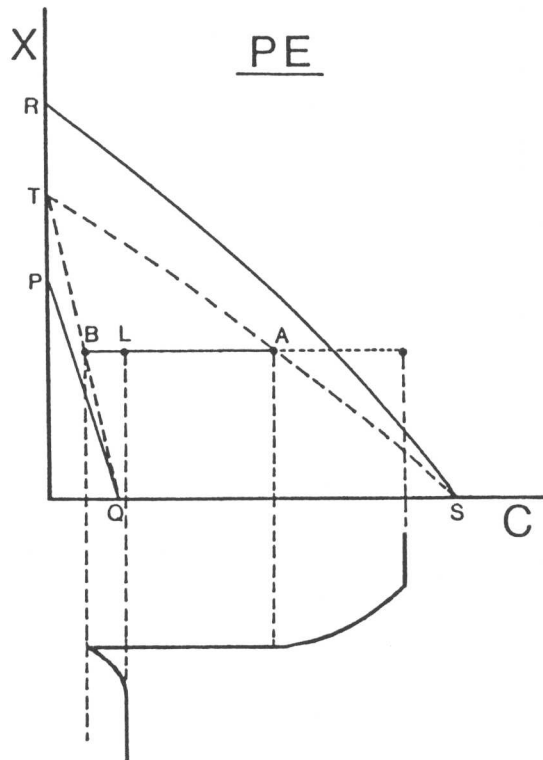


Fig. 7.9 The paraequilibrium growth of austenite as a consequence of the superheating of a sample with a mixture of bainitic ferrite and residual austenite initial microstructure of bulk composition "L" to a temperature T .

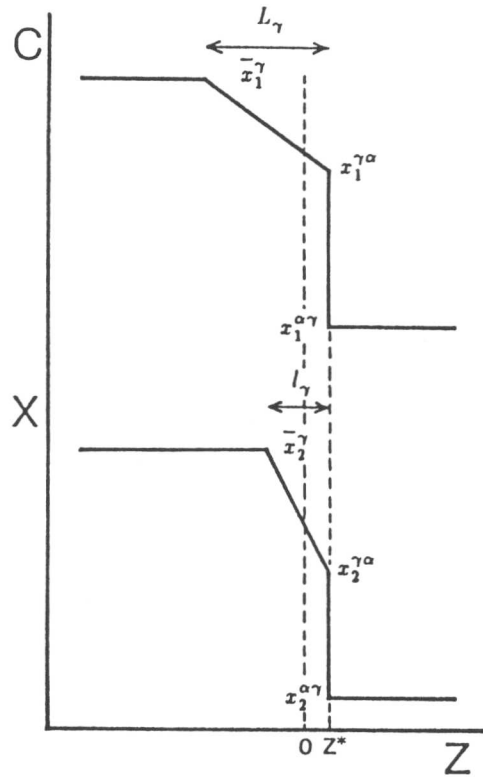


Fig. 7.10 Schematic diagram of carbon and X profiles during the growth of austenite from a fully ferritic initial microstructure assuming linear gradients which exist only in ferrite matrix. z^* designate the position of the transformation interface along a space coordinate normal to the interface.

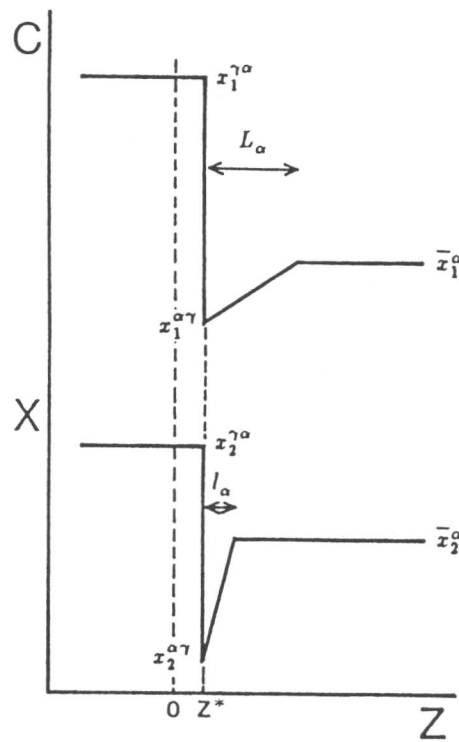


Fig. 7.11 Schematic diagram of carbon and X profiles during the growth of austenite from a mixture of ferrite and austenite assuming linear gradients which exist only in austenite. z^* designate position of the transformation interface along a space coordinate normal to the interface.

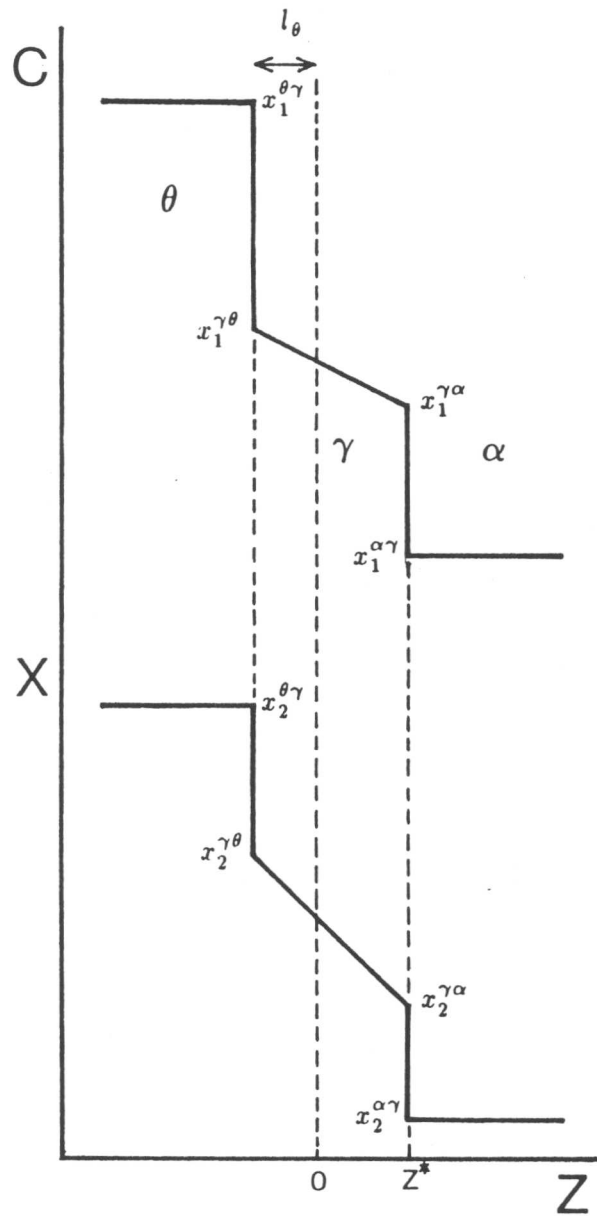


Fig. 7.12 Schematic diagram of carbon and X profiles during the growth of austenite from a mixture of ferrite and cementite particles assuming linear gradients which exist only in austenite. z^* designates the position of the transformation interface along a space coordinate normal to the interface.

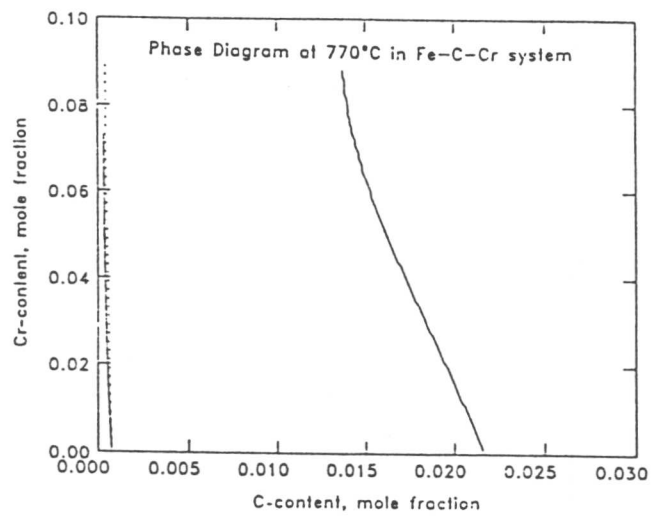
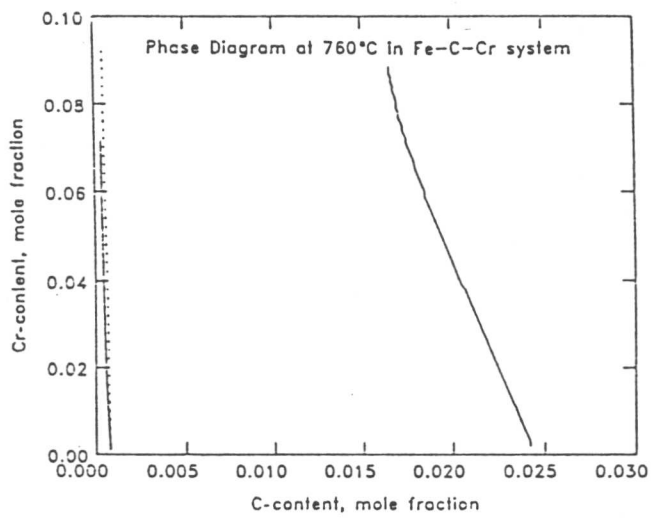
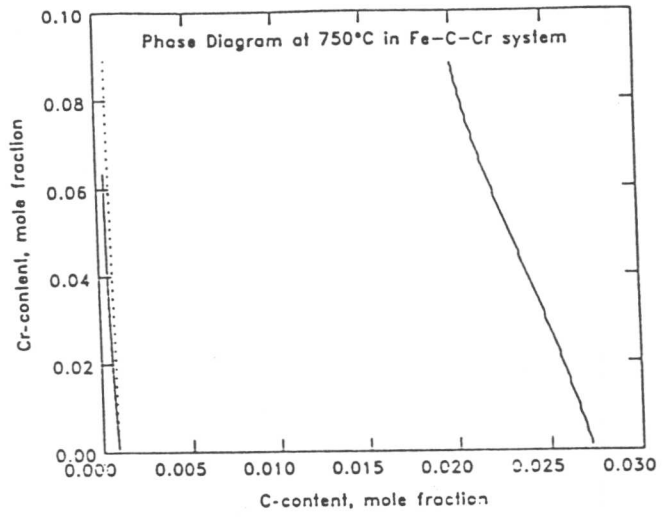


Fig. 7.13 Calculated isothermal sections of the phase diagram in the Fe-0.3C-4.08Cr wt.% alloy at 750, 760 and 770 °C respectively. Dashed lines represent the transition lines from NPLe to PLe condition.

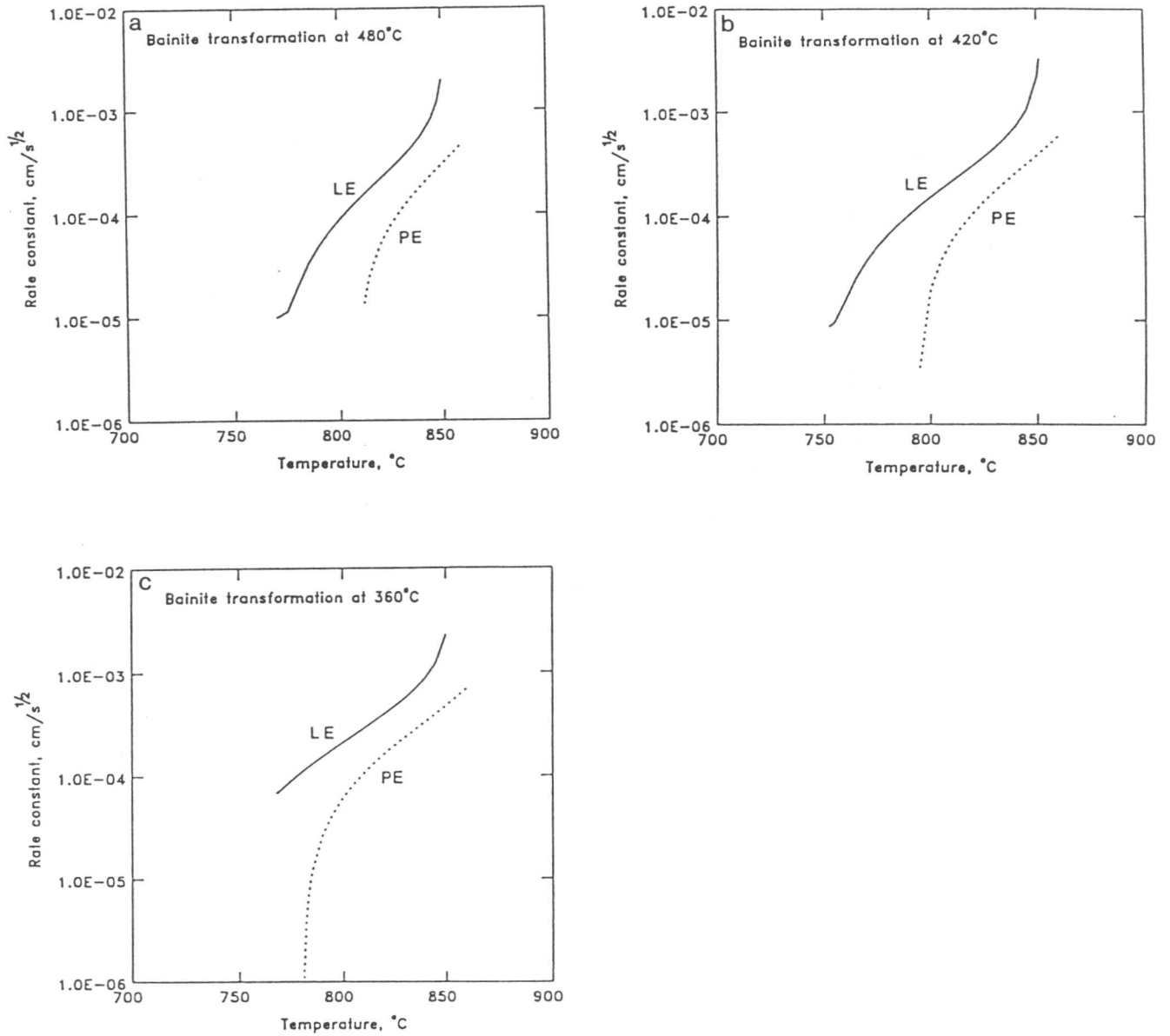


Fig. 7.14 Calculated one dimensional parabolic thickening rate constant of austenite as a function of the reaction temperature during re-austenitisation from a mixture of bainitic ferrite and residual austenite. The bainite transformation treatment was carried out at (a) 480 °C, (b) 420 °C and (c) 360 °C. Solid lines are the rate constant for the local equilibrium growth of austenite and dashed lines for the paraequilibrium growth of austenite.

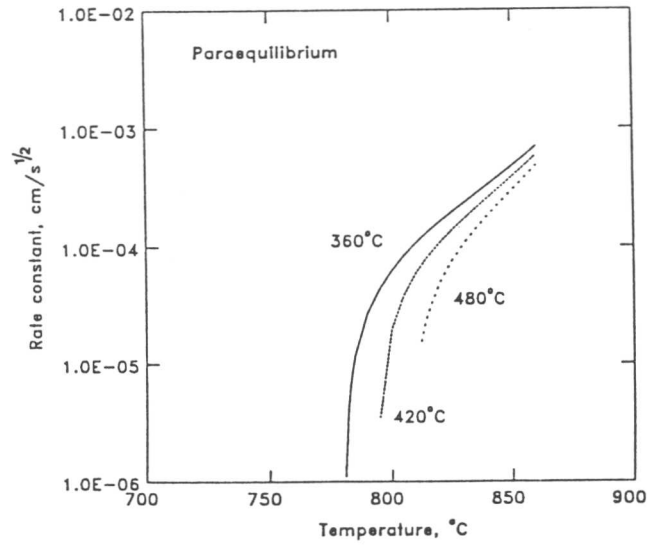


Fig. 7.15 Calculated one dimensional parabolic thickening rate constant of austenite as a function of the reaction temperature during re-austenitisation under paraequilibrium from mixtures of bainitic ferrite and residual austenite obtained at three different bainite transformation temperatures.

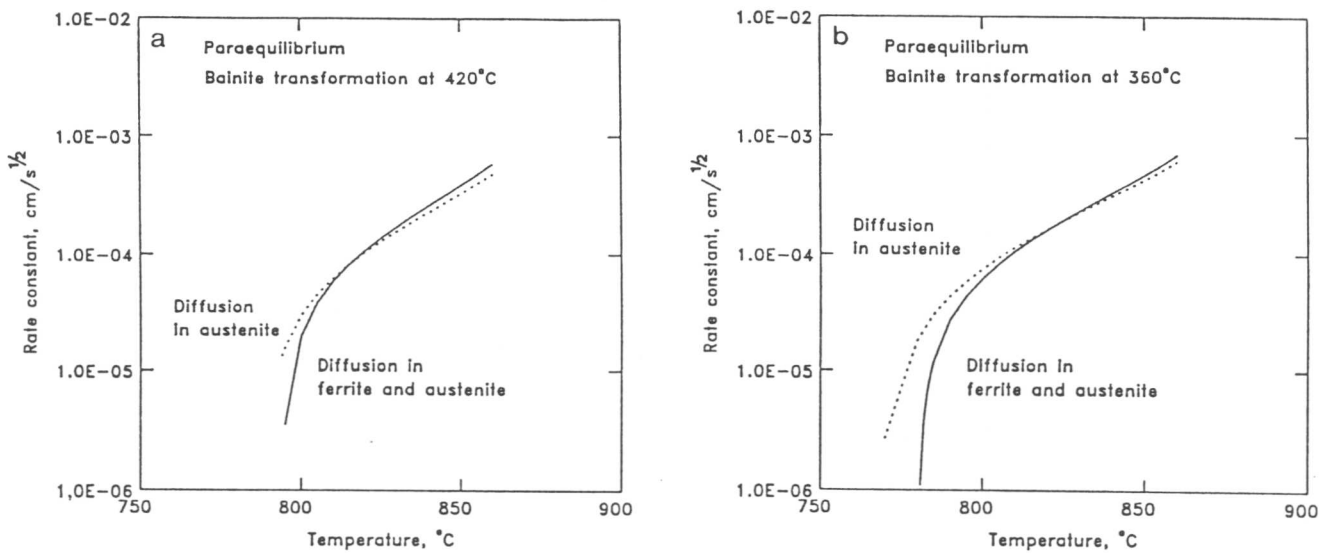


Fig. 7.16 Calculated one-dimensional parabolic thickening rate constant of austenite during re-austenitisation under paraequilibrium from a mixture of bainitic ferrite and residual austenite obtained at (a) 420°C and (b) 360°C. Solid line shows the rate constant as a function of the reaction temperature for the case where diffusion fields exist both in ferrite and austenite, whereas dashed line is for the case with diffusion fields only in austenite.

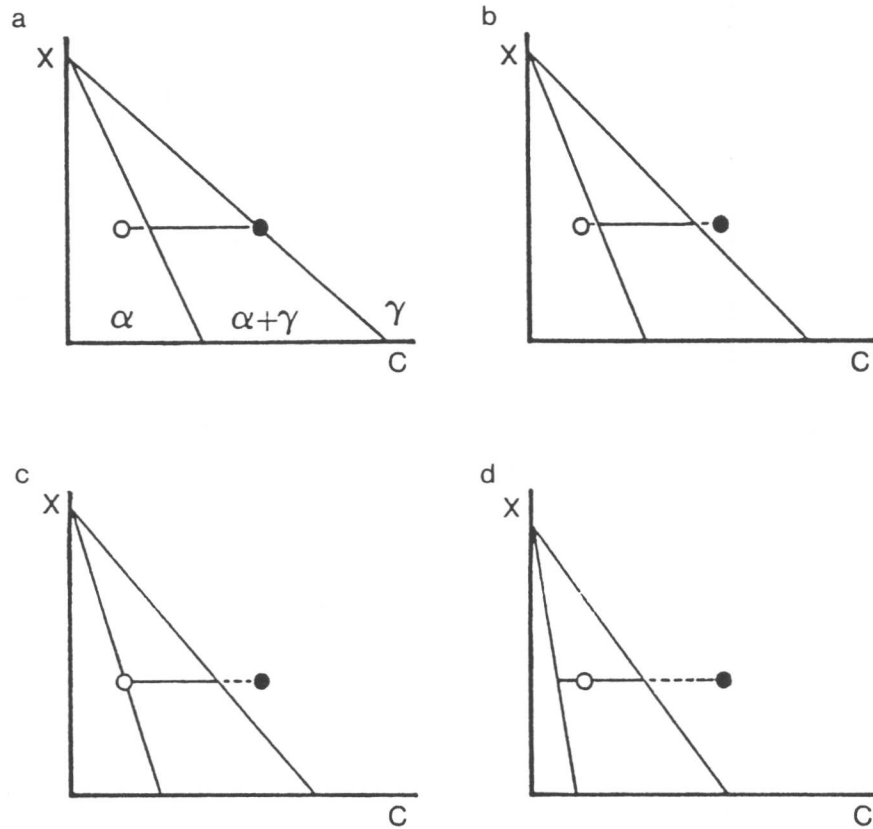


Fig. 7.17 Schematic isothermal sections of the phase diagrams at different temperatures with the paraequilibrium $\alpha/\alpha + \gamma$ and $\gamma/\alpha + \gamma$ phase boundaries, in which the initial carbon concentrations of ferrite and austenite are indicated by open and solid circles respectively.

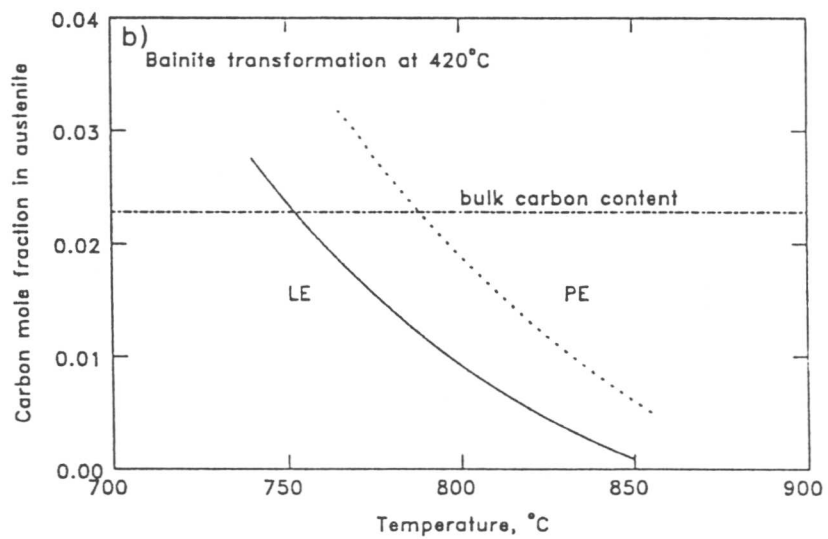
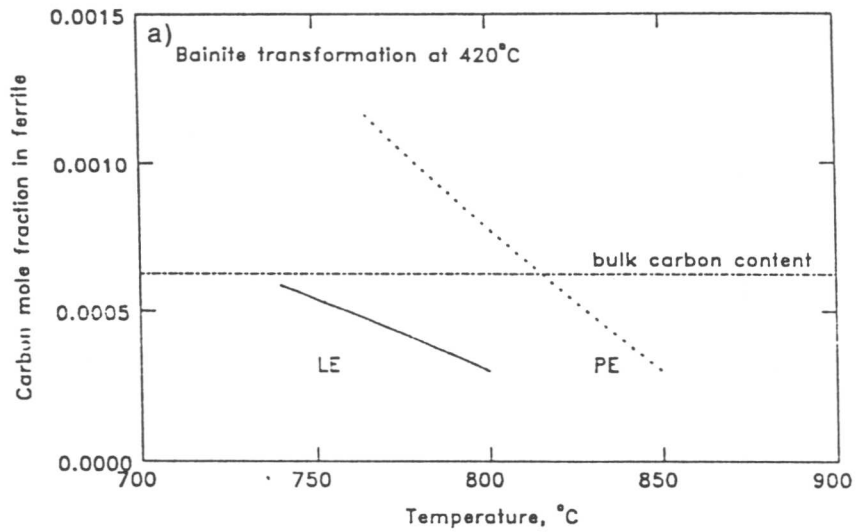


Fig. 7.18 Calculated interface carbon concentrations in ferrite (a) and austenite (b) for the para-equilibrium (solid line) and the local equilibrium (dashed line) growth of austenite from a mixture of bainitic ferrite and austenite formed at 420 °C. Initial carbon concentration in the both phases are also shown.

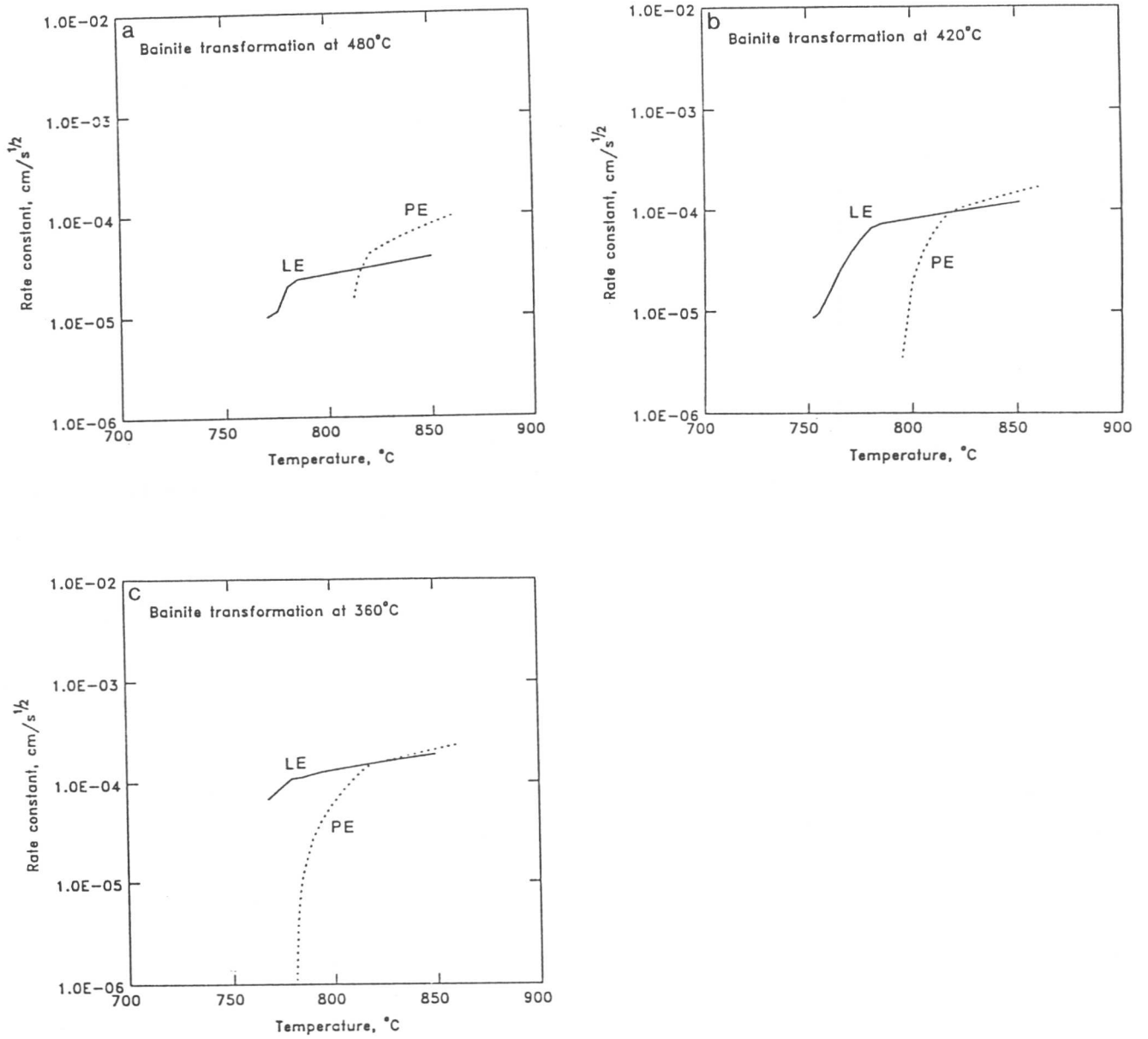


Fig. 7.19 Calculated one dimensional parabolic thickening rate constant of austenite as a function of the reaction temperature during re-austenitisation from a mixture of bainitic ferrite and residual austenite. The bainite transformation treatment was carried out at (a) 480 °C, (b) 420 °C and (c) 360 °C. Solid lines are the rate constant for the local equilibrium growth of austenite and dashed lines for the paraequilibrium growth of austenite. The carbon concentration at the interface in austenite was replaced by the bulk carbon content when the calculated $x_1^{\gamma\alpha}$ becomes smaller than the bulk carbon content.

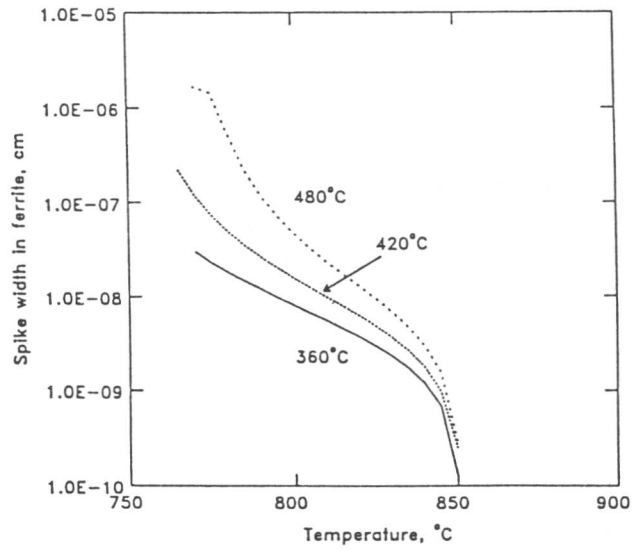


Fig. 7.20 Spike width of the substitutional alloying element calculated by equation 7.80 in the text, as a function of temperature and the initial condition.

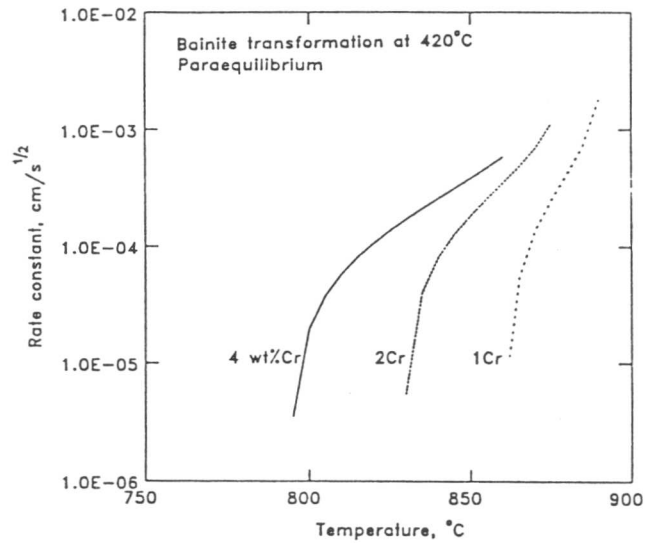


Fig. 7.21 Effect of Cr content on the one dimensional parabolic thickening rate constant of the paraequilibrium growth of austenite. The bainite transformation was carried out at 420°C.

CHAPTER 8

TIME-TEMPERATURE-TRANSFORMATION CURVES AND OVERALL REAUSTENITISATION IN STEELS

8.1 INTRODUCTION

As mentioned in Chapter 1, the prediction of the microstructural development during cooling can be carried out using calculated time-temperature-transformation (TTT) curves for ferrite formation and an assumption of the additivity rule. For many applications, it is just as important to determine TTT curves for reaustenitisation from the initial microstructure of interest. Once TTT curves for various degrees of reaustenitisation are obtained, reaustenitisation during continuous heating, can be calculated adopting Scheil's rule [1] along any heat cycle. This is the major goal of the present work.

8.2 ASSESSMENT OF SCHEIL'S RULE IN REAUSTENITISATION

If the incubation period τ is obtained as a function of temperature, reaustenitisation will start when an integration of τ along a heating pass reaches unity (*i.e.* Scheil's rule)

$$\int_0^{t_s} \tau\{T\}^{-1} dt = 1 \quad (8.1)$$

where the reaction temperature T is now a function of time t , and reaustenitisation starts at time t_s on heating.

The TTT curve for reaustenitisation in a Fe-C-Mn-Ni-Mo alloy reported by Yang [2] (Fig. 8.1) is reanalysed and continuous heating reaustenitisation experiments were conducted on the same alloy as Yang in order to assess the application of Scheil's rule.

Specimens were heated to 1000 °C for 10 min followed by quenching to 460 °C for 30 min allowing the bainite transformation completed. The specimens were then heated directly from the temperature at four different constant heating rates, 5, 10, 20 and 50 °C s⁻¹. Reaustenitisation-start temperatures were determined by deviations of the relative length change from a linear thermal expansion curve. The observed results were plotted against heating rate in Fig. 8.2.

An empirical expression for τ was obtained by regression analysis using Yang's isothermal data for the smallest detectable reaustenitisation from the mixture of bainite and residual austenite:

$$\log \tau = -57.737 \log T + 173.42 \quad (8.2)$$

where τ and T are measured in s and K respectively.

The reaustenitisation start temperatures during continuous heating were calculated using equation 8.2 and are presented in Fig. 8.2. The agreement between experiment and calculation is reasonably good.

8.3 GROWTH OF AUSTENITE

Reaustenitisation in steels proceeds by a nucleation and growth mechanism. When the retained austenite is present in the initial microstructure, it may not be necessary to nucleate new austenite since the reaction can proceed by the growth of the retained austenite.

Assuming one-dimensional growth, and if the austenite/ferrite interfacial area per unit volume is S_V , the increase in volume fraction of austenite ΔV_γ during heat treatment is given by:

$$\Delta V_\gamma = S_V \alpha_1 t^{1/2}. \quad (8.3)$$

Adopting the extended volume concept (see Appendix), ξ the volume fraction of newly transformed austenite normalised by the maximum degree of reaction $\theta = V_\gamma^e - V_{\gamma 0}$ (V_γ^e and $V_{\gamma 0}$ are the equilibrium and initial volume fractions of austenite), is expressed as follows:

$$\xi\{t\} = 1 - \exp\left[-\frac{S_V \alpha_1}{\theta} t^{1/2}\right]. \quad (8.4)$$

When reaustenitisation proceeds not only by the one-dimensional thickening of austenite plates but also by lengthening of the plates, $\xi\{t\}$ should be then expressed by the parabolic thickening rate constants in two directions. Assuming that the initial volume of an austenite plate in the starting microstructure is $a_0 c_0^2$, and that at time t is ac^2 , the volume fraction change ΔV_γ at time t during isothermal reaustenitisation can be expressed as follows:

$$\begin{aligned} \Delta V_\gamma &= n(ac^2 - a_0 c_0^2) \\ &= n\{(a_0 + \alpha_1 t^{1/2})(c_0 + \beta t^{1/2})^2 - a_0 c_0^2\} \\ &= n\{(6a_0 c_0 + c_0^2)\alpha_1 t^{1/2} + (9a_0 + 6c_0)\alpha_1^2 t + 9\alpha_1^3 t^{3/2}\} \end{aligned} \quad (8.5)$$

where β is the parabolic lengthening rate constant which was assumed to be $3\alpha_1$ after [3], and n is the number of growing austenite plates per unit volume. The volume fraction of newly transformed austenite normalised by the maximum degree of reaction θ is thus given by:

$$\xi\{t\} = 1 - \exp\left[-\frac{n}{\theta}\{(6a_0 c_0 + c_0^2)\alpha_1 t^{1/2} + (9a_0 + 6c_0)\alpha_1^2 t + 9\alpha_1^3 t^{3/2}\}\right]. \quad (8.6)$$

Yang and Bhadeshia [4] derived the time required to obtain a small increase in the volume fraction of austenite τ using equation 8.4 as follows:

$$\begin{aligned} \tau &\simeq \left[\frac{\Delta \xi \theta}{S_V \alpha_1}\right]^2 \\ &= \left[\frac{\Delta V_\gamma}{S_V \alpha_1}\right]^2. \end{aligned} \quad (8.7)$$

Therefore the incubation period τ is proportional to α_1^{-2} . If this theory is acceptable, the plot of $\log\{\tau\}$ against $\log\{\alpha_1^{-2}\}$ should show a linear correlation as shown by Yang [2]. It should be noted, however, that there are poor linear correlations between τ and α_1^{-2} as shown in Fig. 8.3 a. The slopes of the *log-log* plot are 1.56 for the smallest detectable reaustenitisation and 1.80 for the 0.05 of increase in the volume fraction of austenite (Fig. 8.3 b), which are expected to be unity from the theory. When $\log\{-\ln\{1 - \xi\}\}$ is plotted against $\log\{t\}$, the slope of the plot should be 1/2 in Yang's theory at the early stage of reaustenitisation. The slope of the plot is, however, not always 1/2 as shown in Fig. 8.4. These results may indicate that equation 8.6 could be more appropriate for an expression of the kinetics of reaustenitisation from a mixture of bainitic ferrite and austenite than equation 8.4. For simplification, the initial dimension of the retained austenite is assumed here to be $a_0 = 0.2 \mu\text{m}$ and $c_0 = 5 \mu\text{m}$. Equation 8.6 becomes as follows:

$$\xi\{t\} = 1 - \exp\left[-\frac{31n\alpha_1}{\theta}t^{1/2}\{1 + 1.03\alpha_1t^{1/2} + 0.29\alpha_1^2t\}\right]. \quad (8.8)$$

The slope of the plot of $\log\{-\ln\{1 - \xi\}\}$ against $\log\{t\}$ varies with α_1 as shown in Fig. 8.5. The slope should then vary with temperature since α_1 depends on the reaction temperature. The slope of the plot of $\log\{-\ln\{1 - \xi\}\}$ against $\log\{t\}$ varies from 0.51 to 1.42 when α_1 is altered between 0.01 and 10 $\mu\text{m s}^{-1/2}$. When α_1 becomes 1.0 $\mu\text{m s}^{-1/2}$ ($1 \times 10^{-4} \text{ cm s}^{-1/2}$), the slope reaches around unity.

Using calculated parabolic thickening rate constants for Yang's alloy [2] and for the Fe-0.3C-4.08Cr wt.% alloy, the slopes of the plot of $\log\{-\ln\{1 - \xi\}\}$ against $\log\{t\}$ calculated as discussed above were compared with the observed slopes at 680, 700 and 710 °C for Yang's alloy [2] and at 778, 785 and 805 °C for the Fe-0.3C-4.08Cr wt.% alloy (Fig. 8.6). A reasonable agreement between experiment and calculated results was obtained. This suggests that equation 8.6 is applicable to the kinetic calculation of reaustenitisation from mixtures of bainitic ferrite and austenite where the initial austenite is plate in shape and grows in two directions; *i.e.* lengthening and thickening.

The effective number of austenite plates per unit volume which can grow during reaustenitisation; *i.e.* the number n in equation 8.6, can be evaluated from the observed data discussed above. The 50% reaustenitisation time (*i.e.* the time for $\xi = 0.5$) was used. The calculated n values are 1.30×10^{-4} at 680 °C, 2.91×10^{-5} at 700 °C and 5.49×10^{-4} at 710 °C for Yang's alloy, and 4.30×10^{-4} at 778 °C, 8.31×10^{-4} at 785 °C and 5.33×10^{-4} at 805 °C for the Fe-0.3C-4.08Cr wt.% alloy. Although there are significant scatter in the calculated n values, especially in Yang's alloy, the average value for each alloy is used for further analysis since the same starting microstructure was used for each alloy.

The TTT curve for a 0.05 increase in the volume fraction of austenite (*i.e.* $\Delta V_\gamma = 0.05$) was calculated and compared with the observed data [2] in Fig. 8.7. A reasonable agreement was obtained at high temperatures but not at temperatures below 690 °C. This may be because the theory does not take into account of the effect of soft impingement. Since the maximum degree of reaction at low temperatures is not very large in comparison with 0.05, the growth rate of austenite may decrease significantly by soft impingement before ΔV_γ reaches 0.05.

The effect of reaction temperature on the increase in the volume fraction of austenite was calculated using equation 8.6 for the Fe-0.3C-4.08Cr wt.% alloy with bainite + 0.3 of retained austenite starting microstructure (Fig. 8.8). The calculated results were rearranged to show the TTT curves for different degrees of ΔV_γ (Fig. 8.9). The calculated TTT curve for $\Delta V_\gamma = 0.05$ was compared with the observed values in the present experiments (Fig. 8.10). The agreement is reasonably good. It should, however, be noted that the formation of austenite was observed *during* heating when the reaction temperature is higher than 785 °C. The observed values in Fig. 8.10 may represent overestimates.

8.4 AUSTENITE FORMATION INCLUDING NUCLEATION AND GROWTH

Examples of the nucleation and growth reaustenitisation processes include the reheating of martensite or mixtures of ferrite and carbides. Although the morphology of the austenite formed depends strongly on the initial microstructure (Chapter 6), the simplest assumption is the spherical austenite model. The growth is then three-dimensional and the appropriate parabolic rate constant α_3 is used. The formation of austenite is assumed to occur from a carbon supersaturated ferrite matrix. The paraequilibrium carbon concentration at 500 °C was

used, without any proof, as the matrix carbon concentration after tempering during heating, since there is no knowledge about the amount of carbon left in the matrix before the reaction. The rate constant α_3 is given by [5]:

$$\begin{aligned}\frac{x_1^{\alpha\gamma} - \bar{x}_1^\alpha}{x_1^{\alpha\gamma} - x_1^{\gamma\alpha}} &= H_3\{D_{11}^\alpha\} - \frac{B_1 D_{12}^\alpha}{D_{11}^\alpha - D_{22}^\alpha} [H_3\{D_{22}^\alpha\} - H_3\{D_{11}^\alpha\}] \\ \frac{x_2^{\alpha\gamma} - \bar{x}_2^\alpha}{x_2^{\alpha\gamma} - x_2^{\gamma\alpha}} &= H_3\{D_{22}^\alpha\}\end{aligned}\quad (8.9)$$

where

$$\begin{aligned}H_3\{D_{ii}^\alpha\} &= \frac{\alpha_3^2}{2D_{ii}^\alpha} \left[1 - \left(\frac{\pi}{4D_{ii}^\alpha} \right)^{0.5} \alpha_3 \exp\left\{ \frac{\alpha_3^2}{4D_{ii}^\alpha} \right\} \operatorname{erfc}\left\{ \left(\frac{\alpha_3^2}{4D_{ii}^\alpha} \right)^{0.5} \right\} \right] \\ B_1 &= \frac{x_2^{\alpha\gamma} - x_2^{\gamma\alpha}}{x_1^{\alpha\gamma} - x_1^{\gamma\alpha}}\end{aligned}$$

where D_{11}^α and D_{22}^α are diffusivities of carbon and substitutional alloying element in ferrite, and the x 's are chemical compositions at the interface.

Using the extended volume concept with the nucleation rate I and the growth rate α_3 , the volume fraction of austenite ξ at time t normalised by the maximum degree of reaction θ (note that θ here is equal to V_γ^e) is given by:

$$\begin{aligned}\xi\{t\} &= 1 - \exp\left[- \int_0^t I \frac{4}{3\theta} \pi \alpha_3^3 (t-t')^{3/2} dt'\right] \\ &= 1 - \exp\left[- \frac{4\pi\alpha_3^3}{3\theta} \int_0^t I(t-t')^{3/2} dt'\right].\end{aligned}\quad (8.10)$$

The nucleation rate I is a function of temperature, driving force for nucleation, site density and time. To simplify the calculation, I is assumed to have the following form:

$$I\{t\} = N_0 \nu_1 \exp(-\nu_1 t) \quad (8.11)$$

where N_0 is the initial nucleation site density and ν_1 is the rate constant for nucleation. Substituting the expression of I into equation 8.10, the following relation is obtained:

$$\xi\{t\} = 1 - \exp\left[- \frac{4\pi\alpha_3^3 N_0 \nu_1}{3\theta} \int_0^t \exp\{-\nu_1 t'\} (t-t')^{3/2} dt'\right]. \quad (8.12)$$

The total number of particles N at time t can be calculated from equation 8.11, namely;

$$N\{t\} = \int_0^t I dt' = \int_0^t N_0 \nu_1 e^{-\nu_1 t'} dt' = N_0 (1 - e^{-\nu_1 t}). \quad (8.13)$$

Therefore, the time required to exhaust 95% of the nucleation sites is roughly equal to $3/\nu_1$.

At a temperature T , the following relation can be obtained from equation 8.12 and be used to determine the values ν_1 and N_0 .

$$\log\{-\ln\{1 - \xi\}\} = \log K_T + \log\left[\int_0^t e^{-\nu_1 t'} (t-t')^{3/2} dt'\right] \quad (8.14)$$

where $K_T = 4\pi\alpha_3^3 N_0 \nu_1 / 3\theta$. By altering the value ν_1 in the second term, the slope of the plot of the both sides of the equation against $\log t$ can be made identical. Then the value ν_1 obtained here will be substituted into the expression of K_T giving the value N_0 at temperature

T using the calculated α_3 from thermodynamic knowledge as discussed earlier. Once the values in equation 8.12 are obtained, the time required to obtain the increase in the volume fraction of austenite ΔV_γ can be obtained.

When the rate constant ν_1 in the nucleation function is altered, the slope of the plot of $\log\{-\ln\{1-\xi\}\}$ against $\log\{t\}$ decreases with ν_1 as it can be seen in Fig. 8.11. Since the slopes of the plot which were obtained in the present experiments (Fig. 8.12) were close to unity between 778 and 805 °C, the rate constant ν_1 is said to be about 2.0 s^{-1} in this temperature range. Using the normalised volume fraction, $\nu_1 = 2.0\text{ s}^{-1}$ and α_3 (Fig. 8.13) which was calculated using equation 8.9 with the thermodynamic equations discussed in Chapter 7, the initial nucleation site density N_0 was obtained as a function of the reaction temperature (Fig. 8.14). N_0 increases slightly with reaction temperature, which may assist in increasing the rate of reaustenitisation with reaction temperature. Using N_0 , ν_1 and α_3 , the effect of temperature on the kinetics of reaustenitisation was calculated (Fig. 8.15).

8.5 CONCLUSIONS

The diffusional growth theory discussed in the previous chapter was applied to overall reaustenitisation either from mixtures of bainite and austenite where growth of the pre-existing austenite dominates the reaction, or from a martensitic initial microstructure where the nucleation of austenite is necessary. The analysis leads the following concluding remarks.

- 1) Reaustenitisation from mixtures of bainite and austenite can be expressed by the parabolic growth theory of the pre-existing austenite films.
- 2) Reaustenitisation from the mixture of bainite and austenite seems to proceed by the growth of the pre-existing austenite films in two directions; lengthening and thickening.
- 3) Observed time-temperature-transformation curves for reaustenitisation from the mixtures of bainite and austenite can be reproduced successfully by the growth theory.
- 4) The formation of austenite including nucleation and growth was modelled using a simple expression for nucleation and the three-dimensional parabolic rate constant.
- 5) This analysis showed that the initial nucleation site density of austenite from the martensitic initial microstructure increases with reaction temperature.

REFERENCES

1. J. W. Christian: *"The Theory of Transformation in Metals and Alloys"*, 2nd ed. Part 1, Pergamon, Oxford, 1981.
2. J-R. Yang: *Ph. D. Thesis, University of Cambridge* 1988.
3. J. R. Bradley, J. M. Rigsbee and H. I. Aaronson: *Metall. Trans. A*, 1977, **8A**, 323.
4. J-R. Yang and H. K. D. H. Bhadeshia: *"Welding Metallurgy of Structural Steels"*, TMS-AIME, Warrendale, Ohio, ed. J. Y. Koo, 1987, 549.
5. D. E. Coates: *Metall. Trans.*, 1973, **4**, 1077.

8.6 APPENDIX

When there are n^e interfaces between α and γ per unit volume at the beginning of the reaction, and these thicken parabolically, the actual volume fraction of newly formed austenite is V_γ and the volume fraction of newly formed austenite assuming that there is no impingement is V_γ^e , the increase in V_γ and V_γ^e ; *i.e.* dV_γ and dV_γ^e , can be expressed by the increase in the thickness of austenite dq as follows:

$$dV_\gamma = n dq$$

$$dV_\gamma^e = n^e dq$$

where n is the number of interfaces per unit volume which can grow at time t . Since the thickness of ferrite plates has a distribution, a thinner ferrite plate can be exhausted by growing austenite earlier than a thicker one. So the number of interfaces which has already been encountered by the adjacent interface is $\Delta n = n^e - n$. Although the distribution function of the thickness of ferrite plates is not known, the simplest assumption is $\Delta n = \frac{V_\gamma}{\theta} n^e$, where $\theta = 1 - V_{\gamma 0}$ with the initial volume fraction of austenite given by $V_{\gamma 0}$. Therefore the relation between dV_γ and dV_γ^e is as follows:

$$\begin{aligned} dV_\gamma &= \frac{n}{n^e} dV_\gamma^e \\ &= \frac{n^e - (V_\gamma/\theta)n^e}{n^e} dV_\gamma^e \\ &= \left(1 - \frac{V_\gamma}{\theta}\right) dV_\gamma^e \end{aligned}$$

which leads to the relation:

$$-\theta \ln\left\{1 - \frac{V_\gamma}{\theta}\right\} = V_\gamma^e.$$

Therefore,

$$\frac{V_\gamma}{\theta} = 1 - \exp\left\{-\frac{V_\gamma^e}{\theta}\right\}$$

which is the same as the extended volume concept.

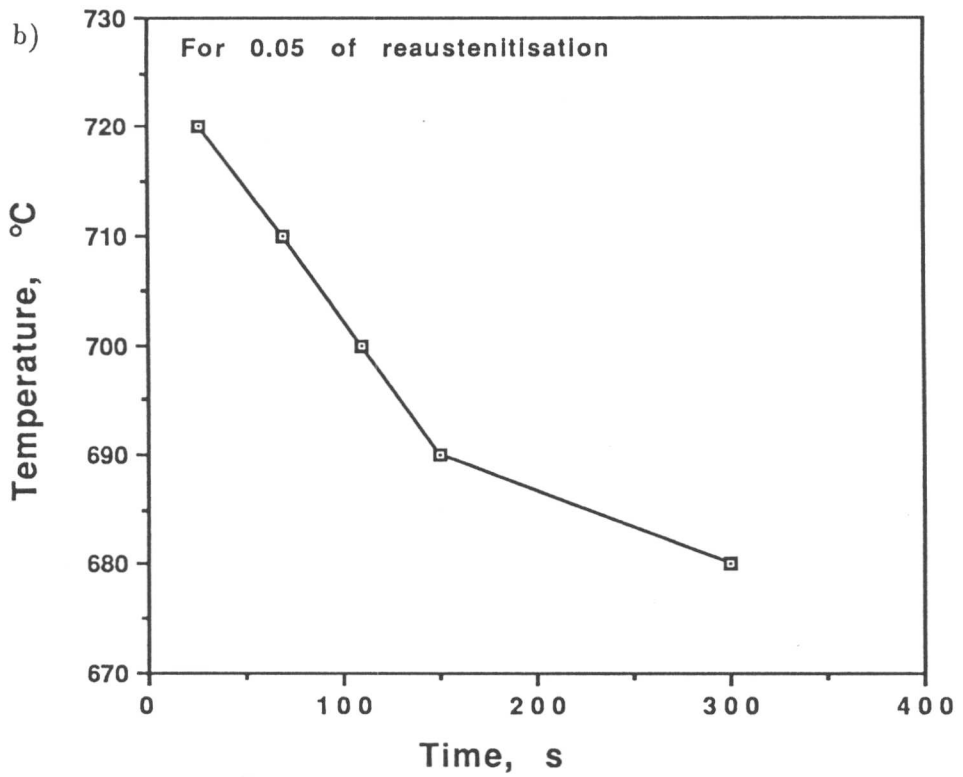
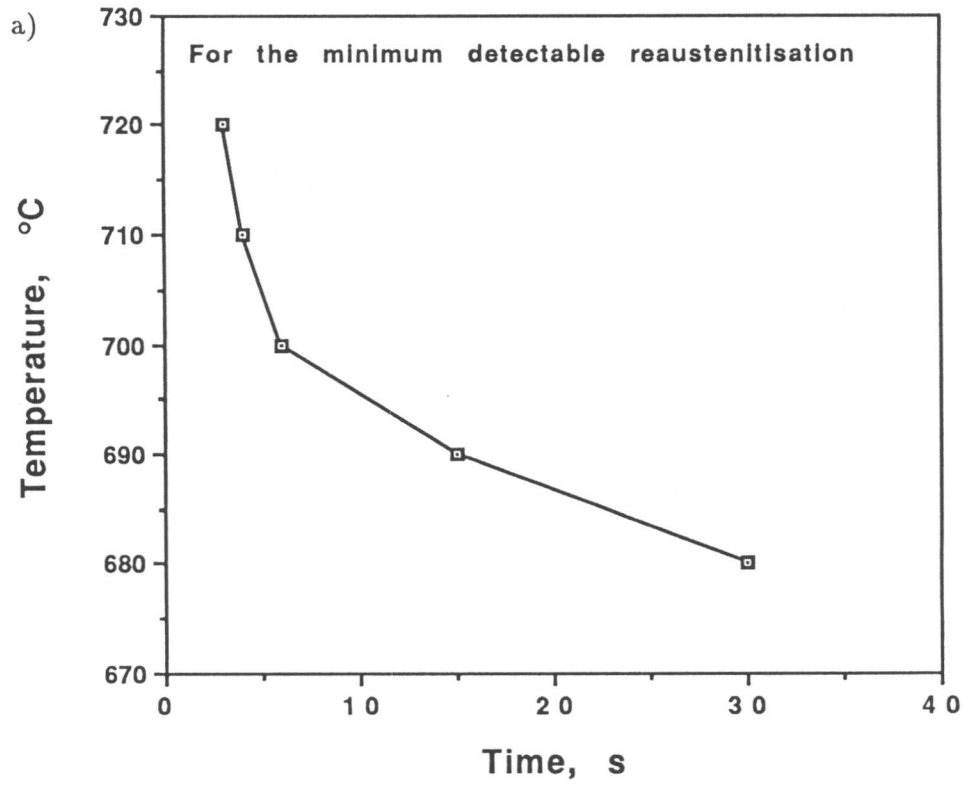


Fig. 8.1 TTT curves for reaustenitisation from a mixture of bainite and austenite in a Fe-C-Mn-Ni-Mo alloy (after Yang [2]). a) is for the minimum detectable reaustenitisation and b) for 0.05 of increase in the volume fraction of austenite.

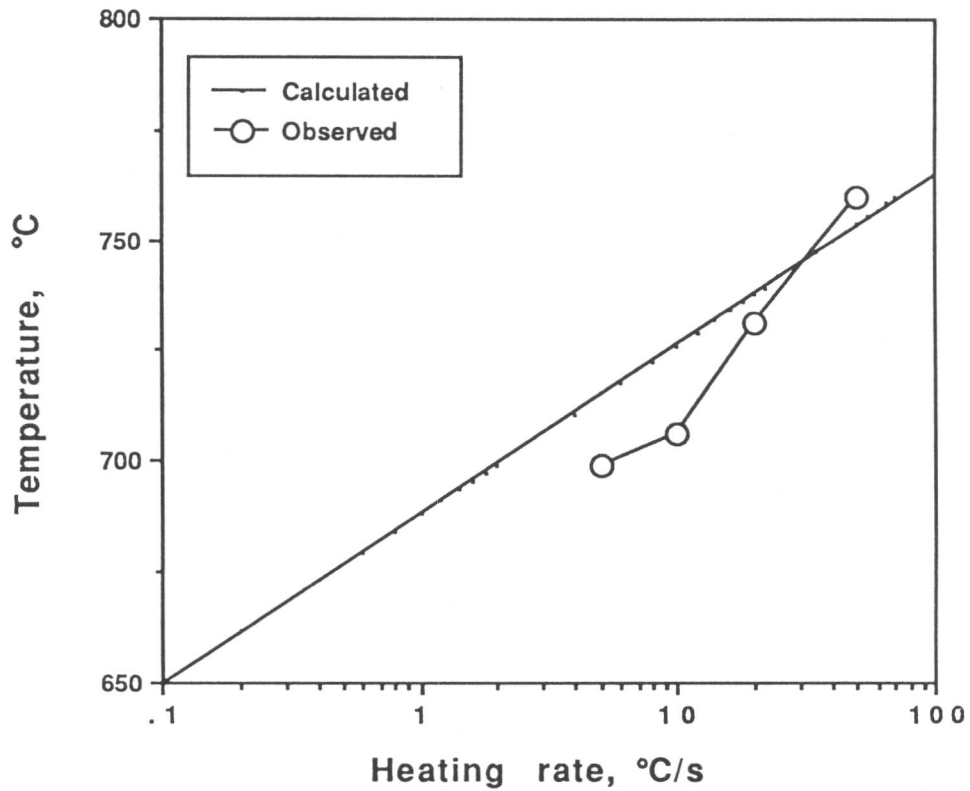


Fig. 8.2 Calculated (line) and observed (plots) re-austenitisation-start temperatures during continuous heating at constant heating rates from a mixture of bainite and austenite in the Fe-C-Mn-Ni-Mo alloy as a function of heating rate.

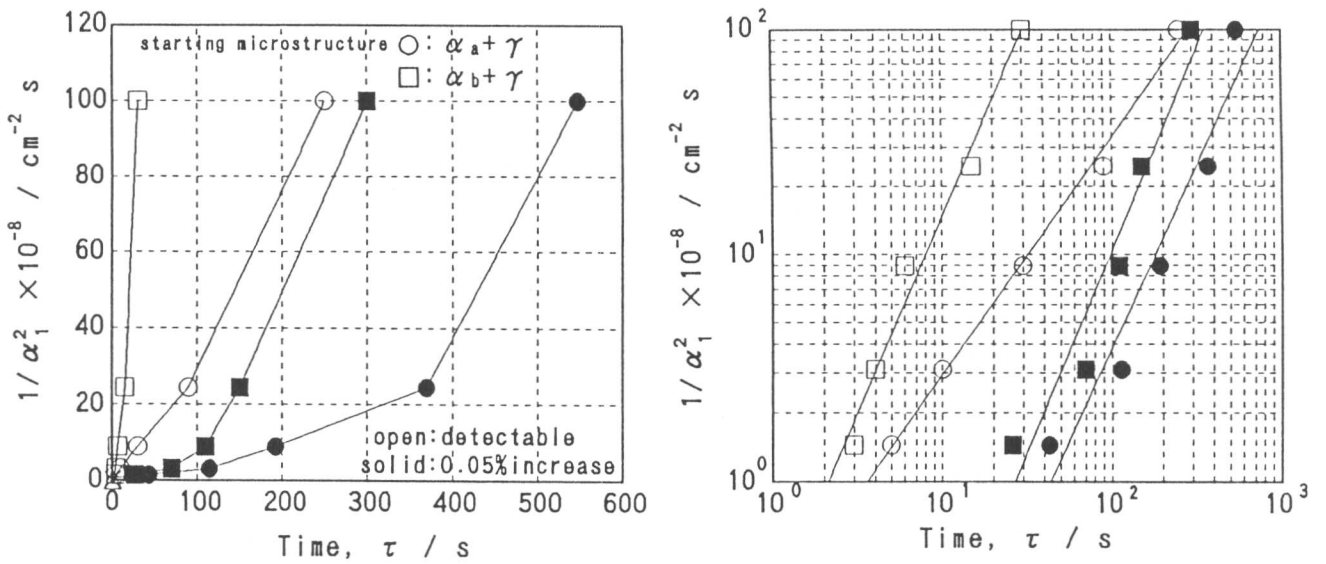


Fig. 8.3 Relation between τ and α_1^{-2} plotted (a) in linear scale and (b) in logarithmic scale.

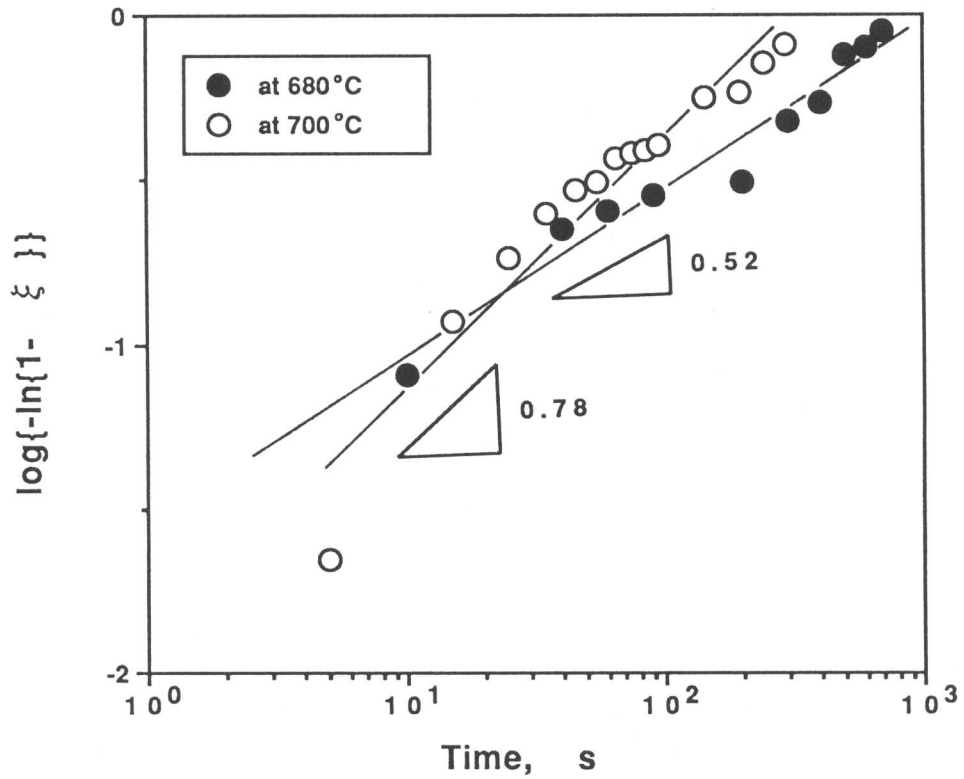


Fig. 8.4 $\log\{-\ln\{1 - \xi\}\}$ v.s. $\log\{t\}$ plots in the Fe-C-Mn-Ni-Mo alloy (after Yang [4]).

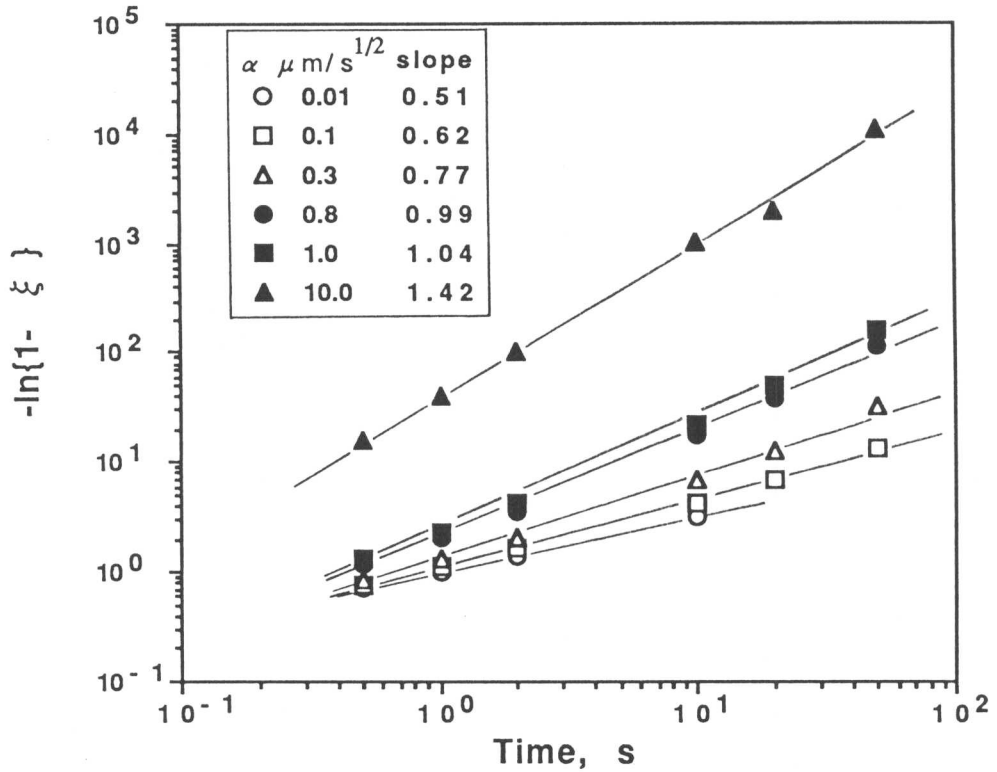


Fig. 8.5 Change in the slope of the plot of $\log\{-\ln\{1 - \xi\}\}$ against $\log\{t\}$ with the parabolic thickening rate constant α_1 .

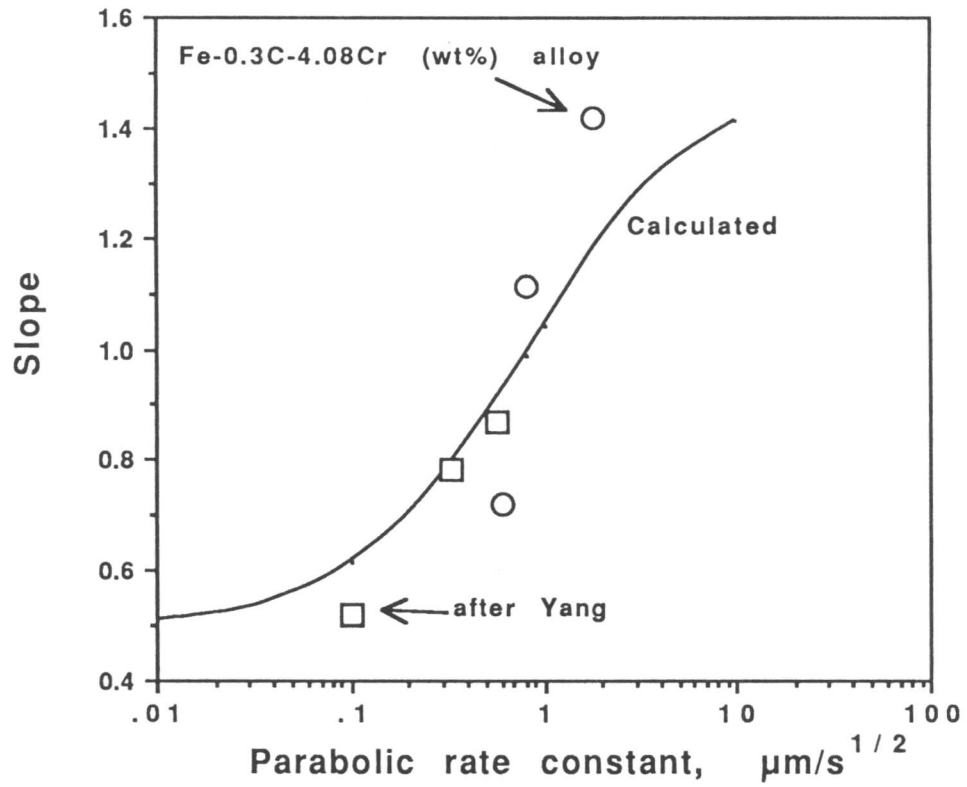


Fig. 8.6 Comparison between observed and calculated slopes of the plot of $\log\{-\ln\{1-\xi\}\}$ against $\log\{t\}$.

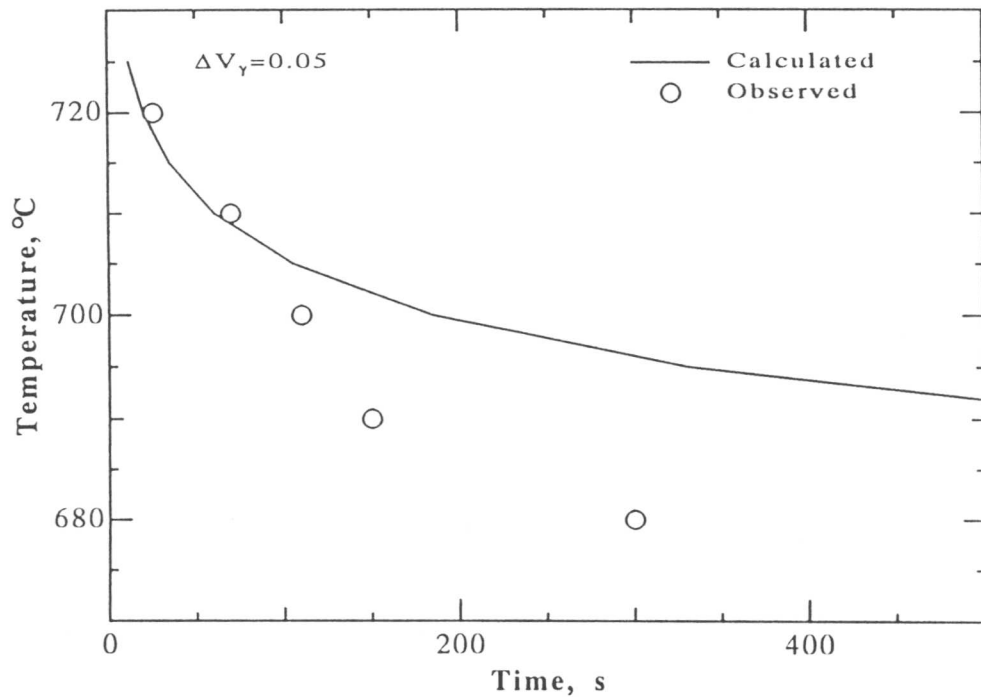


Fig. 8.7 Comparison between calculated (line) and observed (plots [4]) TTT curves for re-austenitization from the mixture of bainite and austenite in the Fe-C-Mn-Ni-Mo alloy.

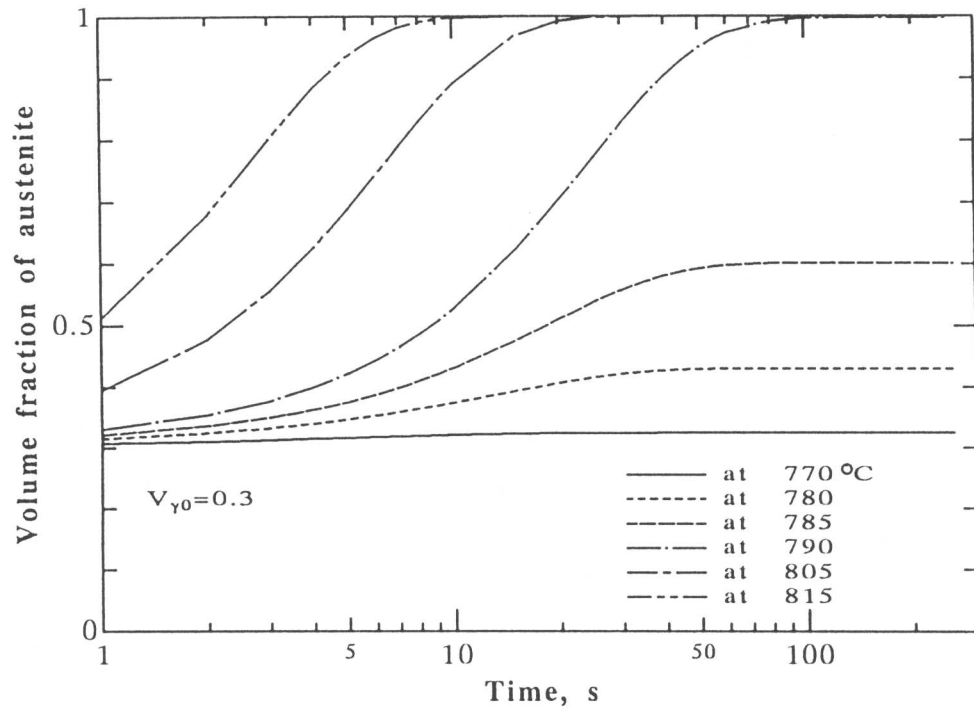


Fig. 8.8 Calculated reaustenitisation behaviour showing the effect of the reaction temperature on the kinetics of reaustenitisation.

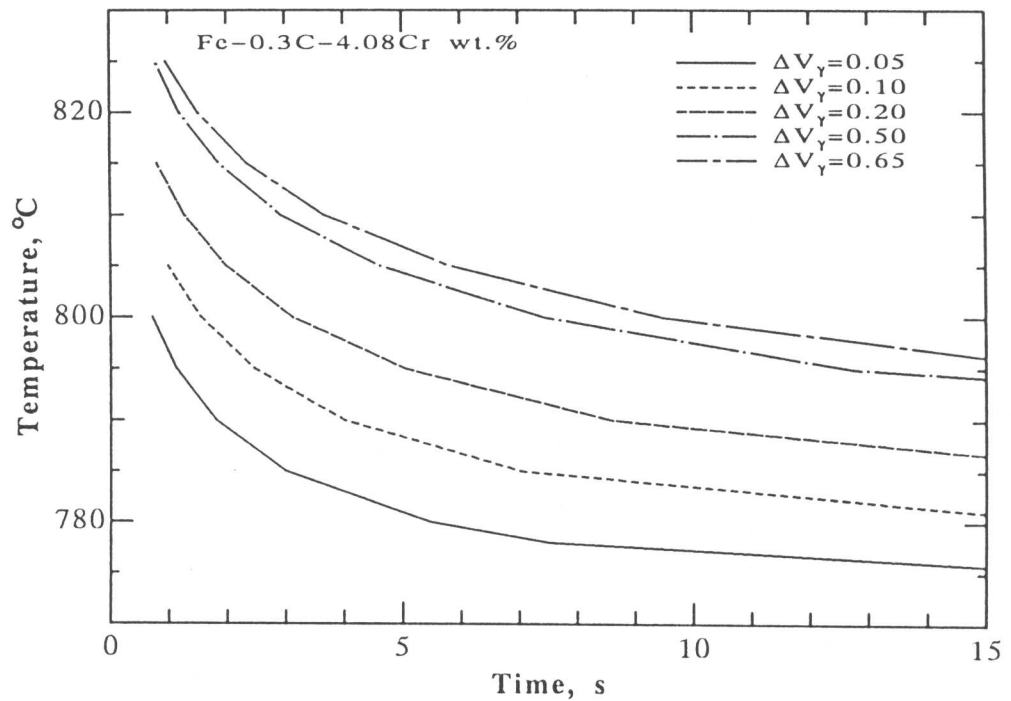


Fig. 8.9 Calculated TTT curves for $\Delta V_{\gamma} = 0.05, 0.10, 0.20, 0.50$ and 0.65 of reaustenitisation from the bainite + 30% of austenite obtained at 420°C in the Fe-0.3C-4.08Cr wt.% alloy.

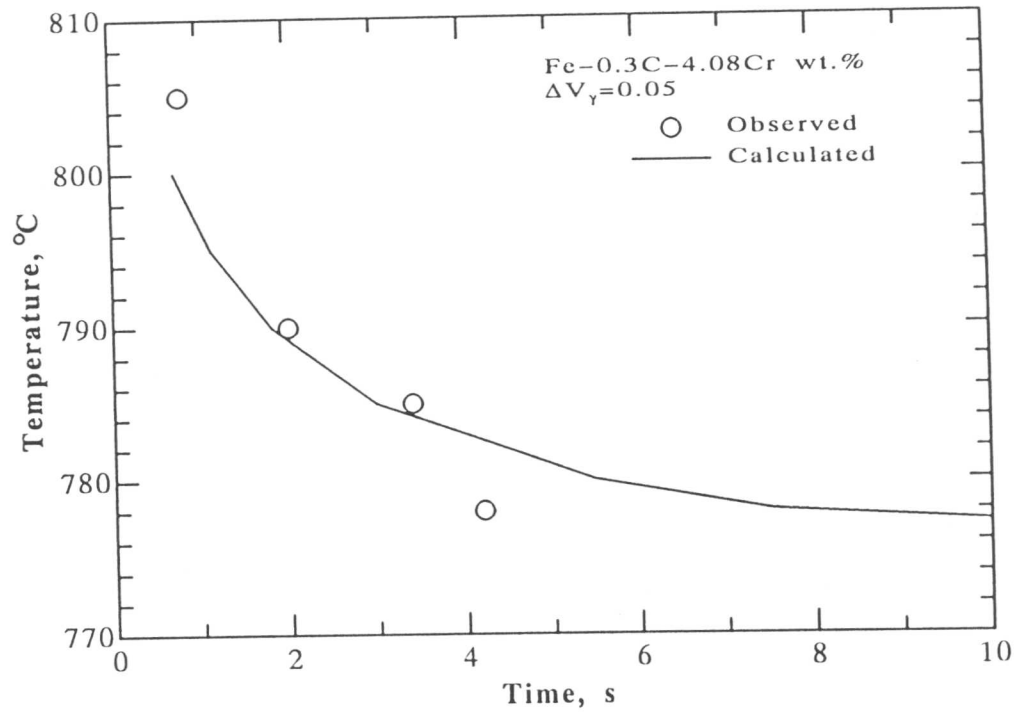


Fig. 8.10 Comparison between calculated (line) and observed (plots) TTT curves for $\Delta V_{\gamma} = 0.05$ from the mixture of bainite and austenite obtained at 420°C in the Fe-0.3C-4.08Cr wt.% alloy.

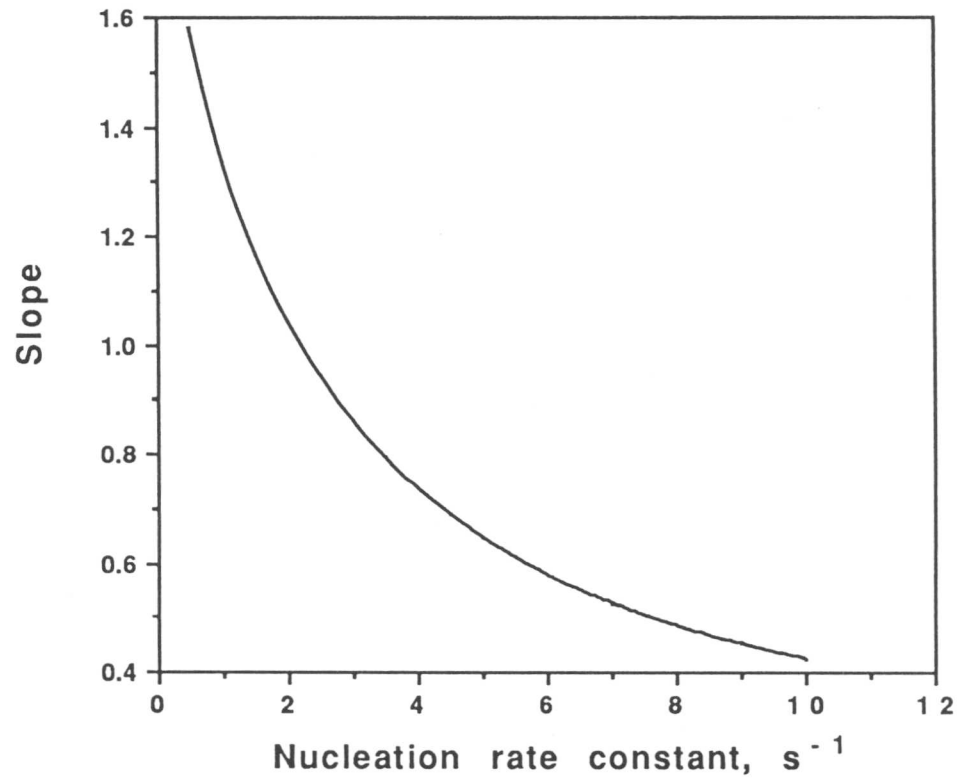


Fig. 8.11 Change in the slope of the plot of $\log\{-\ln\{1 - \xi\}\}$ against $\log\{t\}$ with the nucleation rate constant ν_1 .

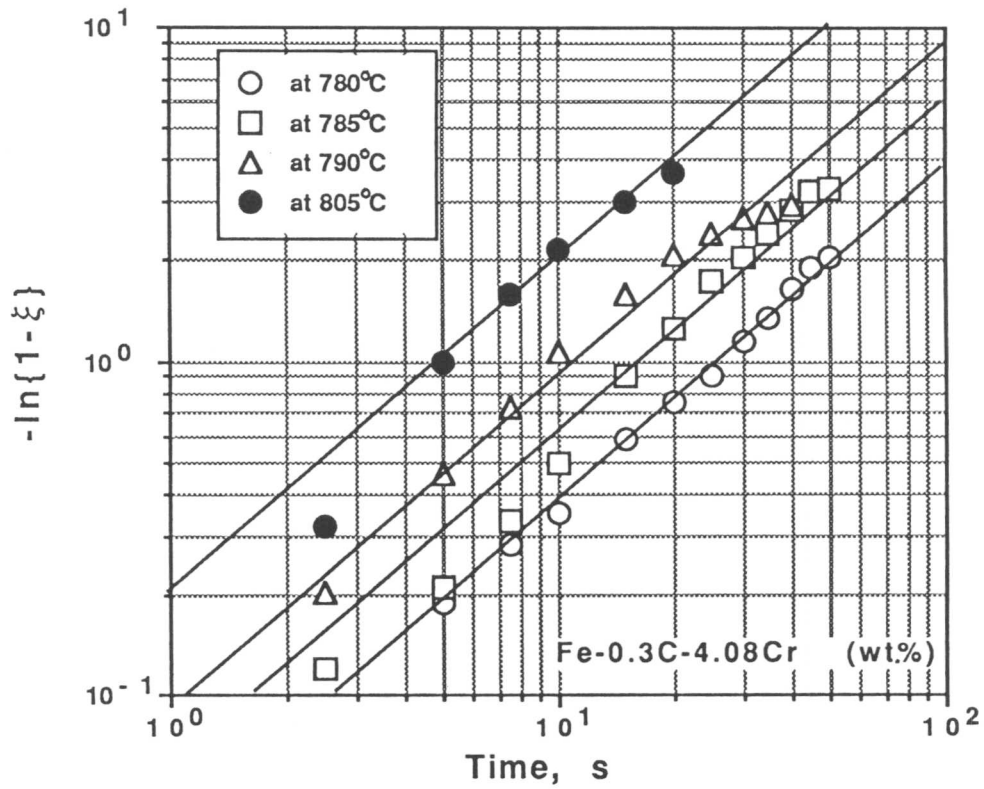


Fig. 8.12 $\log\{-\ln\{1-\xi\}\}$ v.s. $\log\{t\}$ plots for re-austenitisation from martensitic initial microstructure in the Fe-0.3C-4.08Cr wt.% alloy.

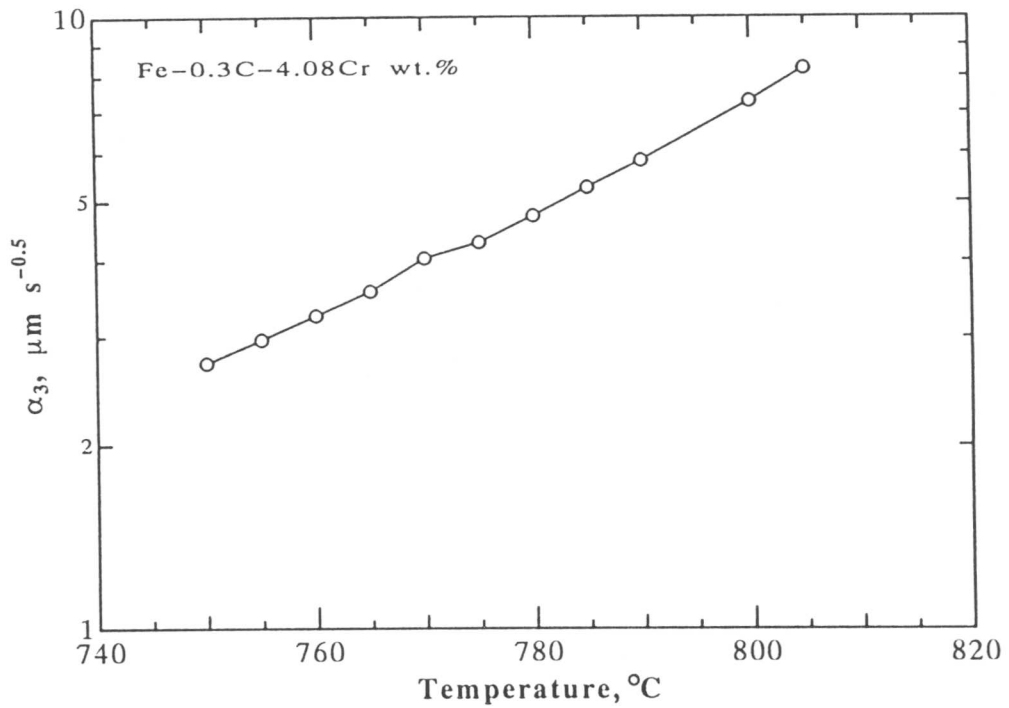


Fig. 8.13 Calculated three-dimensional parabolic rate constant α_3 of austenite formed in a carbon supersaturated ferrite matrix whose carbon concentration is the same as the paraequilibrium carbon concentration at 500 °C.

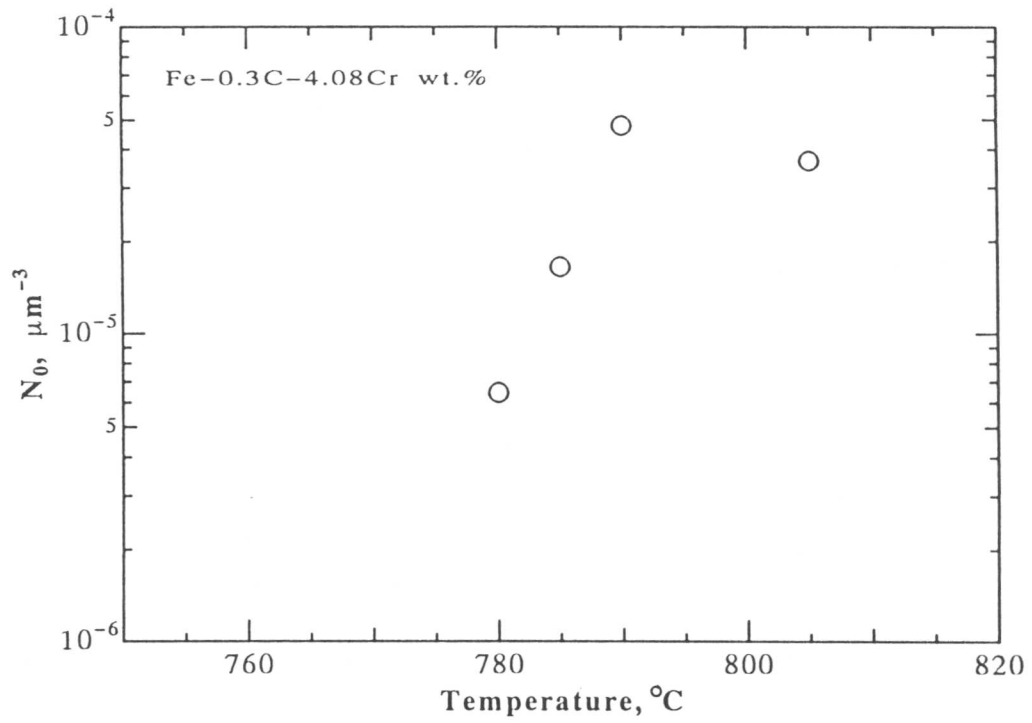


Fig. 8.14 Change in the initial nucleation site density for reaustenitisation N_0 from martensitic initial microstructure with temperature.

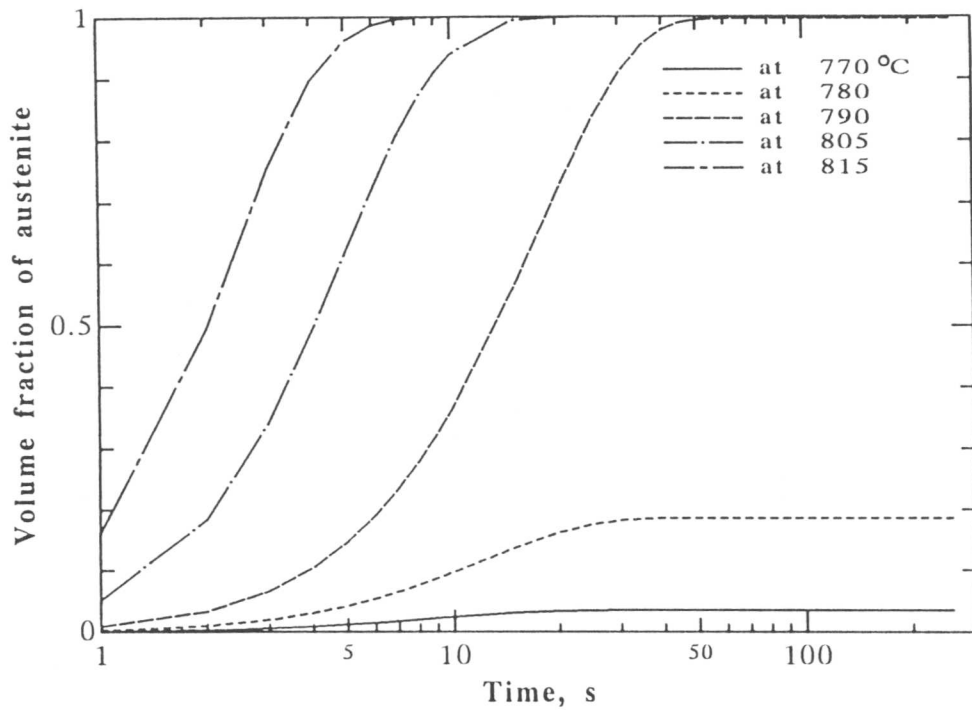


Fig. 8.15 Calculated isothermal reaustenitisation from martensitic initial microstructure.

CHAPTER 9

FURTHER WORK

The ultimate goal of this work is to develop a complete computer model which enables the calculation of microstructural development during austenitisation as a function of alloy chemistry and starting microstructure. Such a model would form a powerful combination with an appropriate computer model for the decomposition of austenite to transformation products such as allotriomorphic ferrite, pearlite, Widmanstätten ferrite, acicular ferrite, bainite and martensite. A grand scheme like this could be applied to a variety of engineering applications, and for the optimisation of material and process designs. Although this final goal is still out of reach, the work presented in this thesis shows that substantial progress can be made for the formation of austenite from well defined initial microstructures.

Since the general problem of austenite formation is strongly dependent on the initial microstructure, it is essential to understand the decomposition products of austenite in steels. The models developed in chapter 2, 3 and 5 illustrate how the details of the mechanism of the bainite and pearlite transformation allow the formation of austenite to be characterised theoretically. It is, however, important to take into account the effect of nucleation if these models are ever to be capable of generally useful application. The diffusional growth theory discussed in chapter 7 can be combined with any nucleation theories which may be developed in the future.

Apart from nucleation theory, the major problems highlighted by the present work, and which need further research are as follows:

- 1) It is necessary to be able to model the dissolution/precipitation of carbides during austenite formation and during heating to the test temperature.
- 2) It is convenient to assume that conditions of local equilibrium or paraequilibrium exist at the transformation interface. However, non-equilibrium growth in which none of the elements achieve equality of chemical potential, is also possible and needs to be investigated. In fact, it would be very useful to experimentally investigate the conditions at the transformation interface using an atom-probe.

COMPUTER PROGRAMS

C Program for the calculation of the time required to decarburise a plate of bainitic ferrite and time for
C a certain amount of cementite.

C

C Typical dataset:

C 1 No. of alloys,

C 0.2 (C) 0.2 (Si) 0.3 (Mn) 0.4(Ni) 0.5(Mo) 0.6 (Cr) 0.1 (V) wt.%

C

IMPLICIT REAL*8(A-H,K-Y), INTEGER(I,J,Z)

DOUBLE PRECISION DIFF(300),CARB(300),C(8),ATIME(40),ATEMP(40)

C HH=PLANCKS CONST.JOULES/SEC, KK=BOLTZMANN'S CONST.JOULES/DEGREE KELVIN

C D=DIFFUSIVITY OF CARBON IN AUSTENITE

C Z=COORDINATION OF INTERSTIAL SITE

C TIME=Time to decarburise a plate of ferrite, seconds

C THICK= thickness of ferrite plate, meters

C PSI=COMPOSITION DEPENDENCE OF DIFFUSION COEFFICIENT

C THETA=NO. C ATOMS/ NO. FE ATOMS

C ACTIV=ACTIVITY OF CARBON IN AUSTENITE

C R=GAS CONSTANT

C X=MOLE FRACTION OF CARBON

C T=ABSOLUTE TEMPERATURE

C SIGMA=SITE EXCLUSION PROBABILITY

C W=CARBON CARBON INTERACTION ENERGY IN AUSTENITE

C IJK1 gives the number of steels, I6 the number of data points

C

HH=6.6262D-34

KK=1.38062D-23

READ(5,*) IJK1

DO 1008 II2=1,IJK1

CALL OMEGA0(W,XBAR,C)

Z=12

A5=1.0D+00

R=8.31432D+00

RADIUS=0.0

VMAX=0.0

M1=0.00

I6=12

DO 222 I7=1,I6

T=50.0D+00*I7+50.0D+00

THICK=0.2D-06

CTEMP=T

STRAIN=400.0D+00

CALL AA3(C,CTEMP,XMAX,STRAIN)

T=T+273.00D+00

II2=0

ICRIT=0

XALPHA=XALPH(T)

A6=(XMAX-XBAR)/290.0D+00

IF(A6.LT. 0.0D+00) GOTO 222

DASH=(KK*T/HH)*DEXP(-(21230.0D+00/T))*DEXP(-31.84D+00)

DO 999 II=1,300

CARB(1)=XBAR

IF (II.GT. 1)GOTO 1000

GOTO 1001

1000 CARB(II)=CARB(II-1)+A6

IF (CARB(II).GT. XMAX) GOTO 1002

1001 X=CARB(II)

II2=II2+1

THETA=X/(A5-X)

ACTIV=CG(X,T,W,R)

ACTIV=DEXP(ACTIV)

DACTIV=DCG(X,T,W,R)

DACTIV=DACTIV*ACTIV

DACTIV=DACTIV*A5/((A5+THETA)**2)

SIGMA=A5-DEXP(-(W)/(R*T))

PSI=ACTIV*(A5+Z*((A5+THETA)/(A5-(A5+Z/2)*THETA+(Z/2)*(A5+Z/2)*

&(A5-SIGMA)*THETA*THETA)))+(A5+THETA)*DACTIV

DIFF(II)=DASH*PSI

IF(DIFF(II).LE. 0.0D+00 .AND. ICRIT.EQ. 0) THEN

ICRIT=II

ENDIF

999 CONTINUE

1002 IF(ICRIT.EQ. 0) GOTO 1012

DO 1333 I=1,II2

IF(I.LT. ICRIT-10) GOTO 1333

```

      DIFF(I)=DIFF(ICRIT-10)
1333 CONTINUE
1012 II3=0
      CALL D01GAF(CARB,DIFF,II2,ANS,ERROR,II3)
      ANS=ANS*1.0D-04/(XMAX-XBAR)
      TIME=(THICK*(XBAR-XALPHA)*DSQRT(3.14159D+00)/(4.0D+00
&*ANS**0.5*(XMAX-XBAR)))**2.0D+00
      ATIME(I7)=TIME
      ATEMP(I7)=CTEMP
222 CONTINUE
      WRITE(6,*) ' TEMP      td,s      t0.01',
&'      t0.02      t0.05      t0.10      t0.50'
      DO 3 JJJ=1,40
      IF(ATEMP(JJJ).EQ. 0) GOTO 3
      TC001=TC(ATEMP(JJJ),C,0.01D+00)
      TC002=TC(ATEMP(JJJ),C,0.02D+00)
      TC005=TC(ATEMP(JJJ),C,0.05D+00)
      TC010=TC(ATEMP(JJJ),C,0.10D+00)
      TC050=TC(ATEMP(JJJ),C,0.50D+00)
      WRITE(6,4) ATEMP(JJJ),ATIME(JJJ),TC001,TC002,TC005,TC010,TC050
      ATIME(JJJ)=0.0D+00
      ATEMP(JJJ)=0.0D+00
4      FORMAT(1H ,F8.2,6D12.4)
3      CONTINUE
1008 CONTINUE
      END
C
C-----
      SUBROUTINE OMEGA(W,XBAR,D)
C SUBROUTINE TO CALCULATE THE CARBON CARBON INTERACTION ENERGY IN
C AUSTENITE, AS A FUNCTION OF ALLOY COMPOSITION. BASED ON .MUCG18
C THE ANSWER IS IN JOULES PER MOL. **7 OCTOBER 1981**
      DOUBLE PRECISION C(8),D(8),W,P(8),B1,B2,Y(8),T10,T20,B3,XBAR
      INTEGER B5,I,U,B4
      READ (5,*) C(1),C(2),C(3),C(4),C(5),C(6),C(7)
      D(1)=C(1)
      D(2)=C(2)
      D(3)=C(3)
      D(4)=C(4)
      D(5)=C(5)
      D(6)=C(6)
      D(7)=C(7)
      D(8)=100.0-C(1)-C(2)-C(3)-C(4)-C(5)-C(6)-C(7)
      WRITE(6,*) ''
      WRITE(6,261) (C(B4),B4=1,7)
      B3=0.0D+00
      C(8)=C(1)+C(2)+C(3)+C(4)+C(5)+C(6)+C(7)
      C(8)=100.0D+00-C(8)
      C(8)=C(8)/55.84D+00
      C(1)=C(1)/12.0115D+00
      C(2)=C(2)/28.09D+00
      C(3)=C(3)/54.94D+00
      C(4)=C(4)/58.71D+00
      C(5)=C(5)/95.94D+00
      C(6)=C(6)/52.0D+00
      C(7)=C(7)/50.94D+00
      B1=C(1)+C(2)+C(3)+C(4)+C(5)+C(6)+C(7)+C(8)
      DO 107 U=2,7
      Y(U)=C(U)/C(8)
107 CONTINUE
      DO 106 U=1,8
      C(U)=C(U)/B1
106 CONTINUE
      XBAR=C(1)
      XBAR=DINT(10000.0D+00*XBAR)
      XBAR=XBAR/10000
      B2=0.0D+00
      T10=Y(2)*(-3)+Y(3)*2+Y(4)*12+Y(5)*(-9)+Y(6)*(-1)+Y(7)*(-12)
      T20=-3*Y(2)-37.5*Y(3)-6*Y(4)-26*Y(5)-19*Y(6)-44*Y(7)
      P(2)=2013.0341+763.8167*C(2)+45802.87*C(2)**2-280061.63*C(2)**3
&+3.864D+06*C(2)**4-2.4233D+07*C(2)**5+6.9547D+07*C(2)**6
      P(3)=2012.067-1764.095*C(3)+6287.52*C(3)**2-21647.96*C(3)**3-
&2.0119D+06*C(3)**4+3.1716D+07*C(3)**5-1.3885D+08*C(3)**6
      P(4)=2006.8017+2330.2424*C(4)-54915.32*C(4)**2+1.6216D+06*C(4)**3

```

```

&-2.4968D+07*C(4)**4+1.8838D+08*C(4)**5-5.5531D+08*C(4)**6
P(5)=2006.834-2997.314*C(5)-37906.61*C(5)**2+1.0328D+06*C(5)**3
&-1.3306D+07*C(5)**4+8.411D+07*C(5)**5-2.0826D+08*C(5)**6
P(6)=2012.367-9224.2655*C(6)+33657.8*C(6)**2-566827.83*C(6)**3
&+8.5676D+06*C(6)**4-6.7482D+07*C(6)**5 +2.0837D+08*C(6)**6
P(7)=2011.9996-6247.9118*C(7)+5411.7566*C(7)**2
&+250118.1085*C(7)**3-4.1676D+06*C(7)**4
DO 108 U=2,7
B3=B3+P(U)*Y(U)
B2=B2+Y(U)
108 CONTINUE
IF (B2 .EQ. 0.0D+00) GOTO 455
W=(B3/B2)*4.187
GOTO 456
455 W=8054.0
456 WRITE (6,261)(C(B4),B4=1,7)
261 FORMAT (4H C=,F6.4,4H SI=,F6.4,4H MN=,F6.4,
&4H NI=,F6.4,4H MO=,F6.4,4H CR=,F6.4,4H V=,F6.4)
RETURN
END
C
C-----
SUBROUTINE AA3(CW,AE3T,XEQ,STRAIN)
C AE3T is read in centigrade
C Matrix C represents chemical composition in weight percent
C STRAIN is in Joules per mole
C XEQ is the paraequilibrium carbon concentration in gamma at AE3T
C
DOUBLE PRECISION X,X1,T,R,A,A1,AFE,A1FE,DA1,DA2,DA1FE,H,H1,S,S1
INTEGER T1,I,NO,U,B4,J99,C99
DOUBLE PRECISION D11,STRAIN
1DEQ,ETEQ,T10,T20,XA,AFEQ,AEQ,ETEQ2,TEQ,
1J,J1,D,D1,W,W1,F,TEST,ERROR,T4,XEQ,FPRO
1,C(8),B1,B2,P(7),Y(7),B3,AE3T,CW(8),Z
Z=0.0D+00
DO 104 I=1,7
C(I)=CW(I)
Z=Z+CW(I)
104 CONTINUE
CW(8)=100.0D+00-Z
B3=0.0D+00
C(8)=(100.0-C(1)-C(2)-C(3)-C(4)-C(5)-C(6)-(C7))/55.84
C(1)=C(1)/12.0115
C(2)=C(2)/28.09
C(3)=C(3)/54.94
C(4)=C(4)/58.71
C(5)=C(5)/95.94
C(6)=C(6)/52.0
C(7)=C(7)/50.94
B1=C(1)+C(2)+C(3)+C(4)+C(5)+C(6)+C(7)+C(8)
DO 107 U=2,7
Y(U)=C(U)/C(8)
107 CONTINUE
DO 106 U=1,7
C(U)=C(U)/B1
106 CONTINUE
B2=0.0
T10=Y(2)*(-3)+Y(3)*2+Y(4)*12+Y(5)*(-9)+Y(6)*(-1)+Y(7)*(-12)
T20=-3*Y(2)-37.5*Y(3)-6*Y(4)-26*Y(5)-19*Y(6)-44*Y(7)
P(2)=2013.0341+763.8167*C(2)+45802.87*C(2)**2-280061.63*C(2)**3
1+3.864D+06*C(2)**4-2.4233D+07*C(2)**5+6.9547D+07*C(2)**6
P(3)=2012.067-1764.095*C(3)+6287.52*C(3)**2-21647.96*C(3)**3-
12.0119D+06*C(3)**4+3.1716D+07*C(3)**5-1.3885D+08*C(3)**6
P(4)=2006.8017+2330.2424*C(4)-54915.32*C(4)**2+1.6216D+06*C(4)**3
1-2.4968D+07*C(4)**4+1.8838D+08*C(4)**5-5.5531D+08*C(4)**6
P(5)=2006.834-2997.314*C(5)-37906.61*C(5)**2+1.0328D+06*C(5)**3
1-1.3306D+07*C(5)**4+8.411D+07*C(5)**5-2.0826D+08*C(5)**6
P(6)=2012.367-9224.2655*C(6)+33657.8*C(6)**2-566827.83*C(6)**3
1+8.5676D+06*C(6)**4-6.7482D+07*C(6)**5 +2.0837D+08*C(6)**6
P(7)=2011.9996-6247.9118*C(7)+5411.7566*C(7)**2
1+250118.1085*C(7)**3-4.1676D+06*C(7)**4
DO 108 U=2,7
B3=B3+P(U)*Y(U)
B2=B2+Y(U)

```

```

108 CONTINUE
    IF(B2 .EQ. 0.0) GOTO 455
    W=(B3/B2)*4.187
    GOTO 456
455 W=8054.0
456 CONTINUE
    X1=C(1)
    R=8.31432
    W1=48570.0
    H=38575.0
    S=13.48
201 XEQ=0.1
    T=AE3T+273.0
    IF (T .LE. 1000) GOTO 20
    H1=105525
    S1=45.34521
    GOTO 19
20 H1=111918
    S1=51.44
19 F=ENERGY(T,T10,T20)+STRAIN
    J=1-DEXP(-W/(R*T))
51 DEQ=DSQRT(1-2*(1+2*J)*XEQ+(1+8*J)*XEQ*XEQ)
    TEQ=5*DLOG((1-XEQ)/(1-2*XEQ))
    TEQ=TEQ+DLOG(((1-2*J+(4*J-1)*XEQ-DEQ)/(2*J*(2*XEQ-1))))**6)
    TEQ=TEQ*R*T-F
    IF (DABS(TEQ) .LT. 1.0) GOTO 50
    ETEQ=5*((1/(XEQ-1))+2/(1-2*XEQ))
    ETEQ2=6*((4*J-1-(0.5/DEQ)*(-2-4*J+2*XEQ+16*XEQ*J))/(1-2*J+(4*J
    1-1)*XEQ-DEQ))+6*(4*J/(2*J*(2*XEQ-1)))
    ETEQ=(ETEQ+ETEQ2)*R*T
    XEQ=XEQ-TEQ/ETEQ
    GOTO 51
50 IF (XEQ .LT. 0.001) GOTO 2444
2444 CONTINUE
802 RETURN
    END
C
C-----
    DOUBLE PRECISION FUNCTION TC(T,C,X)
    DOUBLE PRECISION K, Q, R, T, K0, N, C, X, TT
    INTEGER I
    R=1.987D+00
    Q=8030.0D+00
    K0=36.2D+00*C**0.635
    N=0.62D+00
    TT=T+273.0D+00
    K=K0*DEXP(-Q/R/TT)
    TC=(-DLOG(1.0D+00-X)/K)**(1.0D+00/N)
    RETURN
    END
C-----

```



```

C Program to calculate the parabolic thickening rate constants
C (1, 2, and 3 dimensional) and the time required to obtain a certain
C amount of cementite ignoring the effect of nucleation of cementite.
C
C 25 October 1988
C
C Typical data set
C 0.1 (C) 0.2 (Si) 0.2 (Mn) 0.2 (Ni) 0.2 (Mo) 0.2 (Cr) 0.1 (V)
C 420 --- temperature in deg. C
C 500
C
C
IMPLICIT REAL*8(A-H,K-Y), INTEGER(I,J,Z)
DOUBLE PRECISION S13AAF,CTEMP,T,XALPHA,XGAG,T5,DIFF,B0,B1,B2,A2,DIS
&,DIFF0,T50
EXTERNAL S13AAF
CALL OMEGA(W,XONE)
1 READ (5,*, END=2) CTEMP
T=CTEMP+273.0D0
XALPHA=0.0D0
XGAG=0.25
B0=9.28480435985404817D+00
B1=6880.73079777086696D+00
B2=-1780359.64568034932D+00
DIFF0=4.0D-3*DEXP(-19200.0D0/1.987D0/T)*1.0D-04
DIFF=DF(T)
CALL AL(XONE,XALPHA,XGAG,DIFF0,CTEMP,ALPHA)
A2=1.0D+00/ALPHA**2
DIS=B0+B1/T+B2/T/T
DIS=10.0D0**DIS
WRITE(6,*) 'DISLOCATION DENS., M**2 = ',DIS
WRITE(6,*) 'DIFFUSION COEFF.H, M**2/S = ',DIFF
WRITE(6,*) 'DIFFUSION COEFF.E, M**2/S = ',DIFF0
VE=1.037D-03*XONE
DIS0=10.0D-06
T5=(0.05D0*VE/(DIS/DIS0*9.0*ALPHA*ALPHA*ALPHA))**(2.0/3.0)
T50=(0.5D0*VE/(DIS/DIS0*9.0*ALPHA*ALPHA*ALPHA))**(2.0/3.0)
WRITE(6,*) ' TEMP ALPHA 1/ALPHA**2'
&,' t(0.05) t(0.5)'
WRITE(6,1229) CTEMP, ALPHA, A2, T5, T50
WRITE(6,*) ''
1229 FORMAT(F8.1,4D12.4)
GOTO 1
2 STOP
END
C*****
C FUNCTION GIVING V0
DOUBLE PRECISION FUNCTION V0(T,ALPHA)
HLEN=10.0D-04
HWID=0.2D-04
BETA=3.0D+00*ALPHA
V0=0.05-(((2*BETA/HLEN)+(ALPHA/HWID))*T**0.5 -
&((BETA/HLEN)**2 + 2*ALPHA*ALPHA/(HLEN*HWID))*T +
&ALPHA*BETA*BETA*T**1.5/(HLEN*HLEN*HWID))
RETURN
END
C*****
C FUNCTION GIVING LFG LN(ACTIVITY) OF CARBON IN AUSTENITE
DOUBLE PRECISION FUNCTION CG(X,T,W,R)
DOUBLE PRECISION J,DG,DUMMY,T,R,W,X
J=1-DEXP(-W/(R*T))
DG=DSQRT(1-2*(1+2*J)*X+(1+8*J)*X*X)
DUMMY=5*DLOG((1-2*X)/X)+6*W/(R*T)+((38575.0)-(
&13.48)*T)/(R*T)
CG=DUMMY+DLOG(((DG-1+3*X)/(DG+1-3*X))**6)
RETURN
END
C*****
C FUNCTION GIVING DIFFERENTIAL OF LN(ACTIVITY) OF CARBON IN AUSTENITE, LFG
C DIFFERENTIAL IS WITH RESPECT TO X
DOUBLE PRECISION FUNCTION DCG(X,T,W,R)
DOUBLE PRECISION J,DG,DDG,X,T,W,R
J=1-DEXP(-W/(R*T))
DG=DSQRT(1-2*(1+2*J)*X+(1+8*J)*X*X)

```

```

      DDG=(0.5/DG)*(-2.4*J+2*X+16*J*X)
      DCG=-((10/(1-2*X))+(5/X))+6*((DDG+3)/(DG-1+3*X
&)-(DDG-3)/(DG+1-3*X))
      RETURN
      END
C*****
      SUBROUTINE OMEGA(W,XONE)
C SUBROUTINE TO CALCULATE THE CARBON CARBON INTERACTION ENERGY IN
C AUSTENITE, AS A FUNCTION OF ALLOY COMPOSITION. BASED ON .MUCG18
C THE ANSWER IS IN JOULES PER MOL. **7 OCTOBER 1981**
      DOUBLE PRECISION C(8),W,P(8),B1,B2,Y(8),T10,T20,B3,XONE
      INTEGER B5,I,U,B4
      READ (5,*) C(1),C(2),C(3),C(4),C(5),C(6),C(7)
      WRITE(6,261) (C(B4),B4=1,7)
      B3=0.0D+00
      C(8)=C(1)+C(2)+C(3)+C(4)+C(5)+C(6)+C(7)
      C(8)=100.0D+00-C(8)
      C(8)=C(8)/55.84D+00
      C(1)=C(1)/12.0115D+00
      C(2)=C(2)/28.09D+00
      C(3)=C(3)/54.94D+00
      C(4)=C(4)/58.71D+00
      C(5)=C(5)/95.94D+00
      C(6)=C(6)/52.0D+00
      C(7)=C(7)/50.94D+00
      B1=C(1)+C(2)+C(3)+C(4)+C(5)+C(6)+C(7)+C(8)
      DO 107 U=2,7
      Y(U)=C(U)/C(8)
107 CONTINUE
      DO 106 U=1,8
      C(U)=C(U)/B1
106 CONTINUE
      XONE=C(1)
      XONE=DINT(10000.0D+00*XONE)
      XONE=XONE/10000
      B2=0.0D+00
      T10=Y(2)*(-3)+Y(3)*2+Y(4)*12+Y(5)*(-9)+Y(6)*(-1)+Y(7)*(-12)
      T20=-3*Y(2)-37.5*Y(3)-6*Y(4)-26*Y(5)-19*Y(6)-44*Y(7)
      P(2)=2013.0341+763.8167*C(2)+45802.87*C(2)**2-280061.63*C(2)**3
&+3.864D+06*C(2)**4-2.4233D+07*C(2)**5+6.9547D+07*C(2)**6
      P(3)=2012.067-1764.095*C(3)+6287.52*C(3)**2-21647.96*C(3)**3-
&2.0119D+06*C(3)**4+3.1716D+07*C(3)**5-1.3885D+08*C(3)**6
      P(4)=2006.8017+2330.2424*C(4)-54915.32*C(4)**2+1.6216D+06*C(4)**3
&-2.4968D+07*C(4)**4+1.8838D+08*C(4)**5-5.5531D+08*C(4)**6
      P(5)=2006.834-2997.314*C(5)-37906.61*C(5)**2+1.0328D+06*C(5)**3
&-1.3306D+07*C(5)**4+8.411D+07*C(5)**5-2.0826D+08*C(5)**6
      P(6)=2012.367-9224.2655*C(6)+33657.8*C(6)**2-566827.83*C(6)**3
&+8.5676D+06*C(6)**4-6.7482D+07*C(6)**5 +2.0837D+08*C(6)**6
      P(7)=2011.9996-6247.9118*C(7)+5411.7566*C(7)**2
&+250118.1085*C(7)**3-4.1676D+06*C(7)**4
      DO 108 U=2,7
      B3=B3+P(U)*Y(U)
      B2=B2+Y(U)
108 CONTINUE
      IF (B2.EQ. 0.0D+00) GOTO 455
      W=(B3/B2)*4.187
      GOTO 456
455 W=8054.0
456 WRITE (6,261)(C(B4),B4=1,7)
      WRITE(6,1006)W
1006 FORMAT(' CARBON-CARBON INTERACTION ENERGY IN GAMMA, J/MOL=',F9.4)
261 FORMAT (4H C=,F6.4,4H SI=,F6.4,4H MN=,F6.4,
&4H NI=,F6.4,4H MO=,F6.4,4H CR=,F6.4,4H V=,F6.4)
      RETURN
      END
C*****
C FUNCTION GIVING THE EQUILIBRIUM MOL.FRAC. CARBON IN ALPHA
C BASED ON MY PAPER ON FIRST ORDER QUASICHEMICAL THEORY,METSCI
      DOUBLE PRECISION FUNCTION XALPH(T)
      DOUBLE PRECISION T,CTEMP
      CTEMP=(T-273.0D+00)/900.0D+00
      XALPH=0.1528D-02-0.8816D-02*CTEMP+0.2450D-01*CTEMP*CTEMP
&-0.2417D-01*CTEMP*CTEMP*CTEMP+
&0.6966D-02*CTEMP*CTEMP*CTEMP*CTEMP

```

```

RETURN
END
C*****
C*****
SUBROUTINE AL(XGAG,XAGA,XONE,DIFF,CTEMP,ALPHA)
DOUBLE PRECISION DIFF,ALPHA,XAGA,XGAG,XONE,CTEMP,DUMMY1
&,DER,FUN2,ALPH,DUMMY2,DUMMY3
III=0
ALPHA=DSQRT(DIFF)
DUMMY2=ALPHA
C ABOVE IS A GUESSED VALUE OF ALPHA
4 CALL FUNN(DUMMY1,ALPHA,XGAG,XONE,XAGA,DIFF,CTEMP)
III=III+1
C WRITE(6,20)ALPHA,DUMMY1,DER
46 IF(III .GT. 100) GOTO 3
IF (DABS(DUMMY1) .GT. 0.0001D-06) GOTO 2
GOTO 3
20 FORMAT(3D12.4)
2 DUMMY2=DUMMY1
ALPH=ALPHA*1.00000001D+00
CALL FUNN(FUN2,ALPH,XGAG,XONE,XAGA,DIFF,CTEMP)
DER=(DUMMY1-FUN2)/(ALPHA-ALPH)
ALPHA=ALPHA-(DUMMY1/DER)*0.5D0
GOTO 4
3 WRITE(6,23)CTEMP, ALPHA,DUMMY1
WRITE(6,*) 'ALPHA/SQRT.DIFF =',(ALPHA/DSQRT(DIFF))
23 FORMAT(' CTEMP=',F8.2,' ALPHA (M PER SEC**0.5)=',D12.5,
&' DUMMY1=',D12.5)
WRITE(6,*) 'Fi= ',((XGAG-XAGA)/(XONE-XAGA))
RETURN
END
C*****
SUBROUTINE FUNN(FUN,ALPHA,XGAG,XONE,XAGA,DIFF,CTEMP)
C 'FUN' COMPUTES EQ.2 OF KINSMAN AND AARONSONS TRANSFORMATION AND
C HARDENABILITY PAPER. DIFF=INTEGRATED AVERAGE DIFFUSIVITY OF C IN
C GAMMA, ALPHA = PARABOLIC RATE CONSTANT.
DOUBLE PRECISION DIFF,ALPHA,XAGA,XGAG,XONE,FUN
FUN=DSQRT(3.141593D+00/DIFF)/2.0D+00
FUN=FUN*ALPHA*DEXP(ALPHA*ALPHA/(4.0D+00*DIFF))
FUN=FUN*(1.0D+00-DERF(ALPHA/(2.0D+00*DSQRT(DIFF))))
FUN=(XGAG-XAGA)/(XONE-XAGA)-FUN
RETURN
END
C*****
SUBROUTINE FUNN1(FUN,ALPHA,XGAG,XONE,XAGA,DIFF,CTEMP)
DOUBLE PRECISION DIFF,ALPHA,XAGA,XGAG,XONE,FUN
&,S13AAF
EXTERNAL S13AAF
FUN=ALPHA*ALPHA/4.0D+00/DIFF*DEXP(ALPHA*ALPHA/(4.0D+00*DIFF))
FUN=FUN*S13AAF(ALPHA*ALPHA/(4.0D+00*DIFF), 0)
FUN=(XGAG-XAGA)/(XONE-XAGA)-FUN
RETURN
END
C*****
SUBROUTINE FUNN2(FUN,ALPHA,XGAG,XONE,XAGA,DIFF,CTEMP)
DOUBLE PRECISION DIFF,ALPHA,XAGA,XGAG,XONE,FUN
FUN=ALPHA*ALPHA/(2.0D+00*DIFF)*(1.0D+00-DSQRT(3.141592D+00/DIFF)*
&ALPHA/2.0D+00*DEXP(ALPHA*ALPHA/(4.0D+00*DIFF))
&*(1.0D+00-DERF(ALPHA/(2.0D+00*DSQRT(DIFF))))))
FUN=(XGAG-XAGA)/(XONE-XAGA)-FUN
RETURN
END
C*****
DOUBLE PRECISION FUNCTION DF(KTEMP)
DOUBLE PRECISION R,KTEMP,PHI,DOTO,DTT,F
R=8.3143D+00
PHI=1.0D+00-1.0/(0.5D+00*DEXP(7.2D+03*4.184/(R*KTEMP))
&*DEXP(4.4D+00)+1.0D+00)
DOTO=3.3D-07*DEXP(-19.3D+03*4.184D+00/(R*KTEMP))
DTT=3.0D-04*DEXP(-14.7D+03*4.184D+00/(R*KTEMP))
F=0.86D+00
DF=PHI*DOTO+(1.0D+00-PHI)*F*DTT+(1.0D+00-PHI)
&*(1.0D+00-F)*DOTO
C DIFFUSION OF CARBON IN FERRITE, M*M/S

```

C MCLELLAN ET AL., TRANS. MET. SOC. AIME, VOL.233 (1965) 1938
C R = UNIVERSAL GAS CONSTANT, J/MOL/K
C KTEMP = ABSOLUTE TEMPERATURE
RETURN
END

C
C*****

```

C   FTVSCLR PROGRAM=%H% DATA=&D NAG
C Program to calculate cementite precipitation from a supersaturated
C ferrite based on a nucleation and growth theory. Nucleation occurs
C on the dislocation. The growth of cementite plate is calculated
C using the one-dimensional parabolic thickening rate constant (ALPHA).
C
  IMPLICIT REAL*8(A-H,K-Z), INTEGER(I,J)
  DOUBLE PRECISION X(200),Y(200)
C
C-----
C Initial carbon mole fraction in ferrite (XMOL) and the maximum
C possible volume fraction of cementite (VE).
C
  XMOL=0.0183
  VE=1.00645D+00*4.0D+00*XMOL/(1.0D+00-4.0D+00*XMOL)
C
C-----
C ALPHA : one demensional parabolic rate constant, m/sec**0.5
C DG : activation energy of the nucleation of cementite, J/mole
C
C Typical data set
C 450:Temperature deg.C, 0.1234D-06: Rate constant m/sec**5
C 500          0.3456D-06
C
1  READ(5,*,END=333) T,ALPHA
   DG=180000.0D+00
   WRITE(6,*) 'G* = ',DG
   R=8.314D+00
   TT=T+273.0D+00
C
C-----
C Calculation of the dislocation density in ferrite.
C
  A1=9.28480435985404817D+00
  A2=6880.73079777086696D+00
  A3=-1780359.64568034932D+00
  ROU=A1+A2/TT+A3/TT/TT
  ROU=10.0D+00**ROU
  R0=((2.26D+00-6.4D-03*TT+4.6D-06*TT*TT)*VE/1000.0)
  &  ** (1.0/3.0)*1.0D-06
C
C-----
C N0 : Number of particles per unit volume
C
  N0=VE/(4.0/3.0*3.141593*R0*R0*R0)
C
C-----
C Coefficients in the nucleation function.
C see Christian "The Theory of Transformations in Metals and Alloys"
C
  A=2.8664D-10*3.0D+00**0.5/2.0D+00
  K=(ROU/A)**(1.0/3.0)*2.08D+10*TT*DEXP(-DG/R/TT)*ROU
  VNC=(ROU/A)**(1.0/3.0)*ROU
C
C-----
  WRITE(6,98) T,VE,RMAX,ALPHA,DG,ROU,N0,VNC,K
98  FORMAT(
&' TEMPERATURE, DEG      =',F10.4/
&' EQUILIBRIUM V-THETA   =',D12.4/
&' R-MAX (FROM V-THETA) , um =',D12.4/
&' ALPHA, M/SEC**0.5     =',D12.4/
&' DELTA-G, J/MOLE       =',D12.4/
&' DISLOCATION DENSITY, 1/M**2 =',D12.4/
&' EATA (NO. OF PARTICLE),M**-3=',D12.4/
&' Nv= ROU*N             =',D12.4/
&' NUCLEATION RATE I,   =',D12.4)
C
C-----
C Calculation of time required for 0.05 cementite precipitation
C (TIME), and the total number of particles at the end of the
C reaction (NTOT).
C
  Z=-DLOG(1.0D+00-0.05D+00)
  TIME=(Z*5.0/18.0*VE/K/ALPHA**3.0)**(2.0/5.0)

```

```

30 WRITE(6,99) TIME
99 FORMAT(1H ,TIME FOR 0.05 PRECIPITATION = ',D12.4)
   TC=(30.0*5.0/18.0*VE/K/ALPHA**3.0)**(2.0/5.0)
   DTC=TC/200.0
   DO 20 I=1,200
     X(I)=DTC*(I-1)
     Y(I)=DEXP(-18.0/5.0*K*ALPHA**3.0/VE*X(I)**(5.0/2.0))
20 CONTINUE
   II3=0
   CALL D01GAF(X,Y,200,ANS,ERROR,II3)
   NTOT=K*ANS
   WRITE(6,911) NTOT
911 FORMAT(1H ,NUMBER OF PARTICLE, M**-3 =',D12.4)
   GOTO 1
333 STOP
   END
C
C-----

```

```

C FTVSCLR PROGRAM=%H% NAG DATA=&DATA
C H. K. D. H. Bhadeshia and M. Takahashi
C
C Program to calculate the growth rate based on a plate growth theory
C and the time required to obtain 0.05 cementite precipitation.
C
C Typical dataset:
C 1 40 No. of centigrade-mole fraction carbon pairs, No. of alloys
C 0.2 (C) 0.2 (Si) 0.3 (Mn) 0.4(Ni) 0.5(Mo) 0.6 (Cr) 0.1 (V) wt.%
C 600 ----- temperature in deg.C
C
  IMPLICIT REAL*8(A-H,K-Y), INTEGER(I,J,Z)
  DOUBLE PRECISION DIFF(300),CARB(300)
  &, B0,B1,B2,T5,DIS
C
C XMAXR IS THE EQUILIBRIUM CONC AT PLATE TIP OF RADIUS R, IN GAMMA
C HH=PLANCKS CONST.JOULES/SEC, KK=BOLTZMANN'S CONST.JOULES/DEGREE KELVIN
C
  HH=6.6262D-34
  KK=1.38062D-23
  READ(5,*)I6,IJK1
  DO 1008 I22=1,IJK1
  CALL OMEGA(W,XBAR)
  Z=12
  A5=1.0D+00
  R=8.31432D+00
C
C D=DIFFUSIVITY OF CARBON IN AUSTENITE
C Z=COORDINATION OF INTERSTITIAL SITE
C R=GAS CONSTANT
C X=MOLE FRACTION OF CARBON
C T=ABSOLUTE TEMPERATURE
C SIGMA=SITE EXCLUSION PROBABILITY
C W=CARBON CARBON INTERACTION ENERGY IN AUSTENITE
C
  RADIUS=0.0
  VMAX=0.0
  M1=0.00
  WRITE(6,1009)
1009 FORMAT('*****'/5H )
  DO 222 I7=1,I6
  READ(5,*)T
  XTH=0.25
  XMAX=XTH
  CTEMP=T
  T=T+273.00D+00
  I2=0
  XALPHA=XALPH(T)
  WRITE(6,1005)T,CTEMP,XBAR,XALPHA
  CALL RRAD(RADIUS,XMAX,XALPHA,XBAR,T,R,XMAXR,W)
  A6=(XMAXR-XBAR)/290.0D+00
1005 FORMAT(' ABSOLUTE TEMPERATURE, DEGREES KELVIN =',F8.1/
&' TEMPERATURE IN DEGREES CENTIGRADE =',F8.1/
&' MOL FRAC CARBON IN ALLOY =',F8.4/
&' EQUILIBRIUM MOL FRAC OF C IN FERRITE=',D12.4)
  DIFF0=DF(T)
  CALL VEL(VMAX,DIFF0,RADIUS,XMAX,XBAR,XALPHA)
  CALL VEL3(VMAX,DIFF0,RADIUS,XMAX,XBAR,XALPHA)
  CALL VEL2(VMAX,DIFF0,RADIUS,XMAX,XBAR,XALPHA)
  CALL VEL4(VMAX,DIFF0,RADIUS,XMAX,XBAR,XALPHA)
  B0=9.05839817855180618D0
  B1=7528.72136707062509D0
  B2=-2107436.07233760227D0
  DIS=B0+B1/T+B2/T/T
  DIS=10.0D0**DIS
  WRITE(6,902) DIS
902 FORMAT(1H 'DISLOCATION DENS., M**-2 =',D15.6)
  VE=1.00645D+00*4.0D+00*XBAR/(1.0D+00-4.0D+00*XBAR)
  R0=((2.26D+00-6.4D-03*T+4.6D-06*T*T)*VE/1000.0)
  & *(1.0/3.0)*1.0D-06
  N0=VE/(4.0/3.0*3.14159265D+00*R0*R0)/DIS
  NTOT=N0*DIS
  ASP=15.0D+00
  WRITE(6,903) VE

```

```

903 FORMAT(1H,'MAXIMUM VOLUME FRACTION OF CEMENTITE = ',D15.6)
WRITE(6,904) ASP
904 FORMAT(1H,'ASPECT RATIO OF CEMENTITE = ',F10.4)
WRITE(6,905) R0
905 FORMAT(1H,'AVERAGE PARTICLE SIZE, M = ',D15.6)
WRITE(6,906) NTOT
906 FORMAT(1H,'NUMBER OF PARTICLES, M**-3= ',D15.6)
T5=(VE*0.05D+00)/(3.14159265D+00
& *VMAX*VMAX*VMAX*DIS/ASP*N0)**(1.0D+00/3.0D+00)
WRITE(6,901) VMAX,T5
WRITE(6,*) ''
WRITE(6,*) ''
901 FORMAT(1H,'MAX. VELOCITY, M/SEC = ',D15.4/
&' TIME FOR 0.05 PRECIPITATION OF CEMENTITE, SEC = ',D15.4)
222 CONTINUE
1008 CONTINUE
END
C
C-----
SUBROUTINE OMEGA(W,XBAR)
C SUBROUTINE TO CALCULATE THE CARBON CARBON INTERACTION ENERGY IN
C AUSTENITE, AS A FUNCTION OF ALLOY COMPOSITION. BASED ON .MUCG18
C THE ANSWER IS IN JOULES PER MOL. **7 OCTOBER 1981**
DOUBLE PRECISION C(8),W,P(8),B1,B2,Y(8),T10,T20,B3,XBAR
INTEGER B5,I,U,B4
READ (5,*) C(1),C(2),C(3),C(4),C(5),C(6),C(7)
WRITE(6,261) (C(B4),B4=1,7)
B3=0.0D+00
C(8)=C(1)+C(2)+C(3)+C(4)+C(5)+C(6)+C(7)
C(8)=100.0D+00-C(8)
C(8)=C(8)/55.84D+00
C(1)=C(1)/12.0115D+00
C(2)=C(2)/28.09D+00
C(3)=C(3)/54.94D+00
C(4)=C(4)/58.71D+00
C(5)=C(5)/95.94D+00
C(6)=C(6)/52.0D+00
C(7)=C(7)/50.94D+00
B1=C(1)+C(2)+C(3)+C(4)+C(5)+C(6)+C(7)+C(8)
DO 107 U=2,7
Y(U)=C(U)/C(8)
107 CONTINUE
DO 106 U=1,8
C(U)=C(U)/B1
106 CONTINUE
XBAR=C(1)
XBAR=DINT(10000.0D+00*XBAR)
XBAR=XBAR/10000
B2=0.0D+00
T10=Y(2)*(-3)+Y(3)*2+Y(4)*12+Y(5)*(-9)+Y(6)*(-1)+Y(7)*(-12)
T20=-3*Y(2)-37.5*Y(3)-6*Y(4)-26*Y(5)-19*Y(6)-44*Y(7)
P(2)=2013.0341+763.8167*C(2)+45802.87*C(2)**2-280061.63*C(2)**3
&+3.864D+06*C(2)**4-2.4233D+07*C(2)**5+6.9547D+07*C(2)**6
P(3)=2012.067-1764.095*C(3)+6287.52*C(3)**2-21647.96*C(3)**3-
&2.0119D+06*C(3)**4+3.1716D+07*C(3)**5-1.3885D+08*C(3)**6
P(4)=2006.8017+2330.2424*C(4)-54915.32*C(4)**2+1.6216D+06*C(4)**3
&-2.4968D+07*C(4)**4+1.8838D+08*C(4)**5-5.5531D+08*C(4)**6
P(5)=2006.834-2997.314*C(5)-37906.61*C(5)**2+1.0328D+06*C(5)**3
&-1.3306D+07*C(5)**4+8.411D+07*C(5)**5-2.0826D+08*C(5)**6
P(6)=2012.367-9224.2655*C(6)+33657.8*C(6)**2-566827.83*C(6)**3
&+8.5676D+06*C(6)**4-6.7482D+07*C(6)**5 +2.0837D+08*C(6)**6
P(7)=2011.9996-6247.9118*C(7)+5411.7566*C(7)**2
&+250118.1085*C(7)**3-4.1676D+06*C(7)**4
DO 108 U=2,7
B3=B3+P(U)*Y(U)
B2=B2+Y(U)
108 CONTINUE
IF (B2 .EQ. 0.0D+00) GOTO 455
W=(B3/B2)*4.187
GOTO 456
455 W=8054.0
456 WRITE (6,261)(C(B4),B4=1,7)
WRITE(6,1006)W
1006 FORMAT(' CARBON-CARBON INTERACTION ENERGY IN GAMMA, J/MOL=',F9.4)

```



```

261  FORMAT (4H C=,F7.4,4H SI=,F7.4,4H MN=,F7.4,
      &4H NI=,F7.4,4H MO=,F7.4,4H CR=,F7.4,4H V=,F7.4)
      RETURN
      END
C
C-----
SUBROUTINE RRAD(RADIUS,XMAX,XALPHA,XBAR,T,R,XMAXR,W)
DOUBLE PRECISION RADIUS,XMAX,XBAR,T,R,SIG,MOLVOL,XMAXR
&,XALPHA,RAD,OMEGA,CAPCON,EPSI
SIG=0.7
C SIG=INTERFACIAL ENERGY, JOULES PER METRE SQUARED
  MOLVOL=5.8033D-06*(1.0D+00+3.549D-05*(T-298.0D+00))
C MOLVOL = MOLAR VOLUME OF FERRITE
C RADIUS IS THE CRITICAL RADIUS FOR ZERO GROWTH
C RAD IS THE RATIO OF THE ACTUAL RADIUS TO THE CRITICAL RADIUS
  EPSI=XALPHA*DF(T)
C  CAPCON=(SIG*MOLVOL/(R*T))*((1.0D+00-XALPHA)/(XMAX-XALPHA))
C  &/EPSI
  CAPCON=(SIG*MOLVOL/(R*T))/(XMAX-XALPHA)
  RADIUS=CAPCON*XALPHA/(XMAX-XALPHA)
  OMEGA=(XALPHA-XBAR)/(XALPHA-XMAX)
  RAD=0.2026D+01-0.1917D+01*OMEGA-0.8953D+00*OMEGA*OMEGA
  &+0.3670D+01*OMEGA*OMEGA*OMEGA-0.2519D+01*OMEGA*OMEGA*OMEGA*OMEGA
  RAD=10.00D+00**RAD
  RAD=RADIUS*RAD
  XMAXR=XMAX*(1.0D+00+(CAPCON/RAD))
  WRITE(6,1)SIG,MOLVOL,RADIUS,XMAXR,CAPCON,EPSI
1  FORMAT(' INTERFACIAL ENERGY=',F8.4,' JOULES/METERS SQUARED'/
&' MOLAR VOLUME OF CEMENTITE(METERS CUBED PER MOL)=' ,D15.6/
&' GIBBS THOMPSON CRITICAL RADIUS(METERS)=' ,D15.6/
&' EQUILIBRIUM CONC AT PLATE TIP, MOL FRAC, XMAXR=' ,D15.6/
&' CAPILLARITY CONSTANT CAPCON=' ,D15.6/
&' NON-IDEALITY PARAMETER EPSI=' ,D15.6)
      RETURN
      END
C
C-----
SUBROUTINE RRAD1(RADIUS,XMAX,XALPHA,XBAR,T,R,XMAXR,W)
DOUBLE PRECISION RADIUS,XMAX,XBAR,T,R,SIG,MOLVOL,XMAXR
&,XALPHA,RAD,OMEGA,CAPCON,EPSI
C RADIUS IS THE CRITICAL RADIUS FOR ZERO GROWTH
  XMAXR=XMAX
  RADIUS=6.5D-08
  WRITE(6,9) XMAX,RADIUS
9  FORMAT(1H,'CARBON IN CEMENTITE, MOLE FRACTION = ',F10.4/
&'CRITICAL RADIUS, M = ',D15.4)
      RETURN
      END
C
C-----
SUBROUTINE VEL(VMAX,ANS,RADIUS,XMAX,XBAR,XALPHA)
DOUBLE PRECISION OMEGA,ANS,RADIUS,P,VMAX,XMAX,XBAR
&,XALPHA
  OMEGA=(XALPHA-XBAR)/(XALPHA-XMAX)
  P=(1.0D+00/8.0D+00)*(OMEGA/(1.0D+00-OMEGA))
  VMAX=(ANS*1.0D-04)*P/RADIUS
  WRITE(6,1)VMAX
1  FORMAT(' MAXIMUM GROWTH RATE (EQ.9,MET.TRANS,V6A,1975,P7,=' ,
&D10.4,'METERS PER SECOND')
      RETURN
      END
C
C-----
SUBROUTINE VEL2(VMAX,ANS,RADIUS,XMAX,XBAR,XALPHA)
DOUBLE PRECISION OMEGA,ANS,RADIUS,P,VMAX,XMAX,XBAR
&,XALPHA
  OMEGA=(XALPHA-XBAR)/(XALPHA-XMAX)
  P=(1.0D+00/4.0D+00)*(OMEGA/(1.0D+00-OMEGA))
  VMAX=((10.0D+00)**(-2.5D+00*(1.0D+00-OMEGA)))
  &*(ANS*1.0D-04)*P/RADIUS
  WRITE(6,1)VMAX
1  FORMAT(' MAXIMUM GROWTH RATE (EQ.14,MET.TRANS,V6A,1975,P7,=' ,
&D10.4,'METERS PER SECOND')
      RETURN

```

```

END
C
C-----
SUBROUTINE VEL3(VMAX,ANS,RADIUS,XMAX,XBAR,XALPHA)
DOUBLE PRECISION OMEGA,ANS,RADIUS,P,VMAX,XMAX,XBAR
&,XALPHA
OMEGA=(XALPHA-XBAR)/(XALPHA-XMAX)
P=((OMEGA/(1.0D+00-(2.0D+00/3.14159D+00))*OMEGA-
&(1.0D+00/(2.0D+00*3.14159D+00))*(OMEGA*OMEGA)))*3)
P=P*27.0D+00/(256.0D+00*3.14159D+00)
VMAX=(ANS*1.0D-04)*P/RADIUS
WRITE(6,1)VMAX
1 FORMAT(' MAXIMUM GROWTH RATE (EQ.13,MET.TRANS,V6A,1975,P7,=',
&D10.4,' METERS PER SECOND')
RETURN
END
C
C-----
SUBROUTINE VEL4(VMAX,ANS,RADIUS,XMAX,XBAR,XALPHA)
DOUBLE PRECISION OMEGA,ANS,RADIUS,PECLET,XMAX,XBAR,XALPHA,PI
&,VDUM,DUMMY,VMAX,DD,S2,RAD,DDD
INTEGER I1,I2,I3
WRITE(6,4)
4 FORMAT(' DIFFUSION CONTROLLED GROWTH, TRIVEDI ANALYSIS)
I2=100
DD=0.01
VDUM=DD*VMAX
VMAX=0.5*VMAX
ANS=ANS*1.0D-04
WRITE(6,44)
44 FORMAT(' OMEGA DUMMY VMAX(M/S) PECLET RAD(M)')
OMEGA=(XALPHA-XBAR)/(XALPHA-XMAX)
RAD=0.2026D+01-0.1917D+01*OMEGA-0.8953D+00*OMEGA*OMEGA
&+0.3670D+01*OMEGA*OMEGA*OMEGA-0.2519D+01*OMEGA*OMEGA*OMEGA*OMEGA
RAD=10.0D+00**RAD
RAD=RADIUS*RAD
DO 1 I1=1,I2
PECLET=VMAX*RAD/(2.0D+00*ANS)
S2=-1.073019925D+00*(DLOG10(PECLET))-0.273767575D+00
S2=10.0D+00**S2
PI=3.14159D+00
DUMMY=(DSQRT(PI*PECLET))*(DEXP(PECLET))*(DERFC(DSQRT(PECLET)))
&*(1.0D+00+(RADIUS/RAD)*OMEGA*S2)
DDD=DABS(100.0D+00*(DUMMY-OMEGA))
IF (DDD .GT. 0.1D+00) GOTO 55
WRITE(6,2)OMEGA,DUMMY,VMAX,PECLET,RAD
2 FORMAT(7D12.4)
IF (DDD .LT. 0.01D+00) GOTO 56
55 VMAX=VMAX+VDUM
1 CONTINUE
56 RETURN
END
C
C-----
C FUNCTION GIVING THE EQUILIBRIUM MOL.FRAC. CARBON IN ALPHA
C BASED ON THE PAPER ON FIRST ORDER QUASICHEMICAL THEROY,METSCI
DOUBLE PRECISION FUNCTION XALPH(T)
DOUBLE PRECISION T,CTEMP
CTEMP=(T-273.0D+00)/900.0D+00
XALPH=0.1528D-02-0.8816D-02*CTEMP+0.2450D-01*CTEMP*CTEMP
&-0.2417D-01*CTEMP*CTEMP*CTEMP+
&0.6966D-02*CTEMP*CTEMP*CTEMP*CTEMP
RETURN
END
C
C-----
DOUBLE PRECISION FUNCTION DF(KTEMP)
DOUBLE PRECISION R,KTEMP,PHI,DOTO,DTT,F
R=8.3143D+00
PHI=1.0D+00-1.0/(0.5D+00*DEXP(7.2D+03*4.184/(R*KTEMP))
&*DEXP(4.4D+00)+1.0D+00)
DOTO=3.3D-07*DEXP(-19.3D+03*4.184D+00/(R*KTEMP))
DTT=3.0D-04*DEXP(-14.7D+03*4.184D+00/(R*KTEMP))
F=0.86D+00

```

```
DF=PHI*DOTO+(1.0D+00-PHI)*F*DTT+(1.0D+00-PHI)
&*(1.0D+00-F)*DOTO
C DIFFUSION OF CARBON IN FERRITE, M*M/S
C MCLELLAN ET AL., TRANS. MET. SOC. AIME, VOL.233 (1965) 1938
C R = UNIVERSAL GAS CONSTANT, J/MOL/K
C KTEMP = ABSOLUTE TEMPERATURE
  RETURN
  END
C
C-----
```

```

C PROGRAM TO CALCULATE THE GROWTH RATE OF CEMENTITE ASSUMING
C ONE DIMENSIONAL PARABOLIC THICKENING OF CEMENTITE FROM AUSTENITE.
C KIRKALDY'S METHOD IS USED TO CALCULATE EQUILIBRIUM CONDITIONS.
C
C SEE HASHIGUCHI ET AL., CALPHAD VOL.8 NO.2(1984) PP173-186
C
C THE LINEAR APPROXIMATION IS USED FOR THE CHEMICAL PROFILE IN
C AUSTENITE AHEAD OF THE INTERFACE.
C
C
C M. TAKAHASHI, 19.1.1990
C
C IMPLICIT REAL*8 (A-H,K-Z)
C DOUBLE PRECISION C(8),Y(8),K(8),X(8),C0(8),W0(8),CB(3),DUM(3)
C &,G(8),E(8,8),WW(8),G2(8),LFX(2,8),GM(8),AC(8)
C COMMON/TRANS/C0,W0
C COMMON/COEFF/G,E,WW,GFE3C
C COMMON/HILL/G2,LFX,LCV,GM,AC,DDG,GFEC
C READ(5,*) III
C III=0
27 III=III+1
C IF (III .GT. III) GOTO 26
C READ(5,*) (W0(I),I=1,7)
C READ(5,*) TI,DCT,TF
C READ(5,*) SECS,DSEC,SECF,IN
C CALL CONV(1,W0,C0)
C IM=0
C WRITE(6,*) 'INITIAL COMPOSITIONS'
C WRITE(6,198)
C WRITE(6,199) (W0(I),I=1,7)
C WRITE(6,199) (C0(I),I=1,7)
199 FORMAT(1H,'7F9.5)
198 FORMAT(1H,' C SI MN NI
C &,' CR MO CU ')
C WRITE(6,*)
C CALL OMEGA(W)
C CC=0.0D+00
C DO 1 I=1,7
C CC=CC+C0(I)
1 CONTINUE
C C0(8)=1.0D+00-CC
C KK=0.0D+00
C DO 2 I=2,7
C K(I)=C0(I)/C0(8)
C KK=KK+K(I)
C IF (C0(I) .EQ. 0.0D+00) GOTO 2
C IM=I
2 CONTINUE
C YY=0.0D+00
C DO 3 I=2,7
C Y(I)=K(I)/(1.0D+00+KK)
C YY=YY+Y(I)
3 CONTINUE
C Y(8)=1.0D+00-YY
C CTEMP=TI
20 CTEMP=CTEMP+DCT
C T=CTEMP+273.0D+00
C IF (CTEMP .GT. TF) GOTO 25
C
C THERMODYNAMIC PARAMETERS
C IN ORDER OF SI,MN,NI,CR,MO,CU.
C
C DG=46150.0D+00/3.0-19.205D+00*T/3.0
C GFE3C=1.332D+04-64.718*T+7.481*T*DLOG(T)-DG
C G(2)=28535.0D+00-DG
C G(3)=-14263.0D+00+10.0D+00*T-DG
C G(3)=-13532.0D+00-DG
C G(4)=20338.0D+00-2.368D+00*T-DG
C G(5)=-24418.0D+00+16.61D+00*T-2.749D+00*T*DLOG(T)-DG
C G(6)=-19644.0D+00-0.628*T-DG
C G(7)=28535.0D+00-DG
C
C E(1,1)=4.7859D+00+5066.0D+00/T
C E(1,2)=4.84D+00-7370.0D+00/T
C E(1,2)=14795.0D+00/T

```

```

E(1,3)=-4811.0D+00/T
E(1,4)=-2.2D+00+7600.0D+00/T
E(1,5)=24.4-38400.0D+00/T
E(1,6)=3.855D+00-17870.0D+00/T
E(1,7)=4200.0D+00/T
C
E(2,2)=26048.0D+00/T
E(3,3)=2.406D+00-175.6D+00/T
C
E(3,3)=0.2D+00
E(4,4)=-721.7D+00/T
E(5,5)=7.655D+00-3154.0D+00/T-0.661D+00*DLOG(T)
E(6,6)=-2330.0D+00/T
E(7,7)=-0.161D+00-7834.0D+00/T
C
WW(2)=0.0D+00
WW(3)=8351.0D+00-15.188D+00*T
WW(4)=0.0D+00
WW(5)=1791.0D+00
WW(6)=0.0D+00
WW(7)=0.0D+00
C-----
G2(2)=123000D+00
G2(3)=-48500D+00
G2(4)=46000D+00
G2(5)=-251160D+00+118.0D+00*T
G2(6)=-267200D+00
G2(7)=-46000.0D+00+55.0D+00*T
LFX(1,2)=-108280.0D+00
LFX(1,3)=730.0D+00-10.0D+00*T
LFX(1,4)=-14600.0D+00
LFX(1,5)=13110.0D+00-31.82D+00*T+2.748D+00*T*DLOG(T)
LFX(1,6)=9686.0D+00
LFX(1,7)=49752.0D+00-9.431D+00*T
LFX(2,2)=0.0D+00
LFX(2,3)=0.0D+00
LFX(2,4)=8800.0D+00
LFX(2,5)=0.0D+00
LFX(2,6)=0.0D+00
LFX(2,7)=-8594.0D+00+5.05D+00*T
LCV=-21058.0D+00-11.581D+00*T
C
GM(2)=28535.0D+00
GM(2)=0.0D+00
GM(3)=-13532.0D+00
GM(4)=14540.0D+00-2.367D+00*T
GM(5)=-850.0D+00-14.58D+00*T
GM(6)=502.0D+00
GM(7)=28535.0D+00
AC(2)=0.0D+00
AC(3)=8350.0D+00-15.2D+00*T
AC(4)=0.0D+00
AC(5)=1790.0D+00
AC(6)=0.0D+00
AC(7)=0.0D+00
GFEC=1.332D+04-64.718*T+7.481*T*DLOG(T)
DDG=46150.0D+00-19.221D+00*T
C-----
C
C CALCULATION OF THE MAXIMUM FREE ENERGY CHANGE
CALL GCM(T,GMAX,XCEM)
WRITE(6,*) 'GMAX=',GMAX
C DIFFUSIVITY OF X IN GAMMA
D22=DIFX(T)
WRITE(6,*) 'D22=',D22
C FE-C CASE
C CALL FUNCFC(T,XGA)
CALL FUNCFC2(T,XGA)
CALL ALP(T,ALPHA,XGA,D11,W)
WRITE(6,195) CTEMP,XGA,ALPHA
195 FORMAT(1H,'FE-C : AT TEMP =',F8.2,' C-EQ=',F8.6,
& ' ALPHA=',D12.6)
C
IF (IM .EQ. 0) GOTO 24
C PARAEQUILIBRIUM CASE
C CALL FUNCP(T,XGA,IM)

```

```

CALL FUNCP2(T,XGA,IM)
CALL ALP(T,ALPHA,XGA,D11,W)
WRITE(6,194) CTEMP,XGA,ALPHA
194 FORMAT(1H,'PARA : AT TEMP =',F8.2,' C-EQ=',F8.6,
& ' ALPHA=',D12.6)
C
C DETERMINATION OF THE FINAL EQUILIBRIUM
CALL FUNCQ(T,C0,X,Y,IM)
C CALL FUNCOR(T,C0,X,Y,IM)
XEQ1=X(1)
XEQ2=X(IM)
YEQ1=Y(1)
YEQ2=Y(IM)
WRITE(6,196) CTEMP
196 FORMAT(1H,'AT TEMPERATURE DEG C =',F8.2)
WRITE(6,*) 'EQUILIBRIUM COMPOSITIONS'
WRITE(6,91) XEQ1,XEQ2,YEQ1,YEQ2
91 FORMAT(1H,' CGC=',F9.5,' MGC=',F9.5,' CCG=',F9.5,
& ' MCG=',F9.5)
89 FORMAT(1H,' C0(IM)-X(IM) = ',D12.5)
IF (X(1) .GT. C0(1)) GOTO 25
C
C IF(YEQ2 .GT. C0(IM)) THEN
C DMAX=YEQ2
C DMIN=C0(IM)
C ELSE
C DMAX=C0(IM)
C DMIN=YEQ2
C ENDIF
DMAX=0.25D+00
DMIN=C0(1)
C DMIN=0.0D+00
C
C
C DETERMINATION OF A TIE LINE
C
C CB(3)=(9.0*YEQ2+C0(IM))/10.0D+00
CB(3)=C0(1)+1.0D-05
C CB(3)=0.24D+00
C CB(3)=CB(IM)
DEL=CB(3)
DCB=1.0D-10
C
10 CB(1)=CB(3)-DCB
CB(2)=CB(3)+DCB
C IF(CB(3) .LT. C0(IM)+2.0D-10) GOTO 30
DO 5 I=1,3
DO 23 I3=1,8
C(I3)=0.0D+00
23 CONTINUE
C C(IM)=CB(I)
C C(1)=0.24D+00
C(IM)=C0(IM)
C(1)=CB(I)
C(8)=1.0D+00-C(IM)-C(1)
C WRITE(6,*) 'C1,CIM=',C(1),C(IM)
CALL FUNCQ(T,C,X,Y,IM)
C CALL FUNCOR(T,C,X,Y,IM)
C WRITE(6,*) 'C1,CIM=',C(1),C(IM)
C WRITE(6,*) 'C0,CGC=',C0(1),X(1)
C WRITE(6,188) I,X(1),X(IM),Y(IM)
188 FORMAT(1H,'I2,' X1=',F9.5,' X2=',F9.5,' Y2=',F9.5)
C
C CALCULATION OF THE GROWTH RATE, ALPHA CM/SEC**0.5
C
CALL AL(T,X,Y,ALPHA,DUM(I),W,D11,IM)
5 CONTINUE
C WRITE(6,*) 'DUM 1 2 3=',DUM(1),DUM(2),DUM(3)
IF (ABS(DUM(3)) .LT. ALPHA/1.0D+02) GOTO 30
IF (ABS(0.25D+00-CB(3)) .LT. 1.0D-04) THEN
WRITE(6,*) 'ENTER THE NPLE REGIME'
GOTO 30
ENDIF
DEL=CB(3)-2.0*DCB*DUM(3)/(DUM(2)-DUM(1))

```

```

C WRITE(6,*) 'CB3,DEL=',CB(3),DEL
IF (DEL .LT. DMIN) THEN
  DEL=(CB(3)+DMIN)/2.0D+00
ENDIF
IF (DEL .GT. DMAX) THEN
  DEL=(CB(3)+DMAX)/2.0D+00
ENDIF
C WRITE(6,*) 'CB3,DEL=',CB(3),DEL
C WRITE(6,*) 'ALPHA,DUM=',ALPHA,DUM(3)
IF (DUM(3) .GT. 0.0D+00) THEN
  CBUL=CB(3)
  CB(3)=DEL
ELSE
  CB(3)=(CB(3)+CBUL)/2.0
ENDIF
GOTO 10
30 WRITE(6,*) 'LOCAL EQUILIBRIUM'
WRITE(6,*) ' IN AUSTENITE'
WRITE(6,198)
WRITE(6,199) (X(I),I=1,7)
WRITE(6,*) ' IN CEMENTITE'
WRITE(6,199) (Y(I),I=1,7)
WRITE(6,193) CTEMP,X(1),ALPHA
193 FORMAT(1H 'L-EQ : AT TEMP =',F8.2,' C-EQ=',F8.6,
& ' ALPHA=',D12.6)
WRITE(6,*) ''
C
C CALCULATION OF NUCLEATION
IF (IN .EQ. 1) GOTO 24
CALL NUC(C0,D11,T)
C
C
24 GOTO 20
25 GOTO 27
26 STOP
END
C
C-----
C CALCULATION OF NUCLEATION RATE AND VOLUME FRACTION OF
C CEMENTITE ASSUMING A PILLBOX TYPE NUCLEUS
C
C-----
C CONSTANTS IN NUCLEATION FUNCTION
SUBROUTINE NUC(C0,D11,T)
IMPLICIT REAL*8 (A-H,K-Z)
DOUBLE PRECISION C0(8)
CTEMP=T-273.0D+00
N=1.0D+15
SV=5.0D+08
NA=6.022D+23
V=1.285D-23
A4=8.268D-30
KK=8.314D+00*1.0D+07/NA/V
PAI=3.141592654D+00
EP=1.0D+00
SIGE=1.0D+00
AR=3.0D+00
PHAI=GMAX*1.0D+07/NA/V
CJ=SV*N*(2.0D+00*C0(1)*D11*V*EP**0.5)
&/(A4*(3.0D+00*KK*T)**0.5)
CJ=CJ*DEXP(-4.0D+00*PAI*SIGE*SIGE*EP
&/(PHAI*PHAI*KK*T))
CJ1=12.0D+00*KK*T*A4*SIGE/(D11*C0(1)*V*PHAI*PHAI)
VTETA=4.0D+00*C0(1)
CJ0=AR*AR*ALPHA*ALPHA/VTETA*CJ
WRITE(6,*) 'CJ0=',CJ0
WRITE(6,*) 'CJ1=',CJ1
WRITE(6,*) 'D11=',D11
C-----
C CALCULATION OF VOLUME FRACTION OF CEMENTITE
SEC=SECS
YE=0.0D+00
YO=0.0D+00
200 SEC=SEC+DSEC

```

```

IF(SEC .GT. SECF) GOTO 202
XMIN=0.0D+00
XMAX=SEC
XX=XMAX-XMIN
DO 201 II=1,150
  IO=II*2.0D+00-1.0D+00
  IE=II*2.0D+00
  XO=XX/300.0D+00*IO+XMIN
  XE=XX/300.0D+00*IE+XMIN
  IF (LOG(CJ1/XO) .GT. 3.5D+00) GOTO 201
  YO=YO+(XMAX-XO)**1.5*DEXP(-CJ1/XO)
  IF (XMAX .LE. XE) GOTO 201
  YE=YE+(XMAX-XE)**1.5*DEXP(-CJ1/XE)
201 CONTINUE
  XE=CJ0*XX/300.0D+00*(4.0/3.0*YE+2.0/3.0*YO)
  XXE=1.0D+00-DEXP(-XE)
  WRITE(6,299) CTEMP,SEC,XXE
  IF (XXE .GT. 0.95D+00) GOTO 202
299 FORMAT(1H ,TEMP=',F6.1,' TIME=',D12.4,' V-TETA=',D12.4)
GOTO 200
202 RETURN
END
C
C-----
C SUBROUTINE TO CALCULATE ONE DIMENSIONAL RATE CONSTANT
C ASSUMING THE LINEAR GRADIENT OF CHEMISTRY
C ALPHA = CM/SEC **0.5
C-----
C
SUBROUTINE AL(T,X,Y,ALPHA,DUM,W,D11,IM)
IMPLICIT REAL*8(A-H,K-Z)
DOUBLE PRECISION C0(8),W0(8),X(8),Y(8),G(8),E(8,8),WW(8)
COMMON/TRANS/C0,W0
COMMON/COEFF/G,E,WW,GFE3C
CCG=0.25D+00
D22=DIFX(T)
D11=DIFFG(T,C0(1),X(1),W)
C WRITE(6,*) 'D11=',D11
C WRITE(6,*) 'D22=',D22
D12=D11*E(1,IM)*C0(1)/(1.0D+00+E(1,1)*C0(1))
C D12=0.0D+00
ALPHAC=D11*(C0(1)-X(1))*(C0(1)-X(1))
&/(CCG-C0(1))/(CCG-X(1))
ALPHAC=ALPHAC+D12*(C0(IM)-X(IM))*(C0(IM)-X(IM))
&/(Y(IM)-C0(IM))/(CCG-X(1))
IF(ALPHAC .LT. 0.0D+00) THEN
  ALPHAC=0.0D+00
GOTO 330
ENDIF
ALPHAC=ALPHAC**0.5D+00
330 ALPHAX=D22*(C0(IM)-X(IM))*(C0(IM)-X(IM))
&/(Y(IM)-C0(IM))/(Y(IM)-X(IM))
IF(ALPHAX .LT. 0.0D+00) THEN
  DUM=0.0D+00
GOTO 333
ENDIF
ALPHAX=ALPHAX**0.5D+00
C
DUM=ALPHAC-ALPHAX
IF (DUM .GT. 0.0D+00) THEN
  ALPHA=ALPHAC
ELSE
  ALPHA=ALPHAX
ENDIF
C WRITE (6,*) 'ALPHA,DUM=',ALPHA,DUM
333 RETURN
END
C
C-----
C SUBROUTINE TO CALCULATE ONE DIMENSIONAL RATE CONSTANT
C ASSUMING THE LINEAR GRADIENT OF CHEMISTRY
C ALPHA = CM/SEC **0.5 *****PARAEQUILIBRIUM CONDITION*****
C-----
C

```



```

SUBROUTINE ALP(T,ALPHA,XGA,D11,W)
IMPLICIT REAL*8(A-H,K-Z)
DOUBLE PRECISION C0(8),W0(8),G(8),E(8,8),WW(8)
COMMON/TRANS/C0,W0
COMMON/COEFF/G,E,WW,GFE3C
CCG=0.25D+00
D11=DIFFG(T,C0(1),XGA,W)
ALPHAC=D11*(C0(1)-XGA)*(C0(1)-XGA)
&/((CCG-C0(1))/(CCG-XGA))
ALPHAC=ALPHAC**0.5D+00
ALPHA=ALPHAC
C WRITE(6,*) 'ALPHA,DUM=',ALPHA,DUM
333 RETURN
END
C
C-----
C SUBROUTINE TO CALCULATE THE EQUILIBRIUM INTERFACE CHEMISTRY
C-----
C
SUBROUTINE FUNCOR(T,C,X,Y,IM)
IMPLICIT REAL*8 (A-H,K-Z)
DOUBLE PRECISION X(8),Y(8),E(7,7),WW(7),C0(8),C(8),G(7)
&,YY(3),FUN(3)
COMMON/TRANS/C0,W0
C
C INITIAL GUESS OF X2 AND Y2
C
X1=X(1)
X2=X(IM)
Y2=Y(IM)*4.0/3.0
C
DELTA=1.0D-10
C
499 YY(1)=Y2-DELTA
YY(2)=Y2+DELTA
YY(3)=Y2
DO 10 I=1,3
Y2=YY(I)
C
500 FF=FX Y(T,C,X1,X2,Y2,IM,1)
MM=FX Y(T,C,X1,X2,Y2,IM,0)
DFX=(FX Y(T,C,X1+DELTA,X2,Y2,IM,1)-FX Y(T,C,X1-DELTA,X2,Y2,IM,1))
& /2.0/DELTA
DFY=(FX Y(T,C,X1,X2+DELTA,Y2,IM,1)-FX Y(T,C,X1,X2-DELTA,Y2,IM,1))
& /2.0/DELTA
DMX=(FX Y(T,C,X1+DELTA,X2,Y2,IM,0)-FX Y(T,C,X1-DELTA,X2,Y2,IM,0))
& /2.0/DELTA
DMY=(FX Y(T,C,X1,X2+DELTA,Y2,IM,0)-FX Y(T,C,X1,X2-DELTA,Y2,IM,0))
& /2.0/DELTA
C
IF (ABS(FF) .LT. 1.0D-06 .AND.
& ABS(MM) .LT. 1.0D-06) GOTO 502
DENO=1.0D+00
DET=DFX*DMY-DMX*DFY
DX1=(-FF*DMY+MM*DFY)/DET
DX2=(-MM*DFX+FF*DMX)/DET
IF (X1/DENO+DX1 .LT. 0.0D+00) THEN
X1=X1/2.0/DENO
ELSE
X1=X1/DENO+DX1
ENDIF
IF (X2/DENO+DX2 .LT. 0.0D+00) THEN
X2=X2/2.0/DENO
ELSE
X2=X2/DENO+DX2
ENDIF
C
C WRITE(6,*) X2,Y2,FF
GOTO 500
502 FUN(I)=1.0D+00-(C(IM)-X2)/(C(1)-X1)
& /((3.0*Y2-4.0*X2)*(1.0D+00-4.0*X1))
10 CONTINUE
COEFF=(C(IM)-X2)/(C(1)-X1)
IF (ABS(FUN(3)) .LT. 1.0D-02) GOTO 503

```

```

DUMMY=Y2-2.0*DELTA*FUN(3)/(FUN(2)-FUN(1))
IF (DUMMY .LT. 0.0D+00) THEN
  DUMMY=Y2/2.0D+00
ENDIF
Y2=DUMMY
GOTO 499
503 X(1)=X1
X(IM)=X2
Y(IM)=Y2*3.0/4.0
RETURN
END
C
C
C-----
C FUNCTION TO CALCULATE EQUILIBRIUM FUNCTION F AND M
C IMF=1: F(X,Y) IMF=0: M(X,Y)
C
  DOUBLE PRECISION FUNCTION FXY0(T,C,X1,X2,Y2,IM,IMF)
  IMPLICIT REAL*8 (A-H,K-Z)
  DOUBLE PRECISION E(8,8),WW(8),G(8),C0(8),C(8)
  COMMON/TRANS/C0,W0
  COMMON/COEFF/G,E,WW,GFE3C
  R=8.314D+00
C
C
CG=X1
X1=(C(1)*(3.0*Y2-4.0*X2)-(C(IM)-X2))/(3.0*Y2-4.0*C(IM))
X8=1.0D+00-X1-X2
Y8=1.0D+00-Y2
C
MFE3C=R*T*DLOG(Y8)
MFE=R*T*DLOG(X8)-R*T/2.0*E(1,1)*X1*X1
MC=R*T/3.0*DLOG(X1)+R*T/3.0*E(1,1)*X1
MFE3C=MFE3C+(1-Y8)*WW(IM)*Y2
MFE=MFE-R*T/2.0*E(IM,IM)*X2*X2-R*T*X1*E(1,IM)*X2
MC=MC+R*T/3.0*E(1,IM)*X2
MX= R*T*DLOG(X2)
& +R*T*(E(1,IM)*X1+E(IM,IM)*X2)
MM3C= R*T*DLOG(Y2)
& +Y8*WW(IM)
MM3C=MM3C-Y8*WW(IM)*Y2
C
IF (IMF .EQ. 1) THEN
  FXY0=GFE3C+MFE3C-MFE-MC
ELSE
  FXY0=G(IM)+MM3C-MX-MC
ENDIF
C
RETURN
END
C
C
C-----
C SUBROUTINE TO CALCULATE THE EQUILIBRIUM INTERFACE CHEMISTRY
C-----
C
  SUBROUTINE FUNCO(T,C,X,Y,IM)
  IMPLICIT REAL*8 (A-H,K-Z)
  DOUBLE PRECISION X(8),Y(8),E(8,8),WW(8),X1(3),K(8)
  &,FUN(3),G(8),MM3C(8),MX(8),C0(8),C(8)
  COMMON/TRANS/C0,W0
  COMMON/COEFF/G,E,WW,GFE3C
  R=8.314D+00
C
C
XGA=1.0D-10
DUMMY=1.0D-12
100 X1(1)=XGA-DUMMY
X1(2)=XGA+DUMMY
X1(3)=XGA
DO 10 I=1,3
  XX=0.0D+00
  YY=0.0D+00
  FUN(I)=0.0D+00

```

```

B=DEXP((GFE3C-G(IM)-WW(IM))/R/T+E(1,IM)*X1(I))
X(IM)=C(IM)*(4.0*X1(I)-1.0D+00)/
& (3.0*B*(X1(I)-C(1))+4.0*C(1)-1.0D+00)
Y(IM)=B*X(IM)
XX=XX+X(IM)
YY=YY+Y(IM)
X(1)=X1(I)
X(8)=1.0D+00-X(1)-XX
IF (X(8) .LT. 0.0D+00) THEN
  WRITE(6,*) 'X(8),X(1),XX=',X(8),X(1),XX
ENDIF
Y(8)=1.0D+00-YY
C
C
MFE3C=R*T*DLOG(Y(8))
MFE=R*T*DLOG(X(8))-R*T/2.0*E(1,1)*X(1)*X(1)
MC=R*T/3.0*DLOG(X(1))+R*T/3.0*E(1,1)*X(1)
MFE3C=MFE3C+(1-Y(8))*WW(IM)*Y(IM)
MFE=MFE-R*T/2.0*E(IM,IM)*X(IM)*X(IM)-R*T*X(1)*E(1,IM)*X(IM)
MC=MC+R*T/3.0*E(1,IM)*X(IM)
MX(IM)= R*T*DLOG(X(IM))
& +R*T*(E(1,IM)*X(1)+E(IM,IM)*X(IM))
MM3C(IM)= R*T*DLOG(Y(IM))
& +Y(8)*WW(IM)
MM3C(IM)=MM3C(IM)-Y(8)*WW(IM)*Y(IM)
C
FUN(I)=GFE3C+MFE3C-MFE-MC
C
10 CONTINUE
IF(ABS(FUN(3)) .LT. 1.0D-06) GOTO 20
XGA=X1(3)-2.0*DUMMY*FUN(3)/(FUN(2)-FUN(1))
IF(XGA .LE. 0.0D+00) THEN
  XGA=X1(3)/2.0D+00
ENDIF
GOTO 100
20 DO 30 I=1,8
  X(I)=X(I)
  Y(I)=3.0D+00/4.0D+00*Y(I)
30 CONTINUE
Y(1)=0.25D+00
RETURN
END
C
C-----
C SUBROUTINE TO CALCULATE THE PARAEQUILIBRIUM INTERFACE CHEMISTRY
C-----
C
SUBROUTINE FUNC(T,XGA,IM)
IMPLICIT REAL*8 (A-H,K-Z)
DOUBLE PRECISION X(8),Y(8),E(8,8),WW(8),X1(3)
&,FUN(3),G(8),C0(8),W0(8)
COMMON/TRANS/C0,W0
COMMON/COEFF/G,E,WW,GFE3C
R=8.314D+00
XGA=0.005D+00
C
C
DUMMY=1.0D-08
100 X1(1)=XGA-DUMMY
X1(2)=XGA+DUMMY
X1(3)=XGA
DO 10 I=1,3
  XX=0.0D+00
  FUN(I)=0.0D+00
  K=C0(IM)/C0(8)
  Y(IM)=K/(1+K)
  X(IM)=(1-X1(I))*Y(IM)
  X(1)=X1(I)
  X(8)=1.0D+00-X(1)-X(IM)
  Y(8)=1.0D+00-Y(IM)
C
C
DENO=1.0D+00
C
MFE3C=R*T*DLOG(Y(8))

```

```

MFE=R*T*DLOG(X(8)/DENO)-R*T/2.0*E(1,1)*X(1)*X(1)/DENO/DENO
MC=R*T/3.0*DLOG(X(1)/DENO)+R*T/3.0*E(1,1)*X(1)/DENO
MFE3C=MFE3C+(1-Y(8))*WW(IM)*Y(IM)
MFE=MFE-R*T/2.0*E(IM,IM)*X(IM)*X(IM)/DENO/DENO
MFE=MFE-R*T*X(1)*E(1,IM)*X(IM)/DENO/DENO
MC=MC+R*T/3.0*E(1,IM)*X(IM)/DENO
MX= R*T*DLOG(X(IM)/DENO)
&   +R*T*(E(1,IM)*X(1)+E(IM,IM)*X(IM))/DENO
MM3C= R*T*DLOG(Y(IM))
&   +Y(8)*WW(IM)-Y(8)*WW(IM)*Y(IM)
C
FUN(I)=X(8)*(GFE3C+MFE3C-MFE-MC)
FUN(I)=FUN(I)+X(IM)*(G(IM)+MM3C-MX-MC)
C
C   WRITE(6,*) IM,E(1,1),E(1,IM),E(IM,IM)
C
10  CONTINUE
   IF(ABS(FUN(3)) .LT. 1.0D-10) GOTO 20
   XGA=X1(3)-2.0*DUMMY*FUN(3)/(FUN(2)-FUN(1))
   GOTO 100
20  XGA=X1(3)
   RETURN
   END
C
C-----
C SUBROUTINE TO CALCULATE THE EQUILIBRIUM INTERFACE COMPOSITION
C IN FE-C SYSTEMS
C-----
C
SUBROUTINE FUNCFC(T,XGA)
IMPLICIT REAL*8 (A-H,K-Z)
DOUBLE PRECISION FUN(3),X(3),G(8),E(8,8),WW(8)
COMMON/COEFF/G,E,WW,GFE3C
R=8.314D+00
XGA=0.005D+00
DUMMY=1.0D-08
10  X(1)=XGA-DUMMY
   X(2)=XGA+DUMMY
   X(3)=XGA
   DO 20 I=1,3
     X8=1.0D+00-X(I)
     MFE=R*T*DLOG(X8)-R*T/2.0*E(1,1)*X(I)*X(I)
     MC=R*T/3.0*DLOG(X(I))+R*T/3.0*E(1,1)*X(I)
     FUN(I)=GFE3C-MFE-MC
20  CONTINUE
   IF(ABS(FUN(3)) .LT. 1.0D-06) GOTO 30
   XGA=X(3)-2.0*DUMMY*FUN(3)/(FUN(2)-FUN(1))
   GOTO 10
30  XGA=X(3)
   RETURN
   END
C
C-----
C SUBROUTINE TO CONVERT WT% TO MOLE FRACTION
C   OR MOLE FRACTION TO WT%.
C-----
C
SUBROUTINE CONV(N,WT,C)
IMPLICIT REAL*8 (A-H,O-Z)
DOUBLE PRECISION AN(8), WT(8), C(8), A(8)
AN(1)=12.0115D+00
AN(2)=28.09D+00
AN(3)=54.94D+00
AN(4)=58.71D+00
AN(6)=95.94D+00
AN(5)=52.00D+00
AN(7)=63.55D+00
AN(8)=55.84D+00
IF (N .EQ. 0) GOTO 1
WT(8)=100.0D+00-WT(1)-WT(2)-WT(3)-WT(4)-WT(5)-WT(6)-WT(7)
AT=0.0D+00
DO 2 I=1,8
  A(I)=WT(I)/AN(I)

```

```

      AT=AT+A(I)
2  CONTINUE
   DO 3 I=1,8
      C(I)=WT(I)/AN(I)/AT
3  CONTINUE
   GOTO 4
1  C(8)=1.0D+00-C(1)-C(2)-C(3)-C(4)-C(5)-C(6)-C(7)
   AT=0.0D+00
   DO 5 I=1,8
      A(I)=C(I)*AN(I)
      AT=AT+A(I)
5  CONTINUE
   DO 6 I=1,8
      WT(I)=C(I)*AN(I)/AT*100.0D+00
6  CONTINUE
4  RETURN
   END
C
C-----
C FUNCTION GIVING THE CARBON DIFFUSIVITY IN FERRITE BASED ON
C AGREN'S WORK
C DCA : CM**2/SEC
C
   DOUBLE PRECISION FUNCTION DCA(T)
   DOUBLE PRECISION T,PAI
   PAI=3.141592654D+00
   DCA=0.02D+00*DEXP(-10115.0D+00/T)
   DCA=DCA*DEXP(0.5898D+00*(1.0D+00+2.0/PAI
   &*DATAN(1.4985D+00-15309.0D+00/T)))
   RETURN
   END
C
C-----
C FUNCTION GIVING THE CARBON DIFFUSIVITY IN AUSTENITE
C
   DOUBLE PRECISION FUNCTION DIFFG(T,X1,X2,W)
   IMPLICIT REAL*8(A-H,K-Y), INTEGER(I,J,Z)
   DOUBLE PRECISION DIFF(300),CARB(300)
C HH=PLANCK CONST./S, KK=BOLTZMAN CONST. J/K
   HH=6.6262D-34
   KK=1.38062D-23
   Z=12
   A5=1.0D+00
   R=8.31432D+00
C
C DIFF=DIFFUSIVITY OF CARBON IN AUSTENITE, CM**/SEC
C Z=COORDINATION OF INTERSTIAL SITE
C PSI=COMPOSITION DEPENDENCE OF DIFFUSION COEFFICIENT
C THETA=NO. C ATOMS/ NO. FE ATOMS
C ACTIV=ACTIVITY OF CARBON IN AUSTENITE
C R=GAS CONSTANT
C X=MOLE FRACTION OF CARBON
C T=ABSOLUTE TEMPERATURE
C SIGMA=SITE EXCLUSION PROBABILITY
C W=CARBON CARBON INTERACTION ENERGY IN AUSTENITE
C
   DASH=(KK*T/HH)*DEXP(-(21230.0D+00/T))*DEXP(-31.84D+00)
   XINCR=(X1-X2)/300.0D+00
   DO 1 I=1,300
      CARB(I)=X2+(I-1)*XINCR
      X=CARB(I)
      THETA=X/(A5-X)
      ACTIV=CG(X,T,W,R)
      ACTIV=DEXP(ACTIV)
      DACTIV=DCG(X,T,W,R)
      DACTIV=DACTIV*ACTIV
      DACTIV=DACTIV*A5/((A5+THETA)**2)
      SIGMA=A5-DEXP((-W)/(R*T))
      PSI=ACTIV*(A5+Z*((A5+THETA)/(A5-(A5+Z/2)*THETA+(Z/2)*(A5+Z/2)*
      &(A5-SIGMA)*THETA*THETA)))+(A5+THETA)*DACTIV
      DIFF(I)=DASH*PSI
1  CONTINUE
   II3=0
   CALL DQSES(XINCR,DIFF,300,ANS,ERROR)

```

```

DIFFG=ANS/(X1-X2)
RETURN
END
C
C-----
C FUNCTION GIVING THE CARBON DIFFUSIVITY IN AUSTENITE.
C
DOUBLE PRECISION FUNCTION DIFFG1(T,X,W)
IMPLICIT REAL*8(A-H,K-Y), INTEGER(I,J,Z)
C HH=PLANCK CONST.J/S, KK=BOLTZMAN CONST. J/K
HH=6.6262D-34
KK=1.38062D-23
Z=12
A5=1.0D+00
R=8.31432D+00
C
C DIFF=DIFFUSIVITY OF CARBON IN AUSTENITE, CM**2/SEC
C Z=COORDINATION OF INTERSTIAL SITE
C PSI=COMPOSITION DEPENDENCE OF DIFFUSION COEFFICIENT
C THETA=NO. C ATOMS/ NO. FE ATOMS
C ACTIV=ACTIVITY OF CARBON IN AUSTENITE
C R=GAS CONSTANT
C X=MOLE FRACTION OF CARBON
C T=ABSOLUTE TEMPERATURE
C SIGMA=SITE EXCLUSION PROBABILITY
C W=CARBON CARBON INTERACTION ENERGY IN AUSTENITE
C
DASH=(KK*T/HH)*DEXP(-(21230.0D+00/T))*DEXP(-31.84D+00)
THETA=X/(A5-X)
ACTIV=CG(X,T,W,R)
ACTIV=DEXP(ACTIV)
DACTIV=DCG(X,T,W,R)
DACTIV=DACTIV*ACTIV
DACTIV=DACTIV*A5/((A5+THETA)**2)
SIGMA=A5-DEXP((-W)/(R*T))
PSI=ACTIV*(A5+Z*((A5+THETA)/(A5-(A5+Z/2)*THETA+(Z/2)*(A5+Z/2)*
&(A5-SIGMA)*THETA*THETA)))+(A5+THETA)*DACTIV
DIFFG1=DASH*PSI
RETURN
END
C
C-----
C FUNCTION GIVING LFG LN(ACTIVITY) OF CARBON IN AUSTENITE.
C
DOUBLE PRECISION FUNCTION CG(X,T,W,R)
DOUBLE PRECISION J,DG,DUMMY,T,R,W,X
J=1-DEXP(-W/(R*T))
DG=DSQRT(1-2*(1+2*J)*X+(1+8*J)*X*X)
DUMMY=5*DLOG((1-2*X)/X)+6*W/(R*T)+((38575.0)-
&13.48)*T)/(R*T)
CG=DUMMY+DLOG(((DG-1+3*X)/(DG+1-3*X))**6)
RETURN
END
C
C-----
C FUNCTION GIVING DIFFERENTIAL OF LN(ACTIVITY) OF CARBON
C IN AUSTENITE.
C DIFFERENTIAL IS WITH RESPECT TO X.
C
DOUBLE PRECISION FUNCTION DCG(X,T,W,R)
DOUBLE PRECISION J,DG,DDG,X,T,W,R
J=1-DEXP(-W/(R*T))
DG=DSQRT(1-2*(1+2*J)*X+(1+8*J)*X*X)
DDG=(0.5/DG)*(-2-4*J+2*X+16*J*X)
DCG=-((10/(1-2*X))+(5/X))+6*((DDG+3)/(DG-1+3*X
&)-(DDG-3)/(DG+1-3*X))
RETURN
END
C
C-----
SUBROUTINE OMEGA(W)
C SUBROUTINE TO CALCULATE THE CARBON CARBON INTERACTION ENERGY IN
C AUSTENITE, AS A FUNCTION OF ALLOY COMPOSITION. BASED ON .MUCG18
C THE ANSWER IS IN JOULES PER MOL. **7 OCTOBER 1981**

```

```

COMMON/TRANS/C0,W0
DOUBLE PRECISION C(8),W,P(8),B1,B2,Y(8),T10,T20,B3,XONE
&,C0(8),W0(8)
INTEGER B5,I,U,B4
DO 1 I=1,8
  C(I)=W0(I)
1 CONTINUE
B3=0.0D+00
C(8)=C(1)+C(2)+C(3)+C(4)+C(5)+C(6)+C(7)
C(8)=100.0D+00-C(8)
C(8)=C(8)/55.84D+00
C(1)=C(1)/12.0115D+00
C(2)=C(2)/28.09D+00
C(3)=C(3)/54.94D+00
C(4)=C(4)/58.71D+00
C(5)=C(5)/95.94D+00
C(6)=C(6)/52.0D+00
C(7)=C(7)/50.94D+00
B1=C(1)+C(2)+C(3)+C(4)+C(5)+C(6)+C(7)+C(8)
DO 107 U=2,7
  Y(U)=C(U)/C(8)
107 CONTINUE
DO 106 U=1,8
  C(U)=C(U)/B1
106 CONTINUE
XONE=C(1)
C XONE=DINT(10000.0D+00*XONE)
C XONE=XONE/10000
B2=0.0D+00
T10=Y(2)*(-3)+Y(3)*2+Y(4)*12+Y(5)*(-9)+Y(6)*(-1)+Y(7)*(-12)
T20=-3*Y(2)-37.5*Y(3)-6*Y(4)-26*Y(5)-19*Y(6)-44*Y(7)
  P(2)=2013.0341+763.8167*C(2)+45802.87*C(2)**2-280061.63*C(2)**3
  &+3.864D+06*C(2)**4-2.4233D+07*C(2)**5+6.9547D+07*C(2)**6
  P(3)=2012.067-1764.095*C(3)+6287.52*C(3)**2-21647.96*C(3)**3-
  &2.0119D+06*C(3)**4+3.1716D+07*C(3)**5-1.3885D+08*C(3)**6
  P(4)=2006.8017+2330.2424*C(4)-54915.32*C(4)**2+1.6216D+06*C(4)**3
  &-2.4968D+07*C(4)**4+1.8838D+08*C(4)**5-5.5531D+08*C(4)**6
  P(5)=2006.834-2997.314*C(5)-37906.61*C(5)**2+1.0328D+06*C(5)**3
  &-1.3306D+07*C(5)**4+8.411D+07*C(5)**5-2.0826D+08*C(5)**6
  P(6)=2012.367-9224.2655*C(6)+33657.8*C(6)**2-566827.83*C(6)**3
  &+8.5676D+06*C(6)**4-6.7482D+07*C(6)**5 +2.0837D+08*C(6)**6
  P(7)=2011.9996-6247.9118*C(7)+5411.7566*C(7)**2
  &+250118.1085*C(7)**3-4.1676D+06*C(7)**4
DO 108 U=2,7
  B3=B3+P(U)*Y(U)
  B2=B2+Y(U)
108 CONTINUE
IF (B2 .EQ. 0.0D+00) GOTO 455
W=(B3/B2)*4.187
GOTO 456
455 W=8054.0
456 RETURN
END
C
C-----
C FUNCTION GIVING THE EQUILIBRIUM MOLE FRACTION OF CARBON IN FERRITE.
C
DOUBLE PRECISION FUNCTION XALPH(T)
DOUBLE PRECISION T,CTEMP
CTEMP=(T-273.0D+00)/900.0D+00
XALPH=0.1528D-02-0.8816D-02*CTEMP+0.2450D-01*CTEMP*CTEMP
&-0.2417D-01*CTEMP*CTEMP*CTEMP+
&0.6966D-02*CTEMP*CTEMP*CTEMP*CTEMP
RETURN
END
C-----
C DATA FOR DIFFUSIVITIES OF THE THIRD ELEMENT IN AUSTENITE
C IN ORDER OF SI,MN,NI,CR,MO,CU
BLOCK DATA COEF
COMMON/DIFFUS/D22
DOUBLE PRECISION D22(7)
DATA (D22(J),J=2,7)/
& 6.4D+00,2.41D+00,0.475D+00,4.75D+00,2.73D+00,1.0D+00/
END

```

```

C-----
C FUNCTION TO CALCULATE DIFFUSIVITY OF THE THIRD ELEMENT
C CM**2/SEC
C
DOUBLE PRECISION FUNCTION DIFX(T)
IMPLICIT REAL*8(A-H,K-Z)
DOUBLE PRECISION C0(8),W0(8),D22(7)
COMMON/TRANS/C0,W0
COMMON/DIFFUS/D22
Q=286000.0D+00
K=8.314D+00
D0=0.7D+00
I=1
10 I=I+1
IF(I .GT. 8) GOTO 20
IF(C0(I) .NE. 0) GOTO 20
GOTO 10
20 DIFX=D22(I)*D0*DEXP(-Q/K/T)
RETURN
END
C-----
C SUBROUTINE TO CALCULATE THE MAXIMUM FREE ENERGY CHANGE AVAILABLE
C FOR NUCLEATION OF CEMENTITE FROM AUSTENITE.
C KIRKALDY'S METHOD IS USED.
C SEE HASHIGUCHI ET AL., CALPHAD VOL.8 NO.2(1984) PP173-186
C
C M. TAKAHASHI, 20.11.1989
C
C
SUBROUTINE GCM(T,GMAX,XCEM)
IMPLICIT REAL*8 (A-H,K-Z)
COMMON/TRANS/C0,W0
DOUBLE PRECISION X(8),Y(8),E(8,8),WW(8),X1(3),K(8)
&,FUN(3),G(8),C0(8),Y2(3)
COMMON/COEFF/G,E,WW,GFE3C
R=8.314D+00
XGA=0.01D+00
C
C
DUMMY=1.0D-06
DO 1 I=1,7
X(I)=C0(I)
IF(X(I) .EQ. 0.0D+00) GOTO 1
IFLAG=I
1 CONTINUE
X(8)=C0(8)
YINIT=4.0D+00/3.0D+00*X(IFLAG)
100 Y2(1)=YINIT-DUMMY
Y2(2)=YINIT+DUMMY
Y2(3)=YINIT
DO 10 I=1,3
FUN(I)=0.0D+00
DO 2 II=2,7
IF(II .NE. IFLAG) THEN
Y(II)=0.0D+00
ELSE
Y(II)=Y2(I)
ENDIF
2 CONTINUE
Y(8)=1.0D+00-Y(IFLAG)
C
C
MFE3C=R*T*DLOG(Y(8))+(1.0D+00-Y(8))*WW(IFLAG)*Y(IFLAG)
MFE=R*T*DLOG(X(8))-R*T/2.0*(E(1,1)*X(1)*X(1)+E(IFLAG,IFLAG)
&*X(IFLAG)*X(IFLAG))-R*T*X(1)*E(1,IFLAG)*X(IFLAG)
MC=R*T/3.0*DLOG(X(1))+R*T/3.0*(E(1,1)*X(1)+E(1,IFLAG)
&*X(IFLAG))
MX=R*T*DLOG(X(IFLAG))+R*T*(E(1,IFLAG)*X(1)
&+E(IFLAG,IFLAG)*X(IFLAG))
MM3C=R*T*DLOG(Y(IFLAG))+Y(8)*WW(IFLAG)*(1.0D+00-Y(IFLAG))
C
FC=GFE3C+MFE3C-MFE-MC
FMC=G(IFLAG)+MM3C-MX-MC
FUN(I)=FFC-FMC

```



```

      MUFEC=MFE3C*3.0D+00/4.0D+00+GFE3C
C
10  CONTINUE
    IF(ABS(FUN(3)) .LT. 1.0D-06) GOTO 20
    YINIT=YINIT-2.0*DUMMY*FUN(3)/(FUN(2)-FUN(1))
    IF (YINIT .LT. 0.0D+00) THEN
      YINIT=1.0D-04
    ENDIF
    GOTO 100
20  GMAX=(FMC+FFC)/2.0D+00*3.0D+00/4.0D+00
    XCEM=YINIT*3.0/4.0
    RETURN
    END
C -----
C SUBROUTINE TO CALCULATE PARAEQUILIBRIUM BOUNDARY COMPOSITIONS
C HILLERT-STAFFANSON SUB-REGULAR SOLUTION MODEL IS USED
C 1991.1.8 M.TAKAHASHI
C
SUBROUTINE FUNCP2(T,XGA,IM)
IMPLICIT REAL*8 (A-H,K-Z)
DOUBLE PRECISION X(8),Y(8),G2(8),LFX(2,8),GM(8),AC(8)
&,C0(8),W0(8),X1(3),FUN(3)
COMMON/TRANS/C0,W0
COMMON/HILL/G2,LFX,LCV,GM,AC,DDG,GFEC
R=8.314D+00
XGA=0.005D+00
C
DUMMY=1.0D-08
100 X1(1)=XGA-DUMMY
    X1(2)=XGA+DUMMY
    X1(3)=XGA
    DO 10 I=1,3
      K=C0(IM)/C0(8)
      Y(IM)=K/(1.0D+00+K)
      X(IM)=(1.0D+00-X1(I))*Y(IM)
      X(1)=X1(I)
      DENO=1.0D+00-X(1)
      Y(8)=1.0D+00-Y(IM)
      X(8)=1.0D+00-X(1)-X(IM)
      X(1)=X(1)/DENO
      X(IM)=X(IM)/DENO
      X(8)=X(8)/DENO
C
EG0=-X(IM)*X(1)*G2(IM)+X(IM)*X(IM)*
& (LFX(1,IM)+(3.0D+00-4.0*X(IM))*LFX(2,IM))+X(1)*X(1)*LCV
EG1=-2.0*X(1)*LCV+X(IM)*G2(IM)
EG2=X(8)*X(1)*G2(IM)+X(8)*X(8)*
& (LFX(1,IM)+(1.0D+00-4.0*X(IM))*LFX(2,IM))+X(1)*X(1)*LCV
C
C
FUN(I)=X(8)*
& GFEC-DDG/3 + R*T*DLOG(Y(8))+AC(IM)*Y(IM)*Y(IM)
& - R*T*DLOG(X(8))-R*T*DLOG(1.0D+00-X(1))
& - R*T/3*DLOG(X(1)/(1.0D+00-X(1)))
& - EG0-EG1/3 )
FUN(I)=FUN(I)+X(IM)*
& GM(2)-DDG/3 + R*T*DLOG(Y(IM))+AC(IM)*Y(8)*Y(8)
& - R*T*DLOG(X(IM))-R*T*DLOG(1.0D+00-X(1))
& - R*T/3*DLOG(X(1)/(1.0D+00-X(1)))
& - EG2-EG1/3 )
C
10  CONTINUE
    IF(ABS(FUN(3)) .LT. 1.0D-06) GOTO 20
    XGA=X(1)-2.0*DUMMY*FUN(3)/(FUN(2)-FUN(1))
    IF (XGA .LT. DUMMY) THEN
      XGA=X(1)/2.0D+00
    ENDIF
    IF (XGA .GT. 1.0D+00) THEN
      XGA=(1.0D+00+X(1))/2.0
    ENDIF
    XGA=XGA*DENO
    GOTO 100
20  XGA=X1(3)
    RETURN

```

```

END
C
C -----
C SUBROUTINE TO CALCULATE EQUILIBRIUM BOUNDARY COMPOSITIONS
C IN FE-C-X TERNARY SYSTEM.
C HILLERT-STAFFANSON SUB-REGULAR SOLUTION MODEL IS USED.
C 1991.1.8 M.TAKAHASHI
C
SUBROUTINE FUNCFC2(T,XGA)
IMPLICIT REAL*8 (A-H,K-Z)
DOUBLE PRECISION X(8),Y(8),G2(8),LFX(2,8),GM(8),AC(8)
&,C0(8),W0(8),X1(3),FUN(3)
COMMON/TRANS/C0,W0
COMMON/HILL/G2,LFX,LCV,GM,AC,DDG,GFEC
R=8.314D+00
XGA=0.005D+00
C
DUMMY=1.0D-08
100 X1(1)=XGA-DUMMY
X1(2)=XGA+DUMMY
X1(3)=XGA
DO 10 I=1,3
X(I)=X1(I)
DENO=1.0D+00-X(1)
X(8)=1.0D+00-X(1)
X(1)=X(1)/DENO
X(8)=X(8)/DENO
C
EG0=X(1)*X(1)*LCV
EG1=-2.0*X(1)*LCV
C
C
FUN(I)=GFEC-DDG/3
& - R*T*DLOG(1.0D+00-X(1))
& - R*T/3*DLOG(X(1)/(1.0D+00-X(1)))
& - EG0-EG1/3
C
10 CONTINUE
IF(ABS(FUN(3)) .LT. 1.0D-06) GOTO 20
XGA=X(1)-2.0*DUMMY*FUN(3)/(FUN(2)-FUN(1))
IF (XGA .LT. DUMMY) THEN
XGA=X(1)/2.0D+00
ENDIF
IF (XGA .GT. 1.0D+00) THEN
XGA=(1.0D+00+X(1))/2.0
ENDIF
XGA=XGA*DENO
GOTO 100
20 XGA=X1(3)
RETURN
END
C
C -----
C HILLERT-STAFFANSON SUB-REGULAR SOLUTION MODEL IS USED
C 1991.1.8 M.TAKAHASHI
C IMF=1: F(X,Y) IMF=0: M(X,Y)
C
DOUBLE PRECISION FUNCTION FXY(T,C,X1,X2,Y2,IM,IMF)
IMPLICIT REAL*8 (A-H,K-Z)
DOUBLE PRECISION X(8),Y(8),G2(8),LFX(2,8),GM(8),AC(8)
&,C0(8),W0(8),FUN(3),C(8)
COMMON/TRANS/C0,W0
COMMON/HILL/G2,LFX,LCV,GM,AC,DDG,GFEC
R=8.314D+00
C
X(1)=(C(1)*(3.0*Y2-4.0*X2)-(C(IM)-X2))/(3.0*Y2-4.0*C(IM))
X(1)=X1
X(IM)=X2
X(8)=1.0D+00-X(1)-X(IM)
Y(IM)=Y2
Y(8)=1.0D+00-Y(IM)
DENO=1.0D+00-X(1)
X(1)=X(1)/DENO
X(IM)=X(IM)/DENO

```

```

X(8)=X(8)/DENO
C
EG0=-X(IM)*X(1)*G2(IM)+X(IM)*X(IM)*
& (LFX(1,IM)+(3.0D+00-4.0*X(IM))*LFX(2,IM))+X(1)*X(1)*LCV
EG1=-2.0*X(1)*LCV+X(IM)*G2(IM)
EG2=X(8)*X(1)*G2(IM)+X(8)*X(8)*
& (LFX(1,IM)+(1.0D+00-4.0*X(IM))*LFX(2,IM))+X(1)*X(1)*LCV
C
IF (IMF.EQ.1) THEN
  FXY=GFEC-DDG/3 + R*T*DLOG(Y(8))+AC(IM)*Y(IM)*Y(IM)
& - R*T*DLOG(X(8))-R*T*DLOG(1.0D+00-X(1))
& - R*T/3*DLOG(X(1)/(1.0D+00-X(1)))
& - EG0-EG1/3
ELSE
  FXY=GM(2)-DDG/3 + R*T*DLOG(Y(IM))+AC(IM)*Y(8)*Y(8)
& - R*T*DLOG(X(IM))-R*T*DLOG(1.0D+00-X(1))
& - R*T/3*DLOG(X(1)/(1.0D+00-X(1)))
& - EG2-EG1/3
ENDIF
C
RETURN
END
C
C-----

```

C PROGRAM TO CALCULATE THE CARBON CONCENTRATION IN AUSTENITE WHICH
 C IS IN EITHER PARA- OR ORTHO- EQUILIBRIUM WITH CEMENTITE.
 C KIRKALDY'S METHOD IS USED.

C SEE HASHIGUCHI ET AL., CALPHAD VOL.8 NO.2(1984) PP173-186

C

M. TAKAHASHI, 22.8.1989

C

```

  IMPLICIT REAL*8 (A-H,K-Z)
  DOUBLE PRECISION C(8),Y(8),K(8),X(8)
  &,C0(8),W0(8),CORTHO(8),WORTH0(8),CPARA(8),WPARA(8)
  COMMON/TRANS/C0
  READ(5,*) IALLOY
  READ(5,*)(W0(I),I=1,7)
  READ(5,*) CTEMPU,DTEMP,CTEMPL
  CALL CONV(1,W0,C0)
  WRITE(6,199) (W0(I),I=1,7)
  WRITE(6,199) (C0(I),I=1,7)
199  FORMAT(4H C=,F7.4,4H SI=,F7.4,4H MN=,F7.4,
  &4H NI=,F7.4,4H MO=,F7.4,4H CR=,F7.4,4H V=,F7.4)
  WRITE(6,*)
  CC=0.0D+00
  DO 1 I=1,7
  CC=CC+C0(I)
1  CONTINUE
  C0(8)=1.0D+00-CC
  KK=0.0D+00
  DO 2 I=2,7
  K(I)=C0(I)/C0(8)
  KK=KK+K(I)
2  CONTINUE
  YY=0.0D+00
  DO 3 I=2,7
  Y(I)=K(I)/(1.0D+00+KK)
  YY=YY+Y(I)
3  CONTINUE
  Y(8)=1.0D+00-YY
  C
  C
  WRITE(6,*) T-ACM,C P-WT%C P-M.F.C O-WT%C'
  &,' O-M.F.C O-WT%X O-M.F.X'
  CTEMP=CTEMPU+DTEMP
200 CTEMP=CTEMP-DTEMP
  IF (CTEMP.LT. CTEMPL) GOTO 300
  T=CTEMP+273.0D+00
  CALL FUNCPT(T,Y,K,CPARA)
  CALL CONV(0,WPARA,CPARA)
  CALL FUNCO(T,CORTHO)
  CALL CONV(0,WORTH0,CORTHO)
  WRITE(6,98) T-273.0D+00,WPARA(1),CPARA(1),WORTH0(1),CORTHO(1)
  &,WORTH0(IALLOY),CORTHO(IALLOY)
98  FORMAT(1H ,F8.2, 6D12.4)
  GOTO 200
  C
  C
  300 STOP
  END
  C
  C-----
  C SUBROUTINE TO CALCULATE THE PARAEQUILIBRIUM ACM TEMP.
  C-----
  C
  SUBROUTINE FUNCPT(T,Y,K,X)
  IMPLICIT REAL*8 (A-H,K-Z)
  DOUBLE PRECISION X(8),Y(8),E(7,7),W(7),X1(3),K(8)
  &,FUN(3),G(7),MM3C(8),MX(8)
  R=8.314D+00
  XGA=0.005D+00
  C
  C THERMODYNAMIC PARAMETERS
  C IN ORDER OF SI,MN,NI,CR,MO,CU.
  C
  DG=46150.0D+00/3.0-19.205D+00*T/3.0
  GFE3C=1.332D+04-64.718*T+7.481*T*DLOG(T)-DG
  G(2)=28535.0D+00-DG

```

```

G(3)=-14263.0D+00+10.0D+00*T-DG
C G(3)=-13532.0D+00-DG
G(4)=20338.0D+00-2.368D+00*T-DG
G(5)=-24418.0D+00+16.61D+00*T-2.749D+00*T*DLOG(T)-DG
G(6)=-19644.0D+00-0.628*T-DG
G(7)=28535.0D+00-DG
C
E(1,1)=8910.0D+00/T
E(1,2)=4.84D+00-7370.0D+00/T
E(1,3)=-4811.0D+00/T
E(1,4)=-2.2D+00+7600.0D+00/T
E(1,5)=24.4-38400.0D+00/T
E(1,6)=3.855D+00-17870.0D+00/T
E(1,7)=4200.0D+00/T
C
E(2,2)=26048.0D+00/T
E(3,3)=2.406D+00-175.6D+00/T
C E(3,3)=0.2D+00
E(4,4)=-721.7D+00/T
E(5,5)=7.655D+00-3154.0D+00/T-0.661D+00*DLOG(T)
E(6,6)=-2330.0D+00/T
E(7,7)=-0.161D+00-7834.0D+00/T
C
W(2)=0.0D+00
W(3)=8351.0D+00-15.188D+00*T
W(4)=0.0D+00
W(5)=1791.0D+00
W(6)=0.0D+00
W(7)=0.0D+00
C
C
DUMMY=1.0D-06
100 X1(1)=XGA-DUMMY
X1(2)=XGA+DUMMY
X1(3)=XGA
DO 10 I=1,3
XX=0.0D+00
FUN(I)=0.0D+00
DO 1 II=2,7
X(II)=(1.0D+00-X1(I))*Y(II)
XX=XX+X(II)
1 CONTINUE
X(1)=X1(I)
X(8)=1.0D+00-X(1)-XX
C
C
MFE3C=R*T*DLOG(Y(8))
MFE=R*T*DLOG(X(8))-R*T/2.0*E(1,1)*X(1)*X(1)
MC=R*T/3.0*DLOG(X(1))+R*T/3.0*E(1,1)*X(1)
DO 2 J1=2,7
IF (X(J1) .EQ. 0.0D+00) GOTO 2
MFE3C=MFE3C+(1-Y(8))*W(J1)*Y(J1)
MFE=MFE-R*T/2.0*E(J1,J1)*X(J1)*X(J1)-R*T*X(1)*E(1,J1)*X(J1)
MC=MC+R*T/3.0*E(1,J1)*X(J1)
MX(J1)=R*T*DLOG(X(J1))
& +R*T*(E(1,J1)*X(1)+E(J1,J1)*X(J1))
MM3C(J1)=R*T*DLOG(Y(J1))
& +Y(8)*W(J1)
DO 3 J2=2,7
MM3C(J1)=MM3C(J1)-Y(8)*W(J2)*Y(J2)
3 CONTINUE
2 CONTINUE
C
FUN(I)=FUN(I)+X(8)*(GFE3C+MFE3C-MFE-MC)
DO 15 J3=2,7
FUN(I)=FUN(I)+X(J3)*(G(J3)+MM3C(J3)-MX(J3)-MC)
15 CONTINUE
C
10 CONTINUE
IF(ABS(FUN(3)) .LT. 1.0D-06) GOTO 20
XGA=X1(3)-2.0*DUMMY*FUN(3)/(FUN(2)-FUN(1))
GOTO 100
20 XGA=X1(3)
RETURN

```

```

END
C
C-----
C SUBROUTINE TO CALCULATE THE EQUILIBRIUM ACM TEMP.
C-----
C
SUBROUTINE FUNCO(T,X)
IMPLICIT REAL*8 (A-H,K-Z)
COMMON/TRANS/C0
DOUBLE PRECISION X(8),Y(8),E(7,7),W(7),X1(3),K(8)
&,FUN(3),G(7),MM3C(8),MX(8),C0(8)
R=8.314D+00
XGA=0.01D+00
C
C THERMODYNAMIC PARAMETERS
C IN ORDER OF SI,MN,NI,CR,MO,CU.
C
DG=46150.0D+00/3.0-19.205D+00*T/3.0
GFE3C=1.332D+04-64.718*T+7.481*T*DLOG(T)-DG
G(2)=28535.0D+00-DG
G(3)=-14263.0D+00+10.0D+00*T-DG
C G(3)=-13532.0D+00-DG
G(4)=20338.0D+00-2.368D+00*T-DG
G(5)=-24418.0D+00+16.61D+00*T-2.749D+00*T*DLOG(T)-DG
G(6)=-19644.0D+00-0.628*T-DG
G(7)=28535.0D+00-DG
C
E(1,1)=8910.0D+00/T
E(1,2)=4.84D+00-7370.0D+00/T
E(1,3)=-4811.0D+00/T
E(1,4)=-2.2D+00+7600.0D+00/T
E(1,5)=24.4-38400.0D+00/T
E(1,6)=3.855D+00-17870.0D+00/T
E(1,7)=4200.0D+00/T
C
E(2,2)=26048.0D+00/T
E(3,3)=2.406D+00-175.6D+00/T
C E(3,3)=0.2D+00
E(4,4)=-721.7D+00/T
E(5,5)=7.655D+00-3154.0D+00/T-0.661D+00*DLOG(T)
E(6,6)=-2330.0D+00/T
E(7,7)=-0.161D+00-7834.0D+00/T
C
W(2)=0.0D+00
W(3)=8351.0D+00-15.188D+00*T
W(4)=0.0D+00
W(5)=1791.0D+00
W(6)=0.0D+00
W(7)=0.0D+00
C
C
DUMMY=1.0D-06
100 X1(1)=XGA-DUMMY
X1(2)=XGA+DUMMY
X1(3)=XGA
DO 10 I=1,3
XX=0.0D+00
YY=0.0D+00
FUN(I)=0.0D+00
DO 1 II=2,7
B=DEXP((GFE3C-G(II)-W(II))/R/T+E(1,II)*X1(I))
X(II)=C0(II)*(4.0*X1(I)-1.0D+00)/
& (3.0*B*(X1(I)-C0(1))+4.0*C0(1)-1.0D+00)
Y(II)=B*X(II)
XX=XX+X(II)
YY=YY+Y(II)
1 CONTINUE
X(1)=X1(1)
X(8)=1.0D+00-X(1)-XX
Y(8)=1.0D+00-YY
C
C
MFE3C=R*T*DLOG(Y(8))
MFE=R*T*DLOG(X(8))-R*T/2.0*E(1,1)*X(1)*X(1)

```

```

MC=R*T/3.0*DLOG(X(1))+R*T/3.0*E(1,1)*X(1)
DO 2 J1=2,7
  IF (X(J1) .EQ. 0.0D+00) GOTO 2
  MFE3C=MFE3C+(1-Y(8))*W(J1)*Y(J1)
  MFE=MFE-R*T/2.0*E(J1,J1)*X(J1)*X(J1)-R*T*X(1)*E(1,J1)*X(J1)
  MC=MC+R*T/3.0*E(1,J1)*X(J1)
  MX(J1)= R*T*DLOG(X(J1))
  &   +R*T*(E(1,J1)*X(1)+E(J1,J1)*X(J1))
  MM3C(J1)= R*T*DLOG(Y(J1))
  &   +Y(8)*W(J1)
  DO 3 J2=2,7
    MM3C(J1)=MM3C(J1)-Y(8)*W(J2)*Y(J2)
3  CONTINUE
2  CONTINUE
C
  FUN(I)=GFE3C+MFE3C-MFE-MC
C
10 CONTINUE
  IF(ABS(FUN(3)) .LT. 1.0D-06) GOTO 20
  XGA=X1(3)-2.0*DUMMY*FUN(3)/(FUN(2)-FUN(1))
  GOTO 100
20  XGA=X1(3)
  RETURN
  END
C
C-----
C SUBROUTINE TO CONVERT WT% TO MOLE FRACTION
C   OR MOLE FRACTION TO WT%.
C-----
C
SUBROUTINE CONV(N,W,C)
IMPLICIT REAL*8 (A-H,O-Z)
DOUBLE PRECISION AN(8), W(8), C(8), A(8)
AN(1)=12.0115D+00
AN(2)=28.09D+00
AN(3)=54.94D+00
AN(4)=58.71D+00
AN(5)=95.94D+00
AN(6)=52.00D+00
AN(7)=50.94D+00
AN(8)=55.84D+00
IF (N .EQ. 0) GOTO 1
W(8)=100.0D+00-W(1)-W(2)-W(3)-W(4)-W(5)-W(6)-W(7)
AT=0.0D+00
DO 2 I=1,8
  A(I)=W(I)/AN(I)
  AT=AT+A(I)
2  CONTINUE
DO 3 I=1,8
  C(I)=W(I)/AN(I)/AT
3  CONTINUE
GOTO 4
1  C(8)=1.0D+00-C(1)-C(2)-C(3)-C(4)-C(5)-C(6)-C(7)
  AT=0.0D+00
  DO 5 I=1,8
    A(I)=C(I)*AN(I)
    AT=AT+A(I)
5  CONTINUE
DO 6 I=1,8
  W(I)=C(I)*AN(I)/AT*100.0D+00
6  CONTINUE
4  RETURN
  END
C-----

```

```

C PROGRAM TO CALCULATE THE GROWTH RATE OF PEARLITE ASSUMING THE BULK OR
C INTERFACE DIFFUSION CONTROL.
C
C GAMMA/GAMMA+ALPHA AND GAMMA/GAMMA+THETA INTERFACE COMPOSITIONS
C ARE CALCULATED USING KIRKALDY'S APPROXIMATE METHOD.
C
C                               1991.5.12 M.TAKAHASHI
C
C IMPLICIT REAL*8 (A-H,K-Z)
C DOUBLE PRECISION X(8),Y(8),C0(8),W0(8),WW(8),K(8),G0(8)
C   &,G(8),G2(8),G3(8),G4(8),GM(8),LFX(4,8),AC(8),E(8,8),EA(8,8)
C COMMON/TRANS/C0,W0,K
C COMMON/HILL/G2,LFX,LCV,GM,AC,DDG,GFEC
C   & ,GFE3C,G3,G4,WW,E,EA,G,G0
C READ(5,*) ISAMPLE
C IS=0
10 IS=IS+1
C IF (IS .GT. ISAMPLE) GOTO 100
C READ(5,*) (W0(I),I=1,7)
C READ(5,*) TI,DT,TF
C
C CALL CONV(1,W0,C0)
C
C WRITE(6,*) 'INITIAL COMPOSITION'
C WRITE(6,199)
C WRITE(6,198) (W0(I),I=1,7)
C WRITE(6,198) (C0(I),I=1,7)
199 FORMAT(1H,' C SI MN NI'
C   &,' CR MO CU ')
198 FORMAT(1H,7F9.5)
C WRITE(6,*)
C
C CALL OMEGA(W)
C
C CC=0.0D+00
C DO 11 I=1,7
C   CC=CC+C0(I)
11 CONTINUE
C C0(8)=1.0D+00-CC
C KK=0.0D+00
C DO 12 I=2,7
C   K(I)=C0(I)/C0(8)
C   KK=KK+K(I)
C   IF (C0(I) .EQ. 0.0D+99) GOTO 12
C   IM=I
12 CONTINUE
C YY=0.0D+00
C DO 13 I=2,7
C   Y(I)=K(I)/(1.0D+00+KK)
C   YY=YY+Y(I)
13 CONTINUE
C Y(8)=1.0D+00-YY
C
C
C CTEMP=TI+DT
20 CTEMP=CTEMP-DT
C T=CTEMP+273.0D+00
C IF (CTEMP .LT. TF) GOTO 100
C IFLAGF=0
C IFLAGC=0
C
C
C C THERMODYNAMIC PARAMETERS IN ORDER OF SI,MN,NI,CR,MO,CU
C -----
C THERMODYNAMIC PARAMETERS
C IN ORDER OF SI,MN,NI,CR,MO,CU.
C
C   DG=46150.0D+00/3.0-19.205D+00*T/3.0
C   GFE3C=1.332D+04-64.718*T+7.481*T*DLOG(T)-DG
C   SFG=-11.906D-04*T+8.272D-06*T*T-15.079D-09*T*T*T
C   & +12.857D-12*T*T*T*T
C   G0(1)=-65562.0D+00+32.949*T
C   G0(3)=-20520.0D+00+4.086D+00*T+1500.0D+00*SFG
C   G0(5)=-1534.0D+00-19.472*T+2.749*T*DLOG(T)

```



```

G(2)=28535.0D+00-DG
G(3)=-14263.0D+00+10.0D+00*T-DG
C G(3)=-13532.0D+00-DG
G(4)=20338.0D+00-2.368D+00*T-DG
G(5)=-24418.0D+00+16.61D+00*T-2.749D+00*T*DLOG(T)-DG
G(6)=-19644.0D+00-0.628*T-DG
G(7)=28535.0D+00-DG
C
C E(1,1)=4.7859D+00+5066.0D+00/T
E(1,1)=8910.0D+00/T
C E(1,2)=4.84D+00-7370.0D+00/T
E(1,2)=14795.0D+00/T
E(1,3)=-4811.0D+00/T
E(1,4)=-2.2D+00+7600.0D+00/T
E(1,5)=24.4-38400.0D+00/T
E(1,6)=3.855D+00-17870.0D+00/T
E(1,7)=4200.0D+00/T
C
E(2,2)=26048.0D+00/T
E(3,3)=2.406D+00-175.6D+00/T
C E(3,3)=0.2D+00
E(4,4)=-721.7D+00/T
E(5,5)=7.655D+00-3154.0D+00/T-0.661D+00*DLOG(T)
E(6,6)=-2330.0D+00/T
E(7,7)=-0.161D+00-7834.0D+00/T
C
EA(1,1)=1.3D+00
EA(2,2)=-13.31D+00+44088.0/T
EA(3,3)=3.082D+00-4679.0/T+1509.8*SFG/T
EA(4,4)=2.041D+00-2478.0/T+385.5*SFG/T
EA(5,5)=2.819D+00-6039.0/T
EA(6,6)=-0.219D+00-4772.0/T+402.6*SFG/T
EA(7,7)=0.634D+00-11270.0/T+1006.5*SFG/T
C
WW(2)=0.0D+00
WW(3)=8351.0D+00-15.188D+00*T
WW(4)=0.0D+00
WW(5)=1791.0D+00
WW(6)=0.0D+00
WW(7)=0.0D+00
C-----
G2(2)=123000D+00
G2(3)=-48500D+00
G2(4)=46000D+00
G2(5)=-251160D+00+118.0D+00*T
G2(6)=-267200D+00
G2(7)=-46000.0D+00+55.0D+00*T
G3(2)=404180.0D+00
G3(3)=-145500.0D+00
G3(4)=138000.0D+00
G3(5)=-153640.0D+00+38.860*T
G3(6)=-267200.0D+00
G3(7)=-46000.0D+00+55.0*T
G4(1)=-65563.0D+00+23.815*T
G4(2)=-64818.0D+00+38.543*T
G4(3)=-1800.0D+00+1.276*T
G4(4)=-5650.0D+00-3.35*T
G4(5)=10460.0D+00+0.628*T
G4(6)=10460.0D+00+0.628*T
G4(7)=-6276.0D+00+3.347*T
G4(8)=(-1.0D+00)*ENERGY(T,T10,T20)
C IF (T.LT. 1000.0D+00) THEN
C G4(8)=8933.0D+00-14.406*T+12.083D-03*T*T-11.51D-06*T*T*T
C & +5.23D-09*T*T*T*T
C ELSE
C G4(8)=71659.0D+00-216.84*T+24.773D-02*T*T-12.661D-05*T*T*T
C & +24.397D-09*T*T*T*T
C ENDIF
C-----
C
C CALCULATION OF PARAEQUILIBRIUM COMPOSITIONS (GAMMA/GAMMA+ALPHA)
C
C
C CALL PEQGA0(T,X,Y,IM)

```

```

C   CALL PEQGA(T,X,Y,IM)
C
  PX1GA=X(1)
  PX2GA=X(IM)
  PX1AG=Y(1)
  PX2AG=Y(IM)
C
C
C CALCULATION OF PARAEQUILIBRIUM COMPOSITIONS (GAMMA/GAMMA+THETA)
C
C
C   CALL PEQGC(T,X,Y,IM)
C
  PX1GC=X(1)
  PX2GC=X(IM)
  PX1CG=0.25D+00
  PX2CG=Y(IM)
C
C
C CALCULATION OF VOLUME DIFFUSION CONTROLLED GROWTH RATE OF PEARLITE
C
  SC=5.9D-04/(1000.0D+00-T)/2
  SC=1.0D-04/2.0D+00/(131.12D+00-0.1783*CTEMP
  & +4.238D+00*W0(IM))
  SC=2.0*600.0*1000.0/6.09D09/(1000.0D+00-CTEMP)
  S=1.0D-04/(127.351D+00-0.17368D+00*CTEMP-4.9195*W0(3)
  & +1.7868*W0(5))
  CCC=(PX1GA+PX1GC)/2.0
  D=DIFF(T,CCC,CCC*1.001,W)
C
  VEL1=VD(PX1GA,PX1GC,PX1AG,SC,D,S)
C
  WRITE(6,*)''
  WRITE(6,*) 'Paraequilibrium carbon diffusion control'
  WRITE(6,99) CTEMP,PX1GC,PX2GC,PX1CG,PX2CG
  WRITE(6,69) PX1GA,PX2GA,PX1AG,PX2AG
  WRITE(6,68) VEL1,D
99  FORMAT(1H,'AT Temp=',F6.1,' CGC=',F8.6,' XGC=',
  &F8.6,' CCG=',F8.6,' XCG=',F8.6)
69  FORMAT(1H,' CGA=',F8.6,' XGA=',
  &F8.6,' CAG=',F8.6,' XAG=',F8.6)
68  FORMAT(1H,' V(bulk diff of C) / cm/sec=',D12.5
  &,' Diff. Coef=',D10.4)
C
C
C CALCULATION OF THE INTEFACE COMPOSITIONS (GAMMA/GAMMA+ALPHA)
C IDENTICAL ISOACTIVITY OF CARBON IN GAMMA IS ASSUMED
C
C CALCULATION OF ACTIVITY OF CARBON IN GAMMA
C
  ACTIV=ACG0(T,C0(1),C0(IM),E(1,1),E(1,IM))
  write(6,*) 'ACTIV=',ACTIV
C
  CALL NPGA0(T,X,Y,IM)
  X1GANP=X(1)
  X2GANP=X(IM)
  X1AGNP=Y(1)
  X2AGNP=Y(IM)
C
  X2TRANS=X2AC0(T,X1GANP,ACTIV,E(1,1),E(1,IM))
  write(6,*) 'X2GANP,X2TRANS =',X2GANP,X2TRANS
  IF (X2GANP .LT. X2TRANS) THEN
    WRITE(6,*) 'ENTERING NPLE REGIME FOR FERRITE.....!'
    IFLAGF=1
    X1GA=X1GANP
    X2GA=X2GANP
    X1AG=X1AGNP
    X2AG=X2AGNP
  ELSE
    CALL EQGA0(T,X,Y,ACTIV,IM)
    X1GA=X(1)
    X2GA=X(IM)
    X1AG=Y(1)
    X2AG=Y(IM)
  
```

```

ENDIF
C
C CALCULATION OF THE INTERFACE COMPOSITIONS (GAMMA/GAMMA+THETA)
C IDENTICAL ISOACTIVITY OF CARBON IN GAMMA AT THE INTERFACES IS ASSUMED
C
CALL NPGC0(T,X,Y,IM)
X1GCNP=X(1)
X2GCNP=X(IM)
X1CGNP=0.25D+00
X2CGNP=Y(IM)
C
X2TRANS=X2AC0(T,X1GCNP,ACTIV,E(1,1),E(1,IM))
IF(X2GCNP.GT.X2TRANS) THEN
  WRITE(6,*) 'ENTERING NPLE REGIME FOR CEMENTITE.....'
  IFLAGC=1
  X1GC=X1GCNP
  X2GC=X2GCNP
  X1CG=X1CGNP
  X2CG=X2CGNP
ELSE
  CALL EQGC0(T,X,Y,ACTIV,IM)
  X1GC=X(1)
  X2GC=X(IM)
  X1CG=0.25D+00
  X2CG=Y(IM)
ENDIF
C
C CALCULATION OF BOUNDARY DIFFUSION CONTROLLED GROWTH RATE OF PEARLITE
C
VEL2=VBD(T,X2GA,X2GC,SC,C0(IM),S,IM)
C
50 WRITE(6,*) 'Boundary diffusion controlled growth'
WRITE(6,98) CTEMP,X1GC,X2GC,X1CG,X2CG
WRITE(6,67) X1GA,X2GA,X1AG,X2AG
WRITE(6,66) VEL2
98 FORMAT(1H,'AT Temp=',F6.1,' CGC=',F8.6,' XGC=',
&F8.6,' CCG=',F8.6,' XCG=',F8.6)
67 FORMAT(1H,' CGA=',F8.6,' XGA=',
&F8.6,' CAG=',F8.6,' XAG=',F8.6)
66 FORMAT(1H,' V(boundary diff of X) /cm/sec=',D12.5)
C
C
GOTO 20
C
100 END
C
C-----
C SUBROUTINE TO CALCULATE INTERFACE COMPOSITIONS (GAMMA/GAMMA+ALPHA)
C Kirkaldy's approximate method is used to obtain the first
C guess value of NPLE calculation
C
SUBROUTINE NPGA0(T,X,Y,IM)
IMPLICIT REAL*8 (A-H,K-Z)
DOUBLE PRECISION X(8),Y(8),C0(8),W0(8),WW(8),K(8)
&,XX(3),G(8),G2(8),G3(8),G4(8),GM(8),G0(8)
&,LFX(4,8),AC(8),E(8,8),EA(8,8),FUN(3)
COMMON/TRANS/C0,W0,K
COMMON/HILL/G2,LFX,LCV,GM,AC,DDG,GFEC,
& GFE3C,G3,G4,WW,E,EA,G,G0
C
C write(6,*) 'IM=',IM
R=8.314D+00
XGA=C0(1)+0.01D+00
ITER=0
ACC=1.0D-05
DX1=1.0D-10
200 XX(1)=XGA-DX1
XX(2)=XGA+DX1
XX(3)=XGA
ITER=ITER+1
IF(ITER.GT.10) THEN
  ACC=ACC*10
  ITER=0
ENDIF
ENDIF

```

```

DO 220 I=1,3
  X1=XX(I)
C
  A1=DEXP(G0(1)/R/T+E(1,1)*X1)/
& (1.0D+00+EA(1,1)*X1*DEXP(G0(1)/R/T))
  A2=DEXP(G0(IM)/R/T+E(1,IM)*X1)/
& (1.0D+00+E(1,IM)*X1*DEXP(G0(1)/R/T))
C  write(6,*) 'A1,A2=',A1,A2
  Y1=A1*X1
C
  Y2=C0(IM)
  X2=Y2/A2
C  write(6,*) 'X2AC=',X2
  X0=1.0D+00-X1-X2
  Y0=1.0D+00-Y1-Y2
C
  FFG=DLOG(X0)-1.0/2.0*E(1,1)*X1*X1-1.0/2.0*E(IM,IM)*X2*X2
& -E(1,IM)*X1*X2
  FFA=DLOG(Y0)-1.0/2.0*EA(1,1)*Y1*Y1-1.0/2.0*EA(IM,IM)*Y2*Y2
& -E(1,IM)*Y1*Y2
C
  FUN(I)=G4(8)/R/T+FFG-FFA
C  FUN(I)=Y0-X0*DEXP(G4(8)/R/T
C & +EA(1,1)/2.0*Y1*Y1+E(1,IM)*Y1*Y2
C & +EA(IM,IM)/2.0*Y2*Y2
C & -E(1,1)/2.0*X1*X1-E(1,IM)*X1*X2
C & -E(IM,IM)/2.0*X2*X2)
220 CONTINUE
  IF (ABS(FUN(3)) .LT. ACC) GOTO 100
  DUMMY=XGA-2.0*DX1*FUN(3)/(FUN(2)-FUN(1))
C  write(6,*) 'DUMMY=',DUMMY
C  write(6,*) 'FUN1,2,3=',(FUN(III),III=1,3)
  IF (DUMMY .LT. 0.0D+00) THEN
    DUMMY=XGA/2.0D+00
  ENDIF
  IF (DUMMY .GT. 0.25D+00) THEN
    DUMMY=(0.25D+00+XGA)/2.0
  ENDIF
  XGA=DUMMY
C  write(6,*) 'FUN3,X1=',FUN(3),XGA
  GOTO 200
100 X(1)=X1
  X(IM)=X2
  Y(1)=Y1
  Y(IM)=Y2
C
  RETURN
  END
C
C-----
C SUBROUTINE TO CALCULATE INTERFACE COMPOSITIONS (GAMMA/GAMMA+ALPHA)
C Kirkaldy's approximate method is used to obtain the first
C guess value.
C
SUBROUTINE EQGA0(T,X,Y,ACTIV,IM)
  IMPLICIT REAL*8 (A-H,K-Z)
  DOUBLE PRECISION X(8),Y(8),C0(8),W0(8),WW(8),K(8)
& ,XX(3),G(8),G2(8),G3(8),G4(8),GM(8),G0(8)
& ,LFX(4,8),AC(8),E(8,8),EA(8,8),FUN(3)
  COMMON/TRANS/C0,W0,K
  COMMON/HILL/G2,LFX,LCV,GM,AC,DDG,GFEC,
& GFE3C,G3,G4,WW,E,EA,G,G0
C
  R=8.314D+00
  XGA=C0(1)*1.1D+00
  DX1=1.0D-06
200 XX(1)=XGA-DX1
  XX(2)=XGA+DX1
  XX(3)=XGA
  DO 220 I=1,3
    X1=XX(I)
C
  A1=DEXP(G0(1)/R/T+E(1,1)*X1)/
& (1.0D+00+EA(1,1)*X1*DEXP(G0(1)/R/T))

```

```

A2=DEXP(G0(IM)/R/T+E(1,IM)*X1)/
& (1.0D+00+E(1,IM)*X1*DEXP(G0(1)/R/T))
Y1=A1*X1
C
X2=X2AC0(T,X1,ACTIV,E(1,1),E(1,IM))
C X2=X2AC(T,X1,ACTIV,LCV,G2(IM))
C X2=C0(IM)*(1.0D+00-A1)*X1/
C & ((1.0D+00-A2)*C0(1)+(A2-A1)*X1)
Y2=A2*X2
X0=1.0D+00-X1-X2
Y0=1.0D+00-Y1-Y2
C
FFG=DLOG(X0)-1.0/2.0*E(1,1)*X1*X1-1.0/2.0*E(IM,IM)*X2*X2
& -E(1,IM)*X1*X2
FFA=DLOG(Y0)-1.0/2.0*EA(1,1)*Y1*Y1-1.0/2.0*EA(IM,IM)*Y2*Y2
& -E(1,IM)*Y1*Y2
C
FUN(I)=G4(8)/R/T+FFG-FFA
C FUN(I)=Y0-X0*DEXP(G4(8)/R/T
C & +EA(1,1)/2.0*Y1*Y1+E(1,IM)*Y1*Y2
C & +EA(IM,IM)/2.0*Y2*Y2
C & -E(1,1)/2.0*X1*X1-E(1,IM)*X1*X2
C & -E(IM,IM)/2.0*X2*X2)
220 CONTINUE
IF (ABS(FUN(3)) .LT. 1.0D-06) GOTO 100
DUMMY=XGA-2.0*DX1*FUN(3)/(FUN(2)-FUN(1))
IF (DUMMY .LT. 0.0D+00) THEN
DUMMY=XGA/2.0D+00
ENDIF
IF (DUMMY .GT. 1.0D+00) THEN
DUMMY=(1.0D+00+XGA)/2.0
ENDIF
XGA=DUMMY
GOTO 200
100 X(1)=X1
X(IM)=X2
Y(1)=Y1
Y(IM)=Y2
C
RETURN
END
C
C-----
C SUBROUTINE TO CALCULATE INTERFACE COMPOSITIONS (GAMMA/GAMMA+ALPHA)
C Kirkaldy's approximate method is used to obtain the first
C guess value. -paraequilibrium-
C
SUBROUTINE PEQGA0(T,X,Y,IM)
IMPLICIT REAL*8 (A-H,K-Z)
DOUBLE PRECISION X(8),Y(8),C0(8),W0(8),WW(8)
& ,K(8),XXX(3),FUN1(3),G(8),G2(8),G3(8),G4(8),GM(8)
& ,LFX(4,8),AC(8),E(8,8),EA(8,8),G0(8)
COMMON/TRANS/C0,W0,K
COMMON/HILL/G2,LFX,LCV,GM,AC,DDG,GFEC
& ,GFE3C,G3,G4,WW,E,EA,G,G0
C
R=8.314D+00
C
X1=0.01D+00
DX1=1.0D-06
200 XXX(1)=X1-DX1
XXX(2)=X1+DX1
XXX(3)=X1
DO 220 I=1,3
X1=XXX(I)
C
A1=DEXP(G4(1)/R/T+E(1,1)*X1)/
& (1.0D+00+EA(1,1)*X1*DEXP(G4(1)/R/T))
Y1=A1*X1
X2=(1.0D+00-X1)*K(IM)/(1.0D+00+K(IM))
Y2=(1.0D+00-Y1)*K(IM)/(1.0D+00+K(IM))
X0=1.0D+00-X1-X2
Y0=1.0D+00-Y1-Y2
C

```

```

      FFG=R*T*DLOG(X0)-R*T/2.0*E(1,1)*X1*X1
&   -R*T/2.0*E(IM,IM)*X2*X2
&   -R*T*E(1,IM)*X1*X2
      FFA=R*T*DLOG(Y0)-R*T/2.0*EA(1,1)*Y1*Y1
&   -R*T/2.0*EA(IM,IM)*Y2*Y2
&   -R*T*E(1,IM)*Y1*Y2
      F2G=R*T*DLOG(X2)+R*T*(E(1,IM)*X1+E(IM,IM)*X2)
      F2A=R*T*DLOG(Y2)+R*T*(E(1,IM)*Y1+EA(IM,IM)*Y2)
      FUN1(I)=X0*(G4(8)+FFG-FFA)+X2*(G4(IM)+F2G-F2A)
C
220 CONTINUE
      IF (FUN1(3) .LT. 1.0D-06) GOTO 300
      DUMMY1=X1-2.0*DX1*FUN1(3)/(FUN1(2)-FUN1(1))
      IF (DUMMY1 .LT. 0.0D+00) THEN
        DUMMY1=X1/2.0D+00
      ENDIF
      X1=DUMMY1
      GOTO 200
300 X(1)=X1
      X(IM)=X2
      Y(1)=Y1
      Y(IM)=Y2
C
      RETURN
      END
C
C-----
      DOUBLE PRECISION FUNCTION ACG0(T,X1,X2,E11,E12)
      IMPLICIT REAL*8 (A-H,K-Z)
C
      ACG0=DEXP(DLOG(X1)+E11*X1+E12*X2)
C
      RETURN
      END
C
C-----
      DOUBLE PRECISION FUNCTION X2AC0(T,X1,A,E11,E12)
      IMPLICIT REAL*8 (A-H,K-Z)
C
      X2AC0=(DLOG(A)-DLOG(X1)-E11*X1)/E12
C
      RETURN
      END
C
C-----
      DOUBLE PRECISION FUNCTION ENERGY(T,T10,T20)
      DOUBLE PRECISION T,T10,T20,F,T7
      T7=T-1.0D+02*T20
      IF (T7 .LT. 3.0D+02) GOTO 1
      IF (T7 .LT. 7.0D+02) GOTO 2
      IF (T7 .LT. 9.21D+02) GOTO 3
      IF (T7 .LT. 1.0D+03) GOTO 5
      F=(3.381D+02-3.31D+00*(T7-1.0D+03)+9.83D-03*(T7-9.9999999D+02
&)*1.96D+00-7.11D+00*DSIN(0.034*(T7-1.0D+03)))/(-4.187D+00)
      GOTO 4
1    F=1.38D+00*T7-1.499D+03
      GOTO 4
2    F=1.65786D+00*T7-1.581D+03
      GOTO 4
3    F=1.30089D+00*T7-1.331D+03
      GOTO 4
5    F=-1.0D+00*(1.20D+02-(T7-9.4D+02)*(0.733333333333D+00))
4    ENERGY=(1.41D+02*T10 + F)*4.187D+00
      RETURN
      END
C
C-----
C FUNCTION TO CALCULATE PARAEQUILIBRIUM CARBON DIFFUSION
C CONTROLLED GROWTH RATE OF PEARLITE
C
      DOUBLE PRECISION FUNCTION VD(XGA,XGC,XAG,SC,D,S)
      IMPLICIT REAL*8 (A-H,K-Z)
      A=0.72D+00
      SA=S*7.0D+00/8.0D+00

```

```

SCEM=S/8.0D+00
CCEM=0.25D+00
VD=D/A*S**2/SA/SCEM*(XGA-XGC)/
& (CCEM-XAG)/S*(1.0D+00-SC/S)
RETURN
END
C
C-----
C FUNCTION TO CALCULATE BOUNDARY DIFFUSION CONTROLLED GROWTH RATE
C OF PEARLITE
C
DOUBLE PRECISION FUNCTION VBD(T,XGA,XGC,SC,XBAR,S,IM)
IMPLICIT REAL*8 (A-H,K-Z)
DOUBLE PRECISION CK(8),Q(8)
CK(3)=1.126D-08
CK(5)=2.455D-09
Q(3)=141178.0D+00
Q(5)=138516.0D+00
R=8.314D+00
SA=S*7.0D+00/8.0D+00
SCEM=S/8.0D+00
KDD=CK(IM)*DEXP(-Q(IM)/R/T)
VBD=12.0D+00*KDD/SA/SCEM*(XGA-XGC)/
& XBAR*(1.0D+00-SC/S)
RETURN
END
C
C-----
C SUBROUTINE TO CONVERT WT% TO MOLE FRACTION
C OR MOLE FRACTION TO WT%.
C
SUBROUTINE CONV(N,WT,C)
IMPLICIT REAL*8 (A-H,O-Z)
DOUBLE PRECISION AN(8), WT(8), C(8), A(8)
AN(1)=12.0115D+00
AN(2)=28.09D+00
AN(3)=54.94D+00
AN(4)=58.71D+00
AN(6)=95.94D+00
AN(5)=52.00D+00
AN(7)=63.55D+00
AN(8)=55.84D+00
IF (N .EQ. 0) GOTO 1
WT(8)=100.0D+00-WT(1)-WT(2)-WT(3)-WT(4)-WT(5)-WT(6)-WT(7)
AT=0.0D+00
DO 2 I=1,8
A(I)=WT(I)/AN(I)
AT=AT+A(I)
2 CONTINUE
DO 3 I=1,8
C(I)=WT(I)/AN(I)/AT
3 CONTINUE
GOTO 4
1 C(8)=1.0D+00-C(1)-C(2)-C(3)-C(4)-C(5)-C(6)-C(7)
AT=0.0D+00
DO 5 I=1,8
A(I)=C(I)*AN(I)
AT=AT+A(I)
5 CONTINUE
DO 6 I=1,8
WT(I)=C(I)*AN(I)/AT*100.0D+00
6 CONTINUE
4 RETURN
END
C
C-----
C FUNCTION GIVING LFG LN(ACTIVITY) OF CARBON IN AUSTENITE.
C
DOUBLE PRECISION FUNCTION CG(X,T,W,R)
DOUBLE PRECISION J,DG,DUMMY,T,R,W,X
J=1-DEXP(-W/(R*T))
DG=DSQRT(1-2*(1+2*J)*X+(1+8*J)*X*X)
DUMMY=5*DLOG((1-2*X)/X)+6*W/(R*T)+((38575.0)-
&13.48)*T)/(R*T)

```

```

CG=DUMMY+DLOG(((DG-1+3*X)/(DG+1-3*X))**6)
RETURN
END
C
C-----
C FUNCTION GIVING DIFFERENTIAL OF LN(ACTIVITY) OF CARBON IN
C AUSTENITE. DIFFERENTIAL IS WITH RESPECT TO X.
C
DOUBLE PRECISION FUNCTION DCG(X,T,W,R)
DOUBLE PRECISION J,DG,DDG,X,T,W,R
J=1-DEXP(-W/(R*T))
DG=DSQRT(1-2*(1+2*J)*X+(1+8*J)*X*X)
DDG=(0.5/DG)*(-2.4*J+2*X+16*J*X)
DCG=-((10/(1-2*X))+5/X))+6*((DDG+3)/(DG-1+3*X
&)-(DDG-3)/(DG+1-3*X))
RETURN
END
C
C-----
SUBROUTINE OMEGA(W)
C SUBROUTINE TO CALCULATE THE CARBON CARBON INTERACTION ENERGY IN
C AUSTENITE, AS A FUNCTION OF ALLOY COMPOSITION. BASED ON .MUCG18
C THE ANSWER IS IN JOULES PER MOL. **7 OCTOBER 1981**
COMMON/TRANS/C0,W0,K
DOUBLE PRECISION C(8),W,P(8),B1,B2,Y(8),T10,T20,B3,XONE
&,C0(8),W0(8),K(8)
INTEGER I,U
DO 1 I=1,8
C(I)=W0(I)
1 CONTINUE
B3=0.0D+00
C(8)=C(1)+C(2)+C(3)+C(4)+C(5)+C(6)+C(7)
C(8)=100.0D+00-C(8)
C(8)=C(8)/55.84D+00
C(1)=C(1)/12.0115D+00
C(2)=C(2)/28.09D+00
C(3)=C(3)/54.94D+00
C(4)=C(4)/58.71D+00
C(5)=C(5)/95.94D+00
C(6)=C(6)/52.0D+00
C(7)=C(7)/50.94D+00
B1=C(1)+C(2)+C(3)+C(4)+C(5)+C(6)+C(7)+C(8)
DO 107 U=2,7
Y(U)=C(U)/C(8)
107 CONTINUE
DO 106 U=1,8
C(U)=C(U)/B1
106 CONTINUE
XONE=C(1)
C XONE=DINT(10000.0D+00*XONE)
C XONE=XONE/10000
B2=0.0D+00
T10=Y(2)*(-3)+Y(3)*2+Y(4)*12+Y(5)*(-9)+Y(6)*(-1)+Y(7)*(-12)
T20=-3*Y(2)-37.5*Y(3)-6*Y(4)-26*Y(5)-19*Y(6)-44*Y(7)
P(2)=2013.0341+763.8167*C(2)+45802.87*C(2)**2-280061.63*C(2)**3
&+3.864D+06*C(2)**4-2.4233D+07*C(2)**5+6.9547D+07*C(2)**6
P(3)=2012.067-1764.095*C(3)+6287.52*C(3)**2-21647.96*C(3)**3-
&2.0119D+06*C(3)**4+3.1716D+07*C(3)**5-1.3885D+08*C(3)**6
P(4)=2006.8017+2330.2424*C(4)-54915.32*C(4)**2+1.6216D+06*C(4)**3
&-2.4968D+07*C(4)**4+1.8838D+08*C(4)**5-5.5531D+08*C(4)**6
P(5)=2006.834-2997.314*C(5)-37906.61*C(5)**2+1.0328D+06*C(5)**3
&-1.3306D+07*C(5)**4+8.411D+07*C(5)**5-2.0826D+08*C(5)**6
P(6)=2012.367-9224.2655*C(6)+33657.8*C(6)**2-566827.83*C(6)**3
&+8.5676D+06*C(6)**4-6.7482D+07*C(6)**5 +2.0837D+08*C(6)**6
P(7)=2011.9996-6247.9118*C(7)+5411.7566*C(7)**2
&+250118.1085*C(7)**3-4.1676D+06*C(7)**4
DO 108 U=2,7
B3=B3+P(U)*Y(U)
B2=B2+Y(U)
108 CONTINUE
IF (B2 .EQ. 0.0D+00) GOTO 455
W=(B3/B2)*4.187
GOTO 456
455 W=8054.0

```



```

456 RETURN
END
C
C-----
C FUNCTION GIVING THE EQUILIBRIUM MOLE FRACTION OF CARBON IN
C FERRITE.
C
DOUBLE PRECISION FUNCTION XALPH(T)
DOUBLE PRECISION T,CTEMP
CTEMP=(T-273.0D+00)/900.0D+00
XALPH=0.1528D-02-0.8816D-02*CTEMP+0.2450D-01*CTEMP*CTEMP
&-0.2417D-01*CTEMP*CTEMP*CTEMP+
&0.6966D-02*CTEMP*CTEMP*CTEMP*CTEMP
RETURN
END
C
C-----
C SUBROUTINE TO CALCULATE THE PARAEQUILIBRIUM INTERFACE CHEMISTRY
C
SUBROUTINE PEQGC0(T,X,Y,IM)
IMPLICIT REAL*8 (A-H,K-Z)
DOUBLE PRECISION X(8),Y(8),C0(8),W0(8),WW(8)
&,K(8),X1(3),FUN(3),G(8),G2(8),G3(8),G4(8),GM(8)
&,LFX(4,8),AC(8),E(8,8),EA(8,8),G0(8)
COMMON/TRANS/C0,W0,K
COMMON/HILL/G2,LFX,LCV,GM,AC,DDG,GFEC
&,GFE3C,G3,G4,WW,E,EA,G,G0
R=8.314D+00
XGA=0.005D+00
C
C
DUMMY=1.0D-08
100 X1(1)=XGA-DUMMY
X1(2)=XGA+DUMMY
X1(3)=XGA
DO 10 I=1,3
XX=0.0D+00
FUN(I)=0.0D+00
KK=K(IM)
Y(IM)=KK/(1+KK)
X(IM)=(1-X1(I))*Y(IM)
X(1)=X1(I)
X(8)=1.0D+00-X(1)-X(IM)
Y(8)=1.0D+00-Y(IM)
C
DENO=1.0D+00
C
MFE3C=R*T*DLOG(Y(8))
MFE=R*T*DLOG(X(8)/DENO)
&-R*T/2.0*E(1,1)*X(1)*X(1)/DENO/DENO
MC=R*T/3.0*DLOG(X(1)/DENO)
&+R*T/3.0*E(1,1)*X(1)/DENO
MFE3C=MFE3C+(1-Y(8))*WW(IM)*Y(IM)
MFE=MFE-R*T/2.0*E(IM,IM)*X(IM)*X(IM)/DENO/DENO
MFE=MFE-R*T*X(1)*E(1,IM)*X(IM)/DENO/DENO
MC=MC+R*T/3.0*E(1,IM)*X(IM)/DENO
MX= R*T*DLOG(X(IM)/DENO)
&+R*T*(E(1,IM)*X(1)+E(IM,IM)*X(IM))/DENO
MM3C= R*T*DLOG(Y(IM))
&+Y(8)*WW(IM)-Y(8)*WW(IM)*Y(IM)
C
FUN(I)=X(8)*(GFE3C+MFE3C-MFE-MC)
FUN(I)=FUN(I)+X(IM)*(G(IM)+MM3C-MX-MC)
C
C WRITE(6,*) IM,E(1,1),E(1,IM),E(IM,IM)
C
10 CONTINUE
IF(ABS(FUN(3)) .LT. 1.0D-6) GOTO 20
XGA=X1(3)-2.0*DUMMY*FUN(3)/(FUN(2)-FUN(1))
GOTO 100
20 XGA=X1(3)
RETURN
END
C

```

```

C-----
C SUBROUTINE TO CALCULATE THE EQUILIBRIUM INTERFACE CHEMISTRY
C
  SUBROUTINE NPGC0(T,X,Y,IM)
  IMPLICIT REAL*8 (A-H,K-Z)
  DOUBLE PRECISION X(8),Y(8),C0(8),W0(8),WW(8)
  &,K(8),XX(3),FUN(3),G0(8)
  &,G(8),G2(8),G3(8),G4(8),GM(8),MX(8),MM3C(8)
  &,LFX(4,8),AC(8),E(8,8),EA(8,8)
  COMMON/TRANS/C0,W0,K
  COMMON/HILL/G2,LFX,LCV,GM,AC,DDG,GFEC
  &      ,GFE3C,G3,G4,WW,E,EA,G,G0
C
  R=8.314D+00
C
  XGC=C0(IM)*0.99D+00
  DUMMY=1.0D-6
100 XX(1)=XGC-DUMMY
  XX(2)=XGC+DUMMY
  XX(3)=XGC
  DO 10 I=1,3
  X1=XX(I)
  FUN(I)=0.0D+00
  B=DEXP((GFE3C-G(IM)-WW(IM))/R/T+E(1,IM)*X1)
  Y2=C0(IM)*4.0/3.0
  X2=Y2/B
  X8=1.0D+00-X1-X2
  Y8=1.0D+00-Y2
  IF (X(8) .LT. 0.0D+00) THEN
    WRITE(6,*) 'X8,X1=',X8,X1
  ENDIF
C
C
  MFE3C=R*T*DLOG(Y8)
  MFE=R*T*DLOG(X8)-R*T/2.0*E(1,1)*X1*X1
  MC=R*T/3.0*DLOG(X1)+R*T/3.0*E(1,1)*X1
  MFE3C=MFE3C+(1-Y8)*WW(IM)*Y2
  MFE=MFE-R*T/2.0*E(IM,IM)*X2*X2-R*T*X1*E(1,IM)*X2
  MC=MC+R*T/3.0*E(1,IM)*X2
  MX(IM)= R*T*DLOG(X2)
  &      +R*T*(E(1,IM)*X1+E(IM,IM)*X2)
  MM3C(IM)= R*T*DLOG(Y2)
  &      +Y8*WW(IM)
  MM3C(IM)=MM3C(IM)-Y8*WW(IM)*Y2
C
  FUN(I)=GFE3C+MFE3C-MFE-MC
C
  10 CONTINUE
  IF(ABS(FUN(3)) .LT. 1.0D-02) GOTO 20
  DUMMY1=XGC-2.0*DUMMY*FUN(3)/(FUN(2)-FUN(1))
  IF (DUMMY1 .LT. 0.0D+00) THEN
    DUMMY1=XGC/2.0D+00
  ENDIF
  XGC=DUMMY1
  GOTO 100
20 X(1)=X1
  X(IM)=X2
  Y(1)=0.25D+00
  Y(IM)=3.0D+00/4.0D+00*Y2
  RETURN
  END
C
C-----
C SUBROUTINE TO CALCULATE THE EQUILIBRIUM INTERFACE CHEMISTRY
C
  SUBROUTINE EQGC0(T,X,Y,ACTIV,IM)
  IMPLICIT REAL*8 (A-H,K-Z)
  DOUBLE PRECISION X(8),Y(8),C0(8),W0(8),WW(8)
  &,K(8),XX(3),FUN(3),G0(8)
  &,G(8),G2(8),G3(8),G4(8),GM(8),MX(8),MM3C(8)
  &,LFX(4,8),AC(8),E(8,8),EA(8,8)
  COMMON/TRANS/C0,W0,K
  COMMON/HILL/G2,LFX,LCV,GM,AC,DDG,GFEC
  &      ,GFE3C,G3,G4,WW,E,EA,G,G0

```

```

C
R=8.314D+00
C
XGC=C0(IM)*0.99D+00
7 X2=X2AC0(T,XGC,ACTIV,E(1,1),E(1,IM))
C7 X2=X2AC(T,XGC,ACTIV,LCV,G2(IM))
IF (X2 .LT. 0.0D+00) THEN
XGC=(C0(1)+XGC)/2.0
GOTO 7
ENDIF
DUMMY=1.0D-6
100 XX(1)=XGC-DUMMY
XX(2)=XGC+DUMMY
XX(3)=XGC
DO 10 I=1,3
X1=XX(I)
FUN(I)=0.0D+00
B=DEXP((GFE3C-G(IM)-WW(IM))/R/T+E(1,IM)*X1)
C X2=C0(IM)*(4.0*X1-1.0D+00)/
C & (3.0*B*(X1-C0(1))+4.0*C0(1)-1.0D+00)
C X2=X2AC(T,X1,ACTIV,LCV,G2(IM))
X2=X2AC0(T,X1,ACTIV,E(1,1),E(1,IM))
Y2=B*X2
X8=1.0D+00-X1-X2
Y8=1.0D+00-Y2
IF (X(8) .LT. 0.0D+00) THEN
WRITE(6,*) 'X8,X1=',X8,X1
ENDIF
C
C
MFE3C=R*T*DLOG(Y8)
MFE=R*T*DLOG(X8)-R*T/2.0*E(1,1)*X1*X1
MC=R*T/3.0*DLOG(X1)+R*T/3.0*E(1,1)*X1
MFE3C=MFE3C+(1-Y8)*WW(IM)*Y2
MFE=MFE-R*T/2.0*E(IM,IM)*X2*X2-R*T*X1*E(1,IM)*X2
MC=MC+R*T/3.0*E(1,IM)*X2
MX(IM)=R*T*DLOG(X2)
& +R*T*(E(1,IM)*X1+E(IM,IM)*X2)
MM3C(IM)=R*T*DLOG(Y2)
& +Y8*WW(IM)
MM3C(IM)=MM3C(IM)-Y8*WW(IM)*Y2
C
FUN(I)=GFE3C+MFE3C-MFE-MC
C
10 CONTINUE
IF(ABS(FUN(3)) .LT. 1.0D-02) GOTO 20
DUMMY1=XGC-2.0*DUMMY*FUN(3)/(FUN(2)-FUN(1))
IF (DUMMY1 .LT. 0.0D+00) THEN
DUMMY1=XGC/2.0D+00
ENDIF
XGC=DUMMY1
GOTO 100
20 X(1)=X1
X(IM)=X2
Y(1)=0.25D+00
Y(IM)=3.0D+00/4.0D+00*Y2
RETURN
END
C
C-----
C FUNCTION TO CALCULATE EQUILIBRIUM FUNCTION F AND M
C IMF=1: F(X,Y) IMF=0: M(X,Y)
C
DOUBLE PRECISION FUNCTION FXY0(T,C,X1,X2,Y2,IM,IMF)
IMPLICIT REAL*8 (A-H,K-Z)
DOUBLE PRECISION C(8),C0(8),W0(8),WW(8),K(8),G0(8)
& ,G(8),G2(8),G3(8),G4(8),GM(8),LFX(4,8),AC(8),E(8,8),EA(8,8)
COMMON/TRANS/C0,W0,K
COMMON/HILL/G2,LFX,LCV,GM,AC,DDG,GFEC
& ,GFE3C,G3,G4,WW,E,EA,G,G0
R=8.314D+00
C
C
CG=X1

```

```

      X1=(C(1)*(3.0*Y2-4.0*X2)-(C(IM)-X2))/(3.0*Y2-4.0*C(IM))
      X8=1.0D+00-X1-X2
      Y8=1.0D+00-Y2
C
      MFE3C=R*T*DLOG(Y8)
      MFE=R*T*DLOG(X8)-R*T/2.0*E(1,1)*X1*X1
      MC=R*T/3.0*DLOG(X1)+R*T/3.0*E(1,1)*X1
      MFE3C=MFE3C+(1-Y8)*WW(IM)*Y2
      MFE=MFE-R*T/2.0*E(IM,IM)*X2*X2-R*T*X1*E(1,IM)*X2
      MC=MC+R*T/3.0*E(1,IM)*X2
      MX= R*T*DLOG(X2)
      &   +R*T*(E(1,IM)*X1+E(IM,IM)*X2)
      MM3C= R*T*DLOG(Y2)
      &   +Y8*WW(IM)
      MM3C=MM3C-Y8*WW(IM)*Y2
C
      IF (IMF .EQ. 1) THEN
        FXY0=GFE3C+MFE3C-MFE-MC
      ELSE
        FXY0=G(IM)+MM3C-MX-MC
      ENDIF
C
      RETURN
      END
C
C-----
C FUNCTION GIVING THE CARBON DIFFUSIVITY IN AUSTENITE
C
      DOUBLE PRECISION FUNCTION DIFF(T,X1,X2,W)
      IMPLICIT REAL*8(A-H,K-Y), INTEGER(I,J,Z)
      DOUBLE PRECISION D(300),CARB(300)
C HH=PLANCK CONST./S, KK=BOLTZMAN CONST. /K
      HH=6.6262D-34
      KK=1.38062D-23
      Z=12
      A5=1.0D+00
      R=8.31432D+00
C
C DIFF=DIFFUSIVITY OF CARBON IN AUSTENITE, CM**/SEC
C Z=COORDINATION OF INTERSTIAL SITE
C PSI=COMPOSITION DEPENDENCE OF DIFFUSION COEFFICIENT
C THETA=NO. C ATOMS/ NO. FE ATOMS
C ACTIV=ACTIVITY OF CARBON IN AUSTENITE
C R=GAS CONSTANT
C X=MOLE FRACTION OF CARBON
C T=ABSOLUTE TEMPERATURE
C SIGMA=SITE EXCLUSION PROBABILITY
C W=CARBON CARBON INTERACTION ENERGY IN AUSTENITE
C
      DASH=(KK*T/HH)*DEXP(-(21230.0D+00/T))*DEXP(-31.84D+00)
      XINCR=(X1-X2)/300.0D+00
      DO 1 I=1,300
        CARB(I)=X2+(I-1)*XINCR
        X=CARB(I)
        THETA=X/(A5-X)
        ACTIV=CG(X,T,W,R)
        ACTIV=DEXP(ACTIV)
        DACTIV=DCG(X,T,W,R)
        DACTIV=DACTIV*ACTIV
        DACTIV=DACTIV*A5/((A5+THETA)**2)
        SIGMA=A5-DEXP((-W)/(R*T))
        PSI=ACTIV*(A5+Z*((A5+THETA)/(A5-(A5+Z/2)*THETA+(Z/2)*(A5+Z/2)*
        &(A5-SIGMA)*THETA*THETA)))+(A5+THETA)*DACTIV
        D(I)=DASH*PSI
1      CONTINUE
      I3=0
      CALL DQSES(XINCR,D,300,ANS,ERROR)
      DIFF=ANS/(X1-X2)
      RETURN
      END
C-----

```